DEPOSITION OF CELL WALL COMPONENTS IN CONIFER TRACHEIDS(Dissertation_全文)

AUTHOR(S):

Takabe, Keiji

DEPOSITION OF CELL WALL COMPONENTS IN CONIFER TRACHEIDS

KEIJI TAKABE

1984

DEPOSITION OF CELL WALL COMPONENTS IN CONIFER TRACHEIDS

KEIJI TAKABE

1984

CONTENTS

Table of abbreviations and symbols

a.p.	axial parenchyma
Ara.	arabinose
C	cambium zone
cpm	count per minute
dil H_2SO_4	diluted sulfuric acid
ER	endoplasmic reticulum
G	golgi body
Gal.	galactose
GLC	gas-liquid-chromatography
Glc.	glucose
GV	golgi vesicle
Man.	mannose
$NaClO_2$	sodium chlorite
PATAg	periodic acid-thiocarbohydrazide-silver proteinate
Pl	plastid
r-ER	rough endoplasmic reticulum
r.p.	ray parenchyma
S.	standard
S1	S_1 layer
S2	S_2 layer
S3	S_3 layer
s-ER	smooth endoplasmic reticulum
TLC	thin layer chromatography
W	warty layer
Xyl.	xylose

Introduction

The main components of the cell wall of woody plant are cellulose, hemicelluloses and lignin. Plant anatomists and chemists have been interested in the distribution and the interrelation of cellulose, hemicelluloses and lignin in the cell wall.

The plant cell wall is constructed from the primary wall and the secondary wall. The primary wall is formed in the stages of the cell division and the following radial enlargement of the cell, whereas the secondary wall is formed after complete cell enlargement. Various investigations have been carried out in order to know the sugar composition and the chemical properties of lignin in each cell wall layer, but many questions still remain. This is due to the following difficulties: First, preparation of pure cell wall layer, such as the primary wall or S1, is very difficult because each cell wall layer is extremely thin. Second, even if the pure cell wall layer is prepared, its amount is extremely little. Third, there are two types of the deposition of polysaccharides. One is the appositional deposition, and the other is the internal deposition (Ray, 1967). The sugar composition of each cell wall layer has been presented by Meier and co-worker (1959), Meier (1961) and Côté and co-workers(1968). However, the composition contains some errors in calculation because in their investigations polysaccharides deposited internally were not taken into account. It is necessary to take into

account the amount of the internal deposition of polysaccharides for accurate calculation. If these difficulties are overcome by suitable analytical methods, the sugar composition and the properties of lignin in each cell wall layer will be elucidated more precisely. The elucidation not only gives a better understanding of chemical properties of each cell wall layer, but also provides basic data for processing wood effectively.

In this study, the deposition process of polysaccharide is investigated by analysis of the constituent monosaccharides using gas-liquid-chromatography and analysis of incorporation pattern of radioactive precursor into cell wall. The differentiating xylem was cut from the cambium side to the pith side, hydrolysed and the amount of sugars in each fraction was analyzed by the former method. The incorporation of the radioactive precursor into each cell wall component was analyzed by the latter method. The pattern of deposition of polysaccharides was investigated by LM-autoradiography coupled with chemical analysis. The lignification process of tracheid walls was investigated by UV-microscopy, LM-autoradiography and TEM. The properties of lignin were discussed on the basis of the results of LM-autoradiography.

Biosynthesis of cellulose, hemicelluloses and lignin have have been investigated by many botanists and plant chemists for a long time. However, many questions still remain.

By the development of freeze fracture technique, it became possible to observe the surface of the plasma membrane and the

cell organella. Several workers adapted this technique to algae and plant cells to investigate the site of cellulose synthesis, and suggested "terminal complex" or "rossette" to be the site of cellulose synthesis. There are, however, some questions on the synthetic pathway of cellulose and the cell organella involved in the orientation of cellulose microfibrils.

The cytochemical staining method was applied to investigate the cell organella involved in biosynthesis and/or transport of polysaccharides (mainly hemicelluloses and/or pectins). PATAg test, which was developed by Thiéry (1967), is one of the representative methods to stain polysaccharides selectively. Some investigators suggested the involvement of the Golgi-body in biosynthesis and/or transport of polysaccharides based on the fact that the Golgi-cisternae and the Golgi-vesicles were stained with PATAg. In addition, it was speculated that the ER plays an important role in biosynthesis of polysaccharides. In spite of these investigations, the mechanism of polysaccharide synthesis is still not well elucidated.

On the other hand, the synthetic pathway of lignin is almost perfectly elucidated. However, only few attempts have been performed to elucidate the cell organella involved in biosynthesis of lignin. Hence, it is necessary to investigate further the cell organella involved in biosynthesis of lignin precurcor.

In the present study, TEM-autoradiography adapting to the specimen administered with tritiated glucose or phenylalanine,

and the cytochemical staining were attempted in order to elucidate the cell organella involved in biosynthesis of cell wall components.

The history of studies on the deposition process of cell wall components, the depositing manner of polysaccharides, the distribution of cell wall components in the cell wall, and the cell organella involved in biosynthesis of cell wall components are reviewed in Chapter I.

The deposition process and the depositing manner of polysaccharides, and the distribution of polysaccharides in the cell wall are described in Chapter II.

The lignification process of tracheids is described in Chapter III.

The cell organella involved in biosynthesis of cell wall constituents is described in Chapter IV.

Chapter I

Literature review

1.1 Deposition process and distribution of cell wall constituents

1.1.1 Deposition process and distribution of woody polysaccharides

Main components of the cell wall are cellulose, hemicelluloses and lignin. It is one of the most interesting problems for plant anatomists how these constituents are supplied and deposited to the developing cell wall.

The earlist study on the deposition of polysaccharides to the plant cell wall was carried out by Setterfield and co-worker (1959). Using oat(Avena sativa var. Lanark) coleoptiles administered with tritiated sucrose, they investigated the incorporation of the sucrose into the cell wall by LM-autoradiography after selective extraction of cell wall components. They suggested that wall materials were synthesized in the cell wall from the precursor, because it was found that the radioactivity was distributed all over the cell wall after the selective extractions. In other word, wall materials were deposited by intussusception. However, since the selective extraction of cell wall material was insufficient, they could not obtain the persuasive results.

Ray(1967) administered tritiated glucose to growing oat (Avena sativa var. Victory) coleoptiles and pea(Pisum sativum var. Araska) stem. After selective extraction of cell wall components, the cell wall was observed by TEM-autoradiography. It was shown that the radioactivity at the interior of the cell wall was removed both by extraction with hot diluted sulfuric acid and 17.5% sodium hydroxide, and that the remaining radioactivity was located only at the lumen surface of the cell wall. He, therefore, concluded that cellulose is deposited appositionally, and hemicelluloses internally. However, his conclusion is still inmature because the distribution of the radioactivity before and after selective extraction was not compared with the same cell.

Fujita and co-worker(1978) administered tritiated glucose to a developing cryptomeria(Cryptomeria japonica D.Don) compression wood, and investigated the deposition process of cellulose and hemicellulose. In agreement with Ray's results, they observed that celluolse deposits both in the S1 depositing cells and in the S2-thickening-stage cells, and hemicellulose both in the transitional cells from S1 to S2 development and the cells from S2-thickening-stage to the following secondary wall lignification stage. However, conclusions are based on only the difference of silver-grain distribution on the cell wall. The silver grains located on the lumen surface of the cell wall were attributed to cellulose and those located on the interior of the cell wall were

attributed to hemicellulose, respectively. The results should be supported by chemical analysis of the radioactive cell wall materials.

A few papers have been reported on the deposition and distribution of polysaccharides by chemical analysis. Meier and co-worker(1959), and Meier(1961) investigated the distribution of polysaccharides in the cell wall of Scots pine (Pinus sylvestris), Norway spruce (Picea abies) and silver birch (Betura verrucosa). They made radial sections, which contained cambium and differentiating xylem, observed the sections between crossed nicols in order to check the differentiating stages, and then, excised each section into several fractions by a micromanupulator. After hydrolyzing each fraction, they examined the sugar composition by paper chromatography. Furthermore, they measured the area of cell wall layers on the electron microscopic photograph of transverse sections of tracheids or fibers. On the basis of the proportion of each cell wall layer and the sugar composition of each fraction, they roughly estimated the sugar composition of each cell wall layer after complicated calculation. Côté and co-workers(1968) also investigated the distribution of polysaccharides in the tracheid of compression wood by the same method as Meier and co-worker(1959). However, the calculation of the sugar composition in each cell wall layer based on the increment of sugars accompanied by the cell wall thickening should give better results.

Larson(1969) fed $^{14}CO_2$ to Pinus resinosa, and investigated the incorporation of the radioactivity into the developing cell walls. The differentiating xylem was separated into sevaral fractions according to the method of Meier(1959). The fractions were hydrolyzed and examined on the radioactivity of neutral sugars and lignin. It was shown that xylose increases with the tracheid maturation, mannose remains relatively constant, and both arabinose and galactose decrease remarkably. It was also shown that lignin is accumulated to the cell wall lagging behind the polysaccharide deposition. This method was applied to compression wood of Pinus resinosa(1969). The studies gave accurate cell wall constituent. But since the investigation did not reveal which portion of the cell wall the radioactivity was distribited, the accurate distribution of the cell wall components through the cell wall could not be presented.

In recent years, Hardell and co-worker(1981) collected the individual cell wall layers from spruce(Picea abies) by scratching with specially devised tweezers, and analyzed the sugar composition of each cell wall layer by gas-liquid-chromatography. The results showed no significant differences in the ratio of mannose, xylose and glucose among individual cell wall layers. It was, however, difficult to obtain pure cell wall layers by their method.

There are a few attempts to investigate the localization of polysaccharides by electron microscopic technique combined with

selective degradation of cell wall components (Sinner and co-workers, 1973; 1976; 1979). Parameswaren and co-worker(1982) treated the delignified spruce (Picea abies (L.) Karst.) and beech(Fagus sylvatica L.) particles with purified mannanase, xylanase and avicellase or cellobiohydrolase, and observed the remaining solids by TEM. They suggested that the mannan in spruce is high in S1 and S3, while xylan is higher in S3 than S1. They also suggested that xylan in beech is high in S1 and S3. However, they could not show the localization of polysaccharides quantitatively.

1.1.2 Deposition process and distribution of lignin

As the detection of lignin by microscopic technique is easier than that of polysaccharides, many investigations on the lignin accumulation have been reported. The pioneering study was carried out by Wardrop(1957). He observed the differentiating xylem of Pinus radiata under UV-microscope at a wavelength of 280 nm, because lignin gives an UV-absorption spectrum with an absorption maximum around 280 nm. He showed that lignification begins in the primary wall at the cell corner lagging behind the S1 deposition, and then extends to the middle lamella and secondary walls.

In recent years, Imagawa and co-workers(1976) closely investigated the differentiating tracheids of Japanese larch(Larix leptolepis GORD.) under UV-microscope. They demonstrated that lignification is initiated both at the intercellular layer in the cell corner and at the pit border, extends along both the radial and the tangential wall, and proceeds toward the lumen. They also demonstrated that the cell corners of the tracheid adjacent to the ray is first lignified.

Though UV-microscopy is excellent in dealing with lignin quantitatively, it has a disadvantage of resolving power. A transmission electron microscope has also been employed for the investigation of lignification (Hepler and co-workers; 1970, Wardrop; 1971, 1976, Kutscha and co-worker; 1975). Wardrop(1971)

observed the differentiating xylem of Eucalyptus elaeophora fixed with potassium permanganate, and demonstrated the lignification process as follows: Lignification is initiated at the middle lamella of the cell corners and subsequently occurs at the outer part of S1. It extends along the middle lamella, through the primary wall, and ultimately to the secondary wall.

Kutscha and co-worker(1975) observed balsam fir(Abies balsamea) fixed with potassium permanganate and indicated the lignification process as follows. Lignification is initiated in the middle lamella between pit borders of adjacent tracheids, and extends into the pit border and cell corners. In cell corners, lignin is accumulated in the outer portion of the primary wall or the middle lamella. Lignification proceeds into S1 in the cell corners, leaving the primary wall unlignified at this time. Lignification then proceeds centripetally toward the lumen, lagging behind cell wall thickening.

Kishi and co-workers(1982), however, suggested that the staining intensity is not necessarily proportional to the lignin content. In addition, it is not apparent that potassium permanganate reacts only with lignin. It is, therefore, required to reexamine the results obtained from the specimen fixed with potassium permanganate by another electron microscopic technique.

In recent years, Saka and co-worker(1982) investigated quantitatively the lignification process of loblolly pine (Pinus taeda L.) tracheid by SEM-EDXA technique, and showed as follows.

Prior to S2 formation, lignification is initiated in the cell corner middle lamella and compound middle lamella regions. Subsequently, lignin is rapidly accumulated in both regions. Secondary wall lignification is initiated when the middle lamella lignin concentration is approximately 50% of maximum, and proceeds toward the lumen. As the resolving power of this method is, however, inferior to that of TEM, they could not examine the lignification process of tracheid more closely.

Scott and co-workers(1969), and Fergus and co-workers(1969) applied the UV-microscopy to investigate the distribution of lignin in mature black spruce(Picea mariana Mill.) tracheid. They cut 0.5 um transverse section, took photographs at a wavelength of 280 nm, and measured the silver density of UV-photonegatives. They showed that the lignin concentration of secondary wall, middle lamella, and cell corner middle lamella in earlywood(latewood) are 0.225(0.222)g/g, 0.497(0.60)g/g, and 0.848(1.00)g/g, respectively. In recent years, Saka and co-worker(1982), using a SEM-EDXA technique, investigated the lignin distribution of each cell wall layer in loblolly pine(Pinus taeda L.) tracheid. They showed that the lignin concentration of cell corner, compound middle lamella, S1, S2 and S3 are 0.64g/g, 0.49g/g, 0.25g/g, 0.20g/g and 0.28g/g, respectively. It is noteworthy that the lignin concentration of S2 is lower than those of S1 and S3.

1.2 Cell organelle participating in biosynthesis of cell wall constituent

Many botanists and biochemists have been interested in cellulose biosynthesis for a long time. Preston and co-workers (1951, 1953, 1954, 1955, 1961) observed under electron microscope Valonia, fusiform initials of conifer cambium, parenchyma cells of broad bean internodes, and Chaetomorpha, and found that granular bodies were located on the innermost lamella of the cell wall and accompanied by cellulose microfibrils. Preston(1964) proposed the ordered granule hypothesis on the basis of these observation.

Ledbetter and co-worker(1963) found that the microtubules were observed in the root tips of Phleum pratense L., Spirodela oligorrhiza Kurtz, and Juniperus chinensis L. fixed with gltar-aldehyde-osmium tetroxide, and that the cortical microtubules were parallel to the microfibrils. After that, many investigators confirmed that the direction of the microfibril is the same to that of the microtubule. Hence, it has been believed that the microtubule could be involved in biosynthesis and/or orientation of microfibril. Some exceptions, however, were found in the root hair of radish (Newcomb and co-worker, 1965), the elongating tips of fibers and tracheid (Robards and co-worker, 1967), Cladophorales (Preston and co-worker, 1968) and Pediactum (Gawlick and co-worker, 1969).

In the development of freeze fracture technique, Meuller and co-worker(1976, 1980), Willison and co-worker(1978), Kiermayer and co-worker(1979), Giddings, Jr. and co-workers(1980) and Wada and co-worker(1981) have focused their investigations on the elucidation of the site of cellulose biosynthesis, and they suggested that a terminal complex or rossette on the plasma membrane is the site of cellulose biosynthesis. However, it is still not clear how the precursor of cellulose is transported to the terminal complex or rossette.

The biosynthesis of cell wall polysaccharides has also been investigated by cytochemical methods. PATAg test, which was developed by Thiéry (1967), has been widely used for detecting the polysaccharides at the ultrastructural level. Pickett-Heaps (1968b) adapted the PATAg test to the root tips and coleoptiles of wheat seedlings (Iriticum vulgare). He suggested that the Golgi-body is involved in biosynthesis and/or transport of polysaccharides because the Golgi-cisternae and the Golgi-vesicles are stained positively though the ER-cisternae negatively. Fowke and co-worker (1972), and Ryser (1979) obtained almost the same results as Pickett-Heaps (1968). It is, however, extremely difficult to stain selectively the respective polysaccharides in the wall by this method.

The cell organella involved in biosynthesis of cellulose and hemicelluloses were also investigated by TEM-autoradiography. Northcote and co-worker (1966) and Pickett-Heaps (1966, 1967) ad-

ministered tritiated glucose to root cap cell of wheat(Triticum vulgare) and wheat seedling(Triticum vulgare), respectively, and investigated the distribution of radioactivity by TEM-autoradiography. They suggested that the Golgi-body is involved in transport of wall materials to the cell wall, and the ER may also be involved in the synthesis and the transport of various wall materials. These investigations were, however, insufficient in examining chemically the cell wall component synthesized from the labeled precursor.

Wooding (1968), using sycamore vascular tissue wall administered with tritiated glucose, investigated the sites of cellulose and hemicellulose biosynthesis by comparing the results of TEM-autoradiography to those of chemical analysis. In the chemical analysis, α-cellulose was found to be labelled at an early stage, whereas hemicellulose became labelled after one-hour's incubation. In the TEM-autoradiography, silver grains were found to be distributed only on the developing cell wall at an early stage, whereas they distributed on the Golgi-bodies and their associated vesicles and also on the developing cell wall after one-hour's incubation. He suggested that cellulose is synthesized at or just outside the plasma-membrane, and high-molecular-weight precursors of hemicellulose are contained in the Golgi-body and the Golgi-vesicle.

Only a few workers attempted to investigate the cell organella involved in biosynthesis of lignin. Pickett-Heaps(1968a)

administered tritiated lignin precursor to wheat shoot, and investigated the distribution of radioactivity on the cell organella by TEM-autoradiography. He suggested that the Golgi-bodies and r-ER participated in lignin biosynthesis. Fujita and co-worker(1979) observed the differentiating compression wood administered with tritiated phenylalanine and ferulic acid by TEM-autoradiography, and suggested that the Golgi bodies were involved in lignin biosynthesis. Wardrop(1971, 1976) observed sclerenchyma fibers of Liriodendron tulipifera and sclereids of Pyrus communis, which were fixed with KMnO4, and showed that vesicles supplied their contents to the cell wall, although the origin of the vesicles could not be elucidated.

Chapter II

Deposition of cellulose and hemicelluloses with the tracheid maturation

The investigation of the depositing manner and the deposition process of each cell wall component provides a valuable information about the interrelations among cellulose, hemicelluloses and lignin in the cell wall. It also provides a important information about the chemical composition of each cell wall layer.

Several workers investigated the distribution of polysaccharides by chemical analysis. Meier and co-worker (1959), Meier (1961) and Côté and co-workers (1968) excised the differentiating xylem into several fractions, analyzed the sugar composition, and roughly calculated the polysaccharide composition of each cell wall layer. Larson(1969a,b) also investigated the distribution of cell wall constituents by tracer method. In recent years, Hardell and co-worker (1981) scraped the cell wall layers and analyzed the sugar composition of each cell wall layer. These reports, however, contain some problems presented in Chapter I.

The depositing manner of polysaccharides was investigated by Setterfield and co-worker (1959), Ray (1967) and Fujita and co-worker (1978). Setterfield and co-worker proposed that polysaccharides are deposited to the cell wall by intussusception. On

the contrary, Ray, and Fujita and co-worker proposed that cellulose is deposited to the cell wall by apposition, whereas hemicelluloses by intussusception. As these reports have some problems discussed in Chapter I, the depositing manner of cell wall constituent is still open to speculation.

In this chapter, the deposition process and the depositing manner of polysaccharides are discussed (Takabe and co-workers; 1981, 1983, 1984). In addition, the analysis of sugar composition of each cell wall layer is described.

2.1 Materials and methods

2.1.1 Analysis of sugars by gas-liquid-chromatography

2.1.1.1 Preparation of materials

Cryptomeria (Cryptomeria japonica D.Don) grown at the Kamigamo Experimental Forest, Kyoto University, Kyoto, was used. A block sample was taken from the trunk at breast height on May 29, 1981. Subsequently, a small block (tangential direction: 5mm, radial direction: 5mm, longitudinal direction: 12mm) containing cambium and differentiating xylem was cut from the sample with a razor blade and fixed with 3% glutaraldehyde. After fixation, the small block was washed in phosphate buffer, dehydrated through an ethanol series, and embedded in methyl- and butyl-methacrylate resin.

2.1.1.2 Separation of the differentiating tracheids

The steps in Figure 1 show how accurate transverse, radial, and tangential surfaces of the embedded tissue were prepared using a Sorvall JB-4 microtome equipped with a binocular(10 x 8) and a glass knife, a file, a razor blade, epoxy mounting-blocks, quick adhesive, and a thin plate of gelatin.

First, methacrylate resin which encrusted the specimen was sectioned off with a microtome to expose two tranverse specimen surfaces(step 1), and the resin on the four lateral sides was removed with a file(step 2). The phloem-side tangential surface of the specimen was stuck on a mounting-block with a quick adhe-

sive, and the pith-side tangential surface was sectioned using the microtome(step 3). Changing the mounting-block from the phloem-side to a radial-side an accurate radial surface was made (step 4). The surface was precisely parallel to both the directions of radial files of differentiating tracheids(single arrow) and of the tracheid axis(double arrow). The specimen was separated mechanically from the mounting-block, and the opposite radial-side was adhered to the mounting-block again sandwiching a thin gelatin plate(step 5). After repeating step 4, the specimen was separated from the mounting-block by the irradiation of a supersonic wave in warm water(step 6). Thus by dissolving the gelatin, one can expect that the accurate radial surface elaborated in step 4 is protected from mechanical damage of splitting. Then the pith-side tangential surface was adhered again on the top of a convex-shaped mounting-block, accurate sections were obtained from the two transverse surfaces(step 7), and accurate tangential sections were sliced from the phloem-side of the specimen(step 8).

By the repetition of the steps 7 and 8 in Figure 1, a very accurate tangential section was cut from the phloem-side, that is, the sliced tangential surface was exactly parallel to both the cambium and the tracheid axis. Subsequently, accurate transverse sections, 3-5 μm thick, were prepared from two transverse surfaces, and then mounted in Canada balsam after toluidine-blue-O staining. The sections were viewed under ordinary and pola-

rizing microscopes, and the general differentiation of tracheids and the initiation of the S1 and S3 depositions in each radial file were examined(refer Figure 4a). Then serial tangential sections, 5 μm thick, were made from the cambium-side to the pith-side. At this time, twenty-four serial sheets were collected as one group and put into a mini-vial. Starting from the initiation of radial enlargement of the differentiating tracheids, these procedures were repeated twelve times(refer Figure 4a). After sectioning and collecting the differentiating tracheids, transverse sections were prepared again from two transverse surfaces(see step 7 of Figure 1), and compared with the first transverse sections to determine how much of the specimen was cut away(Figure 4).

2.1.1.2 Quantitative analysis of neutral sugars in each fraction

The collected tangential sections were extracted with acetone three times for two hours to remove the methacrylate resin. The disembedded sections were extracted with a chloroform-methanol mixture (1:1, V/V) three times for four hours, and then air-dried. The dried sections were treated with 4 x crystalline Bacillus subtillis α-amylase(Sigma No. A 6380, 0.5mg/ml in 0.05M phosphate buffer, pH 6.9) for one day at room temperature in the presence of a drop of toluene. After the α-amylase treatment, the cell wall materials were hydrolyzed according to the method of

Saeman and co-workers(1963). To each solution, 250 μg of myo-inositol was added as an internal standard. The unhydrolyzed materials were removed by filtration, and the filtrates were neutralized with saturated barium hydroxide. To remove barium sulfate, the solutions were filtered through the celite layer. The filtrates were passed through Amberlite-IR 120(H^+ form) and evaporated to dryness with a rotary evaporator. The sugars were reduced with sodium borohydride to their corresponding alcohols which were acetylated. The alditol acetates were then extracted with methylene chloride.

The gas chromatograph used in this study was a Shimadzu-GC-5A instrument equipped with a flame ionization detector. Chromatographic peak areas were measured with Shimadzu-Chromatopac E1A electric integrator. A 1.5m x 3mm-o.d. glass column packed with 1.5% ethylene glycol succinate and 1.5% silicone oil(XF-1150) on Gas-Chrom P, was employed at a nitrogen flow rate of 60ml/min. The column was operated isothermally at 185°C with an injection port, and a detector temperature of 230°C. Hydrogen and air flow rates were set at 45ml/min and 900ml/min, respectively.

2.1.2 Tracer method

2.1.2.1 Administration of ^{14}C-glucose

Six- or seven-year-old cryptomeria (Cryptomeria japonica D.Don) grown at the Kyoto Experimental Nursery of Kyoto University Forest was used. Just before administration of the precursor, the tree was fallen, and the internode was removed. A small part of the bark (10 x 10 mm) was scraped away with a knife, and a V-shaped groove, 2 mm wide and 10 mm long, was made in the wood with a razor blade. The bottom of the groove reached the tracheids where the cell wall formation was just completed. D-(U-^{14}C)-Glucose (specific activity: 284 mCi/mmol, concentration: 30 μCi/30 μl aqueous solution, New England Nuclear Corp.) was added dropwise for two hours to the absorbent cotton packed into the groove (Figure 2). After the administration, the specimen was fixed with 3% glutaraldehyde for two hours. After fixation, a part of it was cut into a small block (2 x 2 x 3 mm; radial(R): tangential(T): longitudinal(L)) for light microscopic autoradiography, and the remaining sample was cut into a large block (8 x 3 x 12 mm; R: T: L) for chemical analysis. These blocks were washed in phosphate buffer and embedded in methyl- and buthyl-methacrylate resin in the usual manner.

2.1.2.2 Light microscopic autoradiography

The radioactivity incorporated into the cell walls was observed according to the method mentioned in 2.1.3.3.

2.1.2.3 Fractionation of the differentiating xylem and chemical analysis of the fractions

The differentiating xylem of cryptomeria was fractionated according to the method mentioned in 2.1.1.2. In this case, serial tangential sections, 5 μm in thickness, were cut, and six of them were put into a vial. This procedure was repeated sixteen times. After extraction with acetone and chloroform-methanol (1:1, V/V), and subsequent treatment with α-amylase, sixteen tracheid fractions were hydrolyzed according to the method of Saeman and co-workers(1963). The reaction mixtures were filtered through Whatman glass filter paper A to separate the hydrolyzates from the Klason lignin. After drying the filter papers, the radioactivity of the Klason lignin was counted in 20 ml Packard liquid-scintillation spectrometer-bottles to which 5 ml of dioxane scintillation-fluid (dioxane/ naphthalene/ 2,5-diphenyloxazole/ 1,4-bis-2-(5-phenyloxazol)-benzene: 1 liter/ 120 g/ 5 g/ 0.3 g) was added. The filtrates were passed through Dowex 1 x 8 (carbonate form) column and evaporated to dryness. The hydrolyzates were dissolved by adding 200 μl of distilled water, from which 20 μl was put into the liquid-scintillation vials containing scintillation fluid (5 ml). The radioactivity of the hydrolyzates in each fraction was counted for five 1-minute periods. The remaining solution was dried again. The hydrolyzates were redissolved by adding 10 μl of distilled water with a microsy-

ringe, and 4 μl of the solution was spotted on a plate. Thin-layer chromatography (TLC) was conducted according to the method of Iwakawa and co-workers(1980). After development, the chromatograms were placed in contact with Kodak X-O mat film for two to thirteen weeks in a refrigerator. X-ray films were developed with Rendol (20°C, 7 min,) and fixed with Renfix (20°C, 10 min.).

The radioactivity of neutral sugars separated by TLC was measured as follows: First, the positions of neutral sugars on the TLC plate were confirmed by comparing the plate with the autoradiograph. After scraping off the silica gel from the plate, 0.5 ml of distilled water was added to the silica gel for eluting the sugars. By adding 10 ml of dioxane scintillation-fluid to the extracts, the radioactivity of each extract was counted for five 1-minute periods. In case of low radioactivity (Fraction 9-16), the composition of the radioactive sugars in each fraction was determined by measuring the silver density of the X-ray film exposed for thirteen weeks, with a Sakura Micro-Densitometer (Model PDM-5 Type).

2.1.3 Selective extraction of cell wall component and light microscopic autoradiography

2.1.3.1 Materials

Seven- or eight-year old cryptomeria (Cryptomeria japonica D.Don) was fallen at the middle of July. A disk was obtained

from the internode, and the surface of the disk was cut with a razor brade. The surface of the disk was sealed with a manicure, although a small part of cambium zone (3 x 5 mm: radial and tangential directions) was excluded. Subsequently, tritiated glucose (specific activity: 30.0 Ci/mmol, concentration: 1 mCi/ml aqueous solution, New England Nuclear Corp.) was continuously added dropwise to the non-sealed area of cambium zone for two hours(Figure 3). After administration, small blocks (2 x 2 x 3 mm: radial, tangential, and longitudinal directions) were made, and fixed with 3% gltaraldehyde at 4°C over night. They were washed with phosphate buffer, and embedded in methacrylate resin according to the method of Kushida and co-workers(1979). Serial 1 μm thick transverse sections were cut on a Porter-Blum MT-1 ultramicrotome with a glass knife and mounted on glass-slides. Methacrylate resin was removed with acetone from these sections.

2.1.3.2 Selective extraction of the cell wall components from the thin section

In order to remove lignin, the glass-slide, on which the sections were mounted, was dipped into acidified 2% sodium chlorite solution at 70°C for 15 and 30 minutes.

In order to remove hemicelluloses, the glass-slide was dipped into hot 0.2N sulfuric acid solution for 2 hours.

These procedures were carried out separately, or combined together.

2.1.3.3 Visualization and determination of the radioactivity incorporated into the cell wall

The control section and the sections, which were extracted with different reagents, were coated with the stripping film (London Kodak AR-10). The coated glass-slides were put into a light-tight box containing silica gel, and stored in a refrigerator for several weeks.

In order to visualize the radioactivity, the coated glass-slides were processed by dipping them into D-19 developer for 7 minutes at 20℃, and successively into Fuji-Fix for 10 minutes at 20℃. After fixation, the sections were stained with 1% safranin or 0.5% toluidine blue-O solution.

The determination of the radioactivity incorporated into each tracheid was carried out according to the method of Fujita and co-workers(1981).

2.1.3.4 Determination of the radioactive neutral sugars in the extracts and the residual sections

Two μm thick transverse sections were cut from the specimen block, which was prepared in 2.1.2.1. Three hundreds sheet of the section were collected and put into a vial. This procedure was repeated 4 times.

Methacrylate resin was extracted with acetone. The sections were treated with acidified sodium chlorite solution and/or hot

diluted sulfuric acid according to the methods mentioned in 2.1.3.3. After the treatments, the specimens were centrifuged at 3000 r.p.m. for 10 minutes, and the supernatant fluids were separated from the residual sections. The washing procedure of the sections were repeated twice, and the combined solutions and the residual sections were used in the following analysis.

The extract, which was obtained by the treatment of hot diluted sulfuric acid, was passed through Dowex 1 x 8 (carbonate form) column, and evaporated to dryness. The extract, which was obtained by the treatment of acidified sodium chlorite, was dialyzed against the distilled water, and evaporated to dryness. The dried extracts, the control sections, and the residual sections were hydrolyzed according to the method of Saeman and co-workers(1963). Each hydrolyzate was passed through Dowex 1 x 8 (carbonate form) column, evaporated to dryness, redissolved by adding 20 μl of distilled water, and separated by TLC according to the method of Iwakawa and co-workers. The TLC-autoradiograph was obtained by the method mentioned in 2.1.2.3. The radioactivity of nuetral sugars in each fraction was also measured by the method mentioned in 2.1.2.3.

2.2 Results

2.2.1 Changes in the composition and the amount of neutral sugars during the tracheid wall maturation

2.2.1.1 Changes in the neutral-sugar composition during the tracheid wall maturation

Figure 4 shows the transverse sections of differentiating xylem of cryptomeria subjected to gas-liquid-chromatographic examinations. The separated fractions were as follows:

Fraction 1: the stage of primary wall deposition.

Fractions 2-3: the stage of S1 deposition.

Fractions 4-7: the stage of S2 deposition.

Fraction 8: the stage of S3 deposition.

Fractions 9-12: the final stage of tracheid differentiation.

Figure 5 shows the sugar composition in each fraction. The proportion of glucose was lower in Fraction 1 than in any other fractions. It was slightly higher at S1 than at primary wall formation. During S2 formation, it increased conspicuously and reached a maximum at Fraction 7. It declined at S3 formation, and after that it was approximately constant.

Both mannose and xylose were a relatively minor proportions of the cell wall in Fraction 1. From the S1 stage to the beginning stage of S2, the proportion of mannose and xylose increased

and reached a maximum at Fractions 4 and 5, respectively. They decreased temporarily in subsequent fractions, but increased again at the S3 stage.

Arabinose and galactose comprised relatively large proportions of the hydrolyzate in Fraction 1. The proportion of arabinose continued to decrease with tracheid maturation, and that of galactose also continued to decrease toward Fraction 7, the final stage of S2. But at the S3 stage it increased slightly, and remained constant through the final stage of tracheid differentiation.

2.2.1.2 Changes in the amount of neutral sugars during the tracheid wall maturation

Figure 6 shows the changes in the amount of neutral sugars during the tracheid wall maturation. In Fraction 1, most of tracheids did not complete radial enlargement so that the fraction contained more tracheids with less radial enlargement than any other fractions. Therefore, the amount of sugars in Fraction 1 is not given in Figure 6.

The amount of glucose increased linearly from Fractions 2 to 8 and remained approximately constant from 8 to 12. Mannose increased from Fraction 2 to 9; the amount of increase was especially notable between Fractions 3 and 4, and between 7 and 9. It was noticeable that the amount of mannose continued to increase

toward Fraction 9, whereas that of glucose increased toward Fraction 8 and remained constant from Fractions 8 to 12. Xylose increased from Fractions 2 to 11; the amount of increase was especially notable between Fractions 2 and 5, and between 7 and 8. Between Fractions 5 and 7 xylose increased slightly. Arabinose increased toward Fraction 8; especially the amount of increase between Fractions 7 and 8 was slightly higher than that between the other two adjacent fractions. Galactose increased between Fractions 2 and 4, remained constant between 4 and 7, and increased again between 7 and 9, and finally remained constant from 9 to 12.

Figure 7 shows the amount of increase in neutral sugar with the development of tracheids, that is, the difference in the amount of sugar between the two adjacent fractions. Deposition of glucose was different from those of other sugars. Glucose deposited between the S1 and S3 stages. The amount of glucose deposition in the S2 stage was slightly higher than those in S1 and S3. On the other hand, mannose and xylose deposited actively from the later stage of S1 to the beginning stage of S2, and from the final stage of S2 to the S3 stage. In the middle stage of S2, their depositions were lower, whereas glucose deposition was higher.

2.2.2 Incorporation of the radioactive glucose into cell wall components

2.2.2.1 Light-microscopic autoradiography

Figure 8 shows a light-microscopic autoradiograph of the differentiating xylem of cryptomeria. The incorporation of ^{14}C-glucose into the tracheids occurred between the cells of the cambium and the cells which had completed the S3 formation. Especially, the incorporation was predominant from the cambium cells to the cells depositing S3. Just after the S3 formation, the incorporation temporarily decreased, and then increased at the cells which were about 150 μm from the S3 depositing cells. At the primary wall formation stage, ^{14}C-glucose was incorporated into the radial walls of tracheids rather than into the tangential walls. After that, ^{14}C-glucose was incorporated equally into radial and tangential walls. ^{14}C-glucose was also incorporated actively into the ray and axial parenchyma cells. Almost all of the radioactivity observed locally in both types of parenchyma cells was removed by the treatment with α-amylase(Figure 9).

2.2.2.2 Incorporation of ^{14}C-glucose into the cell-wall components during the tracheid maturation

Figure 10 shows a transverse section of the differentiating

xylem of cryptomeria that was subjected to chemical analysis. The differentiating stages of this sample were as follows:

Fractions 1-2: primary wall formation stage.

Fraction 3: S1 formation stage.

Fractions 4-6: S2 formation stage.

Fractions 7-8: S3 formation stage.

Fractions 9-16: the final cell-wall formation stage.

Figure 11 shows the radioactivity of the hydrolyzates(solid line) and Klason lignin(dashed line) in each fraction. The radioactivity of the hydrolyzates was high in the primary wall formation stage, temporarily decreased in the S1 stage, and then increased sharply in the S2 stage. It decreased during S3 stage. The radioactivity of Klason lignin reached a maximum in Fraction 6, decreased from Fractions 6 to 8, and then gradually increased toward Fraction 11. It is also high in the primary wall formation stage.

Figure 12 shows the autoradiographs of TLC. In Fractions 1 and 2, a large proportion of the radioactivity was incorporated into arabinose, glucose, and galactose. Radioactive xylose was also detected. Only a very small amount of radioactive mannose was detected in this stage. In Fraction 3, the incorporation into arabinose and galactose decreased, whereas that into mannose increased. In Fractions 4-6, large amounts of radioactivity were incorporated into xylose, mannose, and glucose, especially into glucose. In Fractions 7 and 8, the radioactivities of glucose and

mannose were still detected, whereas that of the other sugars were low. In Fractions 9-16, a little radioactivity of glucose was detected, and very little was detected of arabinose and galactose.

Table 1 shows the relative amounts of radioactivity incorporated into the neutral sugars in each fraction. In the primary wall formation stage, galactose and arabinose contents were extremely high, and they comprised 43%. During the S2 stage, galactose and arabinose contents gradually decreased. On the other hand, the percentage of radioactivity in xylose reached a maximum in the early part of the S2 stage, and then decreased. The percentage of radioactivity in mannose showed a relatively low value in the S1 stage, and increased from the S2 to the S3 stages. The percentage of radioactivity in glucose was low in the primary wall formation stage. It was about 43% of the total radioactivity of the neutral sugars contained in Fractions 1 and 2. In the S1 stage, it was still low, and was about 49% of the total. During the S2 formation, it increased sharply and reached a maximum in the S3 stage.

Table 1 The composition of radioactive neutral sugars in each fraction (%).

Fraction	Xyl.	Ara.	Man.	Glc.	Gal.
1	9.0	17.7	6.2	42.2	24.9
2	9.3	18.8	5.8	42.0	24.4
3	11.3	12.7	9.1	49.4	17.5
4	12.8	8.0	12.9	53.5	12.8
5	9.4	5.5	14.2	61.7	9.3
6	8.4	4.6	12.7	67.4	6.9
7	5.5	3.7	15.2	68.2	7.3
8	6.9	3.8	11.5	61.1	16.8
9	6.8	8.2	5.7	64.8	14.5
10	t	11.5	t	62.4	26.1
11	t	13.5	t	64.0	22.5
12	t	7.3	t	73.3	19.4
13	t	7.8	t	75.8	16.4
14	t	6.3	t	80.0	13.7
15	t	6.0	t	81.4	12.6
16	t	5.6	3.8	78.4	12.2

t : trace

2.2.3 Distribution of the labeled cell wall components in the differentiating tracheid walls

2.2.3.1 Distribution of the radioactivity on the differentiating tracheid walls

The differentiating tracheids used in this experiment were numbered from the cell just before S1 deposition toward the cell which completed the cell wall formation. Differentiating stages in many radial files were as follows.

Cells 1-2: S1 formation stage.

Cells 3-6: S2 formation stage.

Cells 7-8: S3 formation stage.

Cells 9-13: probably secondary wall lignification stage.

Figure 13 shows the light microscopic autoradiographs of the control section and the section extracted with hot diluted sulfuric acid. Figure 15 also shows the results of counting silver grains. Tritiated glucose was widely incorporated into the tracheid walls from the cell of S1 formation stage to the cell after S3 formation was completed. Especially, the labeled glucose was actively incorporated into the tracheids of S2 formation stage. The radioactivity was distributed both on the lumen surface of the cell wall and the interior in each tracheid. Particularly, a large proportion of the radioactivity was distributed on the lumen surface of the tracheid in the cells of S1 and S2 formation

stages. An appreciable part of the radioactivity on the interior of the cell wall was removed by the treatment with hot diluted sulfuric acid. This removal mainly occurred in the later part of S1 formation stage, later part of S2 formation stage, S3 formation stage, and secondary wall lignification stage.

Figure 14 shows the light microscopic autoradiographs of the control section, the section extracted with sodium chlorite, and the section extracted with sodium chlorite followed by the extraction with hot diluted sulfuric acid. Figure 16 also shows the results of counting silver grains. The radioactivity on the interior of the cell wall was partially removed by the extraction with sodium chlorite. This phenomenon resembled the results of hot diluted sulfuric acid extraction. After the extraction with sodium chlorite followed by the extraction with hot diluted sulfuric acid, almost all radioactivity remained to be distributed on the lumen surface of the cell wall in the cells of secondary wall formation. The radioactivity on the secondary wall was completely removed in the cells after the S3 formation stage.

2.2.3.2 The composition of the radioactive neutral sugars in the extracts and the residual sections

Figure 17 and Table 2 show the TLC-autoradiographs and the composition of the radioactive neutral sugars in the control sections, the extracts by the treatment with hot diluted sulfuric

acid, and the residual sections. All of the radioactive neutral sugars were extracted by the treatment with hot diluted sulfuric acid. Especially, arabinose and galactose were predominant. They were minor constituents in the residual sections.

Figure 18 and Table 3 show the TLC-autoradiographs and the composition of the radioactive neutral sugars in the control sections, the extracts by the treatment with acidified sodium chlorite solution and the residual sections. Glucose, arabinose, and galactose were extracted by the treatment with acidified sodium chlorite solution. Radioactivity of the Klason lignin in the residual sections was 69 % of that in the control sections.

Figure 19 and Table 4 show the TLC-autoradiographs and the composition of the radioactive neutral sugars in the sections treated with acidified sodium chlorite, the extracts by the treatment with hot diluted sulfuric acid after the sodium chlorite extraction, and the residual sections by sodium chlorite and hot diluted sulfuric acid extractions. All of the neutral sugars were extracted by the treatment with hot diluted sulfuric acid, especially glucose, arabinose and galactose were predominant. On the other hand, glucose, mannose and xylose were the main components in the residual sections, particularly glucose content was extremely high.

Table 2 Composition of radioactive neutral sugars

	Ara.	Xyl.	Man.	Gal.	Glc.
Control	5.5	4.9	9.1	11.6	68.9
Residue ($^{dil}H_2SO_4$)	0.7	4.3	7.7	5.8	81.5
Extracts($^{dil}H_2SO_4$)	17.5	5.3	11.5	25.9	39.8

Table 3 Composition of radioactive neutral sugars

	Ara.	Xyl.	Man.	Gal.	Glc.
Control	5.5	4.9	9.1	11.6	68.9
Residue ($NaClO_2$)	4.7	4.9	8.7	9.6	72.1
Extracts($NaClO_2$)	18.5	7.5	5.1	34.0	34.9

Table 4 Composition of radioactive neutral sugars

	Ara.	Xyl.	Man.	Gal.	Glc.
Residue ($NaClO_2$)	4.7	4.9	8.7	9.6	72.1
Residue ($NaClO_2$-$^{dil}H_2SO_4$)	0.6	5.0	7.9	3.2	83.4
Extracts($NaClO_2$-$^{dil}H_2SO_4$)	19.0	8.4	9.2	28.6	34.8

2.3 Discussion

When discussing the deposition process of polysaccharides from the changes both in the composition and the amount of neutral sugars, attention should be paid to the following points: First, glucose is predominant in hydrolysate, and it derives mostly from cellulose, but some from glucomannan and galactoglucomannan. Therefore, the amount of glucose in the hydrolysate for the most part corresponds to the cellulose content. Second, xylose is a main component of arabinoglucuronoxylan (abbreviated as xylan) and comprised approximately 75% of the xylan in weight. For this reason, xylose can be taken as an index of the xylan content. In the same way, mannose can be used as an index of glucomannan and galactoglucomannan (abbreviated as mannans) content, because mannose is a main component of these polysaccharides. Third, arabinose and galactose can be regarded as indices of the amounts of arabinoglucuronoxylan and galactoglucomannan, respectively. Fourth, since the radioactive precursor is incorporated into the developing cell wall of both tracheid and ray parenchyma, it is necessary to lessen the contamination with polysaccharides in ray parenchyma cell walls.

Figure 7 shows the amount of increase in neutral sugars with the development of tracheid, that is, the difference in the amount of sugar between the two adjacent fractions. Figure 20 also shows the composition of the amount of increase in neutral

sugars.

Comparing Figures 8 and 12, it is obvious that the radioactive glucose, arabinose and galactose in Fractions 14-16 are derived from the cell wall components of ray parenchyma. Hence, the percentage values of Fractions 14-16 show the sugar composition of ray parenchyma cell wall. The similarity of the composition of radioactive neutral sugars in Fractions 10-13 to that in Fraction 14-16 suggests that most of the radioactive sugars containing in Fractions 10-13 may be ascribed to the cell wall materials of ray parenchyma. Therefore, the mean amounts of radioactivity incorporated into each sugar in Fraction 10-16 could be given by subtraction of the radioactivity from the amounts of radioactivity in Fraction 1-8. After subtraction, the composition of the radioactive sugars in each fraction was recalculated (Figure 21).

The result shown in Figure 20 resembles that in Figure 21, except that the arabinose and galactose contents of the former are slightly higher than those of the latter. Therefore, the discussion of the deposition process of woody polysaccharides is made based on the Figures 7, 20 and 21.

Figure 7 indicates that the deposition process of cellulose is different from those of hemicelluloses. Cellulose deposits between the S1 and S3 stages. The amount of cellulose deposition in the S2 stage is slightly higher than those in S1 and S3. On the other hand, hemicelluloses deposit actively from the later

stage of S1 to the beginning stage of S2 and from the final stage of S2 and S3. In the middle stage of S2 hemicellulose depositions decrease, whereas cellulose deposition increases.

The deposition processes of individual hemicelluloses are as follows. Xylan deposition is active between the later stage of S1 and the beginning stage of S2, and between the final stage of S2 and S3 stage, whereas during the middle stage of S2 it decreases. Although the amount of increase in arabinose was less than that in xylose, the profile of the arabinose increment during the secondary wall formation was similar to that of xylose. The pattern of arabinose deposition seems to be in keeping with the xylan deposition process described above. Mannans deposit abundantly between the later stage of S1 and the beginning stage of S2, and between the final stage of S2 and the S3 stage. It is noticeable that deposition of mannans continues in a few tracheids after S3 formation is completed (Figure 7, Fraction 8-9). They are different from deposition pattern of cellulose which complete deposition by the stage of S3 formation.

It is generally accepted that polysaccharides are deposited to the cell wall by "apposition" or "intussusception". In the former polysaccharides are supplied and deposited to the inner surface of the developing cell wall. But, in the latter polysaccharides are supplied and deposited to the interior of the cell wall through the developing cell wall.

On the basis of the results presented in 2.2.3.1 and 2.2.

3.2, the depositing manner of polysaccharides in cryptomeria is discussed. The results that the residual sections were rich in radioactive glucose, mannose and xylose (Figures 17 and 19, Tables 2 and 4) suggest that the most of radioactivity distributed on the lumen surface of the cell wall (Figures 13 and 14) is ascribed to to glucose, mannose and xylose residues of the cell wall polysaccharides. It means that cellulose and main chains of mannans and xylan deposit appositionally to the inner surface of the developing cell wall. On the other hand, the removal of the radioactivity distributed at the interior of the cell wall, and of arabinose and galactose by the treatment with sodium chlorite, and hot diluted sulfuric acid suggest that the major portion of the radioactivity distributed at the interior is due to arabinose and galactose residues of hemicelluloses. They possibly deposit to the cell wall by intussusception, though the main chains of xylan and mannans deposit by apposition. It seems that arabinose and galactose are transported through the developing cell wall and link to the pre-existing main chains of xylan and mannans, respectively, prior to the lignin accumulation.

It could be possible to estimate the distribution of polysaccharides deposited in the cell wall by measuring the amounts of glucose , mannose and xylose, because cellulose and main chains of mannans and xylan are appositionally deposited to the cell wall. The conversion from the amounts of sugars to those of polysaccharides is made by essencially the same method of Meier

(1959). Figure 22 shows the distribution of polysaccharides through the cell wall. S1, outer part of S2 and S3 are rich in hemicelluloses, whereas the middle part of S2 is rich in cellulose. Inner part of S3, which is rich in galactoglucomannan, possibly corresponds to the warty layer.

2.4 SUMMARY

The deposition process and the depositing manner of woody polysaccharides were investigated by GLC of sugar residues, chemical analysis using the radioactive precursor, and LM-autoradiography. The sugar composition of each cell wall layer was discussed on the basis of these investigations.

The deposition process of cellulose was different from those of hemicelluloses. Cellulose deposited between the S1 and S3 stage, especially abundant deposition occurred in the middle part of S2 stage. On the other hand, hemicelluloses deposited actively from the later part of S1 stage to the early part of S2 stage, and from the final part of S2 stage to S3 stage. In the middle part of S2 stage, hemicellulose depositions decreased, whereas cellulose deposition increased. Xylan deposition was active between the later part of S1 stage and the beginning part of S2 stage, and between the final part of S2 stage and S3 stage. Mannans were deposited abundantly between the later part of S1 stage and the beginning part of S2 stage, and between the final part of S2 stage to S3 stage. It was noticed that the deposition of mannans continued in a few tracheids after S3 formation was completed.

The depositing manner of polysaccharides or sugar residues is summarized as follows. Cellulose, and the main chains of mannans and xylan deposit by apposition, whereas galactose and

arabinose residues deposit by intussusception.

The distribution of polysaccharides are shown in Figure 22. S1, outer part of S2 and S3 are rich in hemicelluloses, whereas the middle part of S2 is rich in cellulose.

CHAPTER III

Lignification process of tracheid

The investigation of the lignification of conifer tracheid was initiated by Wardrop (1957). Using an UV-microscope, he observed the differentiating xylem of radiata pine (Pinus radiata), and measured the silver density of UV-photonegatives due to the UV-absorption by lignin. In recent years, Imagawa and co-worker (1976), and Fujita and co-worker (1978) made 0.5 μm thick sections and observed them closely under an UV-microscope. Although these observations were effectual in the study of lignification, this method contained some problems. The data obtained by UV-microscopy are apt to be influenced by the artifacts of sectioning, such as cracks, wrinkles and unevenness of section. The resolving power of an UV-microscope is lower than that of TEM. In addition, it is still uncertain whether a trace amount of lignin can be detected under an UV-microscope.

With the proceeding of the study on lignin biosynthesis, several lignin precursors have been identified. Saleh and co-workers(1967), and Fujita and co-workers(1978) fed tritiated lignin precursors to the differentiating xylem and observed the distribution of the radioactivity on the cell wall by autoradiography.

A few workers (Hepler and co-workers, 1970; Wardrop, 1971; Kutscha and co-worker, 1975), using the specimen fixed with potassium permanganate, also investigated the lignification of the cell wall by TEM. However, it is still ambiguous whether lignin is selectively stained with potassium permanganate.

Though the lignification of the cell wall has been investigated by various microscopic techniques, the results are not necessarily consistent. In this chapter, the UV-microscopy, LM-autoradiography and TEM used to the detection of the lignin in the differentiating xylem are described. The lignification process of tracheid wall is discussed by comparing the results obtained by these methods. In addition, the properties of lignin of the compound middle lamella and the secondary wall are discussed on the basis of the results of LM-autoradiography(Takabe and co-workers, 1981, 1984).

3.1 Materials and method

3.1.1 Specimen preparation

Seven- or eight-year old cryptomeria grown at Kyoto Experimental Nursery, Kyoto University, Kyoto, was used. The internode was obtained from the stem, and tritiated phenylalanine(specific activity: 84 Ci/mmol, concentration: 1.0 mCi/ml, Amersham International plc.) was administered for 1, 2 and 4 hours by the method mentioned in 2.1.2.1. After administration, small blocks were cut from the internode, fixed in 3% gltaraldehyde-1% osumium tetroxide, and embedded in epoxy resin in the usual way.

3.1.2 UV-microscopy

0.5 μm thick transverse section was cut on a Porter-Blum MT-1 ultramicrotome with a glass-knife from the specimen block administered with tritiated phenylalanine for 4 hours. The section was mounted on a 0.5 mm thick quartz-slide, immersed in a glycerine, and covered with 0.18 mm quartz-cover-slip. It was examined under a Leitz UV-microscope (LEITZ-MPV2) at 280 nm wavelength. Photographs were taken on a commercial film, and the silver density of the negative was determined with a Sakura Microdensitometer (Model PDM-5 Type).

3.1.3 Light microscopic autoradiography

One μm thick sections were cut on a Sorvall JB-4 microtome

with a glass-knife from the specimen blocks administered with radioactive phenylalanine for 1, 2 and 4 hours. Light microscopic autoradiography was carried out by the method mentioned in 2.1.3.3. The radioactivity incorporated into the compound middle lamella and secondary walls was determined according to the method of Fujita and co-workers (1981). In this case, the region stained heavily with safranin was regarded as the compound middle lamella, and that stained weakly was regarded as the secondary walls.

3.1.4 TEM-observation of the lignin skeleton

Ultra-thin sections were cut on a LKB-ultramicrotome with a diamond knife from the specimen block administered with radioactive phenylalanine for 4 hours. They were mounted on 100 mesh Mo-grids, which were coated with a formvar support film and followed by evaporation of carbon. Epoxy resin was removed from the sections according to the method of Mayer and co-workers (1961). The sections were hydrolyzed according to the method of Fujii and co-workers(1981). They were observed in a JEM-7 electron microscope at 80 KV.

3.2 Results

3.2.1 UV-microscopy

Numbering of the differentiating tracheids was made by the method mentioned in 2.2.3.1. Differentiating stages in many radial files were as follows.

Cells 1- 4: S1 formation stage.

Cells 5-11: S2 formation stage.

Cells 12-14: S3 formation stage.

Cells 15-25: probably secondary wall lignification stage.

Figures 23, 24 and 25 show the differentiating xylem of cryptomeria photographed in ultraviolet light of wavelength 280 nm. Weak UV-absorption was first detected at the pith-side cell corners in the tracheid 1, which was the beginning of S1 deposition. UV-absorption at the cell corners gradually increased with the development of tracheid wall (Figure 23a).

UV-absorption was spreaded to the compound middle lamella from the cell corners in the tracheid 4, and the absorption area increased all over the compound middle lamella in the tracheid 6. UV-absorption at the compound middle lamella gradually increased during the S2 formation.

UV-absorption at the secondary wall was first detected at the outer portion in the final part of S2 formation stage, and gradually spreaded toward the lumen. It became to be observed all over the secondary wall just after the S3 formation stage,

although the outer portion exhibited a somewhat stronger absorption than the inner portion(Figure 24). In the final part of secondary wall lignification stage, a uniform UV-absorption was observed all over the secondary wall(Figure 25).

Figure 26 shows the densitometer traces of the UV-photomicrograph negatives. UV-absorption at the compound middle lamella was first detected in the tracheid of S1 formation. It gradually increased during the S1 and S2 formation stages, and kept approximately constant after S3 formation stage. UV-absorption at the secondary wall was detected at the outer portion in the middle stage of S2 formation. It gradually proceeded toward the lumen of the tracheid lagging behind the cell wall thickening. In the tracheid just after the S3 formation, UV-absorption can be seen all over the secondary wall, although UV-absorption of the inner portion was weaker than that of the outer portion. The tracheid at the final part of secondary wall lignification showed a uniform UV-absorption of the secondary wall.

3.2.2 LM-autoradiography

Figure 27 shows the amount of the incorporation of tritiated phenylalanine into the compound middle lamella lignin and the secondary wall lignin determined by the method of counting silver grains. The incorporation of radioactive phenylalanine into the compound middle lamella lignin showed the same tendency among the specimens, which were administered for 1, 2, and 4 hours. That

is, the precursor was well incorporated into the compound middle lamella lignin from the S1 formation stage to the early part of S2 formation stage. On the other hand, little incorporation of the precursor into the secondary wall lignin occurred in the specimen incubated for 1 hour. The incorporation into the secondary wall lignin actively occurred from the cells, which began S3 formation, to the cells, which just finished S3 formation, in the specimen incubated for 2 hours. Furthermore, the incorporation of the precursor into the secondary wall lignin remarkably took place from the cells, which began S3 formation, to the cells, which probably finished the lignification of secondary walls.

The results of LM-autoradiography mentioned below were obtained from the specimen administered with radioactive phenylalanine for 4 hours. Figure 28 shows the LM-autoradiograph of the differentiating xylem. Silver grains were first observed at the cell corners in the tracheid at the final part of primary wall formation stage or the beginning part of S1 formation stage. Silver grains were mainly distributed on the cell corners from the S1 formation stage to the early part of S2 formation stage, and after that, they were scarcely distributed at the cell corners. Silver grains on the compound middle lamella were observed from the later part of S1 formation stage to the middle part of S2 formation stage. Silver grains on the secondary wall were remarkably observed from the S3 formation to the final part of

secondary wall lignification, although it was not obvious during the S1 and S2 formation stages.

3.2.3 TEM-observation of the lignin skeleton of the differentiating xylem

Figure 29 shows a pair of the UV-photomicrograph and TEM-photomicrograph of lignin skeleton, which were obtained from the same tracheid. The observation of the lignin skeleton by means of TEM provides more detailed information about the lignin accumulation than that by means of UV-microscopy, though the TEM is inferior to the UV-microscopy for the determination of lignin. Therefore, the radial file observed in 3.2.1 was investigated more closely by means of TEM.

Figure 30 shows the tracheids from the final part of primary wall formation to the S1 formation stage. Lignin residues were first observed at the outer surface of the primary wall of the cell corner in the tracheid just before the S1 formation or the beginning part of S1 formation. The outer surface of the primary wall was gradually accumulated with lignin residue, and the intercellular space was also filled up with the lignin residue with the tracheid maturation. When the tracheid was adjacent to the ray parenchyma, the outer surface of the primary wall and the intercellular space adjacent to the ray parenchyma were accumulated with lignin residue earlier than those not adjacent

to the ray parenchyma. When the intercellular space was relatively wide, the mass of the lignin residue sometimes was observed (Figure 31).

Figure 32 shows the tracheids from the S1 formation to the early part of S2 formation stage. The lignin residue at the intercellular layer was spreaded from the cell corners. In the early part of S1 formation stage, the lignin residue was observed at the outermost part of S1 of the cell corner, and spreaded to the unlignified outermost part of S1 with the tracheid maturation. The lignin residue at the outermost part of S1 neighboring the ray parenchyma was also observed earlier than that not neighboring the ray parenchyma.

Figure 33 shows the tracheids from the S2 formation to the S3 formation stage. The lignin residues at the intercellular layer and the outermost part of S1 had an appreciable density. The primary wall was gradually filled up with the lignin residue. The lignin residue at the secondary wall was spreaded toward the lumen of tracheid, lagging behind the cell wall thickening. At this time, the lignin residue at the outer portion of S1 was much more dense than that at the inner portion of S1 (Figure 34).

Figure 35 shows the tracheids at the S3 formation stage. The lignin residue at the secondary wall was continuously spreaded toward the lumen, and reached to the lumen surface of the cell wall. At this time, the outer portion of the secondary wall

showed a high density of the lignin residue. When the secondary wall lignification was completed, the secondary wall showed a uniform density of the lignin residue, though the warty layer had slightly more dense lignin residue than the secondary wall(Figure 36).

3.3 Discussion

The lignification of the differentiating xylem was investigated by means of UV-microscopy, TEM adapting to the observation oflignin skeleton of differentiating tracheids, and LM-autoradiography to detect the incorporated tritiated phenylalanine. These methods have both advantage and disadvantage in order to investigate the lignin accumulation. UV-microscopy has an advantage for quantitative determination of lignin by measuring the silver density of UV-photo negatives, although it has low resolving power. In addition, the result of Figure 29 suggests that the detection of lignin by UV-microscopy is not possible when the lignin concentration is low. TEM adapting to the observation of lignin skeleton of the differentiating tracheid has a great advantage to observe closely the lignin accumulation because of the high resolving power. However, it is not possible to determine the amount of lignin from the silver density of TEM-negatives. In order to know the sites of lignin accumulation by these two methods, it is necessary to compare the UV-absorption or the lignin residue of the two adjacent tracheids in the same radial file. On the other hand, the site, where the lignin accumulation takes place, can be detected by means of LM-autoradiography. In addition, when the labeled lignin precursor is effectively incorporated into the cell wall, it is expected to detect sensitively the site of lignin accumulation. The resolving power of

LM-autoradiography is, however, slightly lower than that of UV-microscopy. Therefore, the lignification process is discussed by combining the advantages of these three methods.

Lignin accumulation is initiated at the outer surface of the primary wall of the cell corner in the tracheid just before S1 formation or beginning S1 formation. Wardrop (1957) and Imagawa (1976) reported that the lignin accumulation at the cell corner occurs lagging behind the S1 formation. The difference between their results and the result obtained in this study is probably derived from the low sensitivity of UV-microscopy shown in Figure 29. Lignification at the outer surface of the primary wall gradually proceeds with the cell wall maturation. Lignin is also filled up step by step in the intercellular space with the tracheid maturation. Lignification of the outer surface of the primary wall and the intercellular space is probably finished at the early part of S2 formation. When the intercellular space is relatively wide, a mass of lignin is produced. Lignification of the intercellular layer and the outermost part of S1 is initiated at the cell corner in the S1 formation stage and gradually proceeds to the unlignified intercellular layer and the outermost part of S1, respectively. The lignin spreads at the whole of the intercellular layer and the outermost part of S1. The lignification of P is initiated in the tracheid beginning S2 formation. The lignification of I, P and the outermost part of S1 proceed during the S2 formation stage and cease at the S3 formation stage. When

the tracheid comes into contact with the ray parenchyma, the outer surface of the primary wall, intercellular space, and the outermost part of S1 are lignified earlier in ray parenchyma side than in the opposite side.

Lignification of the secondary wall is initiated at the outermost part of S1 and gradually proceeds toward the lumen. The amount of lignin accumulated to the secondary wall during the S2 formation stage is relatively small. In the tracheids after the S3 formation stage, lignin accumulation actively occurs all over the secondary wall. At this time, the lignin precursor is continuously supplied to all over the secondary wall, and the amount of lignin in the secondary wall is gradually increased by the repeated linking of the monolignol radicals.

Sarkanen(1971) suggested that "bulk-polymer" is produced by one time addition of the monolignol in peroxidase solution, whereas "endwise polymer" is produced by a slow time addition of the monolignol in the enzyme solution. On the basis of his hypothesis and the results in Figure 27, the characteristics of lignin are discussed. In lignification of the compound middle lamella, the lignin precursor is rapidly supplied and the mono-radicals are concentrated in the narrow space. As the condition resembles that of "one time addition of the monolignol", a bulk polymer could be formed in the compound middle lamella. On the other hand, the supply of lignin precursor into the secondary walls might be slower than that into the compound middle lamella,

and the lignin precursors diffuse all over the secondary wall, especially at the tracheids just after the S3 formation. Thus, lignification of secondary wall may proceed at the condition of "slow time addition of monolignol" to lead end-wise polymer.

3.4 SUMMARY

The lignification process of tracheid wall was investigated by UV-microscopy, LM-autoradiography and TEM. The properties of lignin of the compound middle lamella and the secondary wall were discussed on the basis of the results of LM-autoradiography.

Lignification was initiated at the outer surface of the primary wall of the cell corner in the tracheid just before S1 formation or beginning S1 formation. Lignin was filled up step by step in the intercellular space with the tracheid maturation. Lignification of the intercellular layer and the outermost part of S1 was initiated at the cell corner in the S1 formation stage, and gradually proceeded to the unlignified intercellular layer and outermost part of S1, respectively. The lignification of P was initiated in the tracheid beginning S2 formation. When the tracheid came into contact with the ray parenchyma, the outer surface of the primary wall, intercellular space, and the outermost part of S1 in ray parenchyma side were lignified earlier than those in the opposite side. Lignification of the secondary wall was initiated at the outmost part of S1 and gradually pro-

ceeded toward the lumen. In the tracheids after the S3 formation stage, lignin accumulation actively occurred all over the secondary wall.

The compound middle lamella lignin might probably be rich in "bulk polymer", whereas the secondary wall lignin "end-wise polymer".

CHAPTER IV

Cell organella involved in biosynthesis of cell wall constituents

The main components of cell wall is cellulose, hemicelluloses and lignin.

It has been accepted that "terminal complex" or "rossete" on the plasma-membrane is the site of cellulose synthesis. It is, however, still open to speculation how the precursor of cellulose is synthesized and transported to the site of synthesis. There are few investigation on the cellulose synthesis in woody plants.

Pickett-Heaps (1968b) and Wooding (1968) suggested that the Golgi-bodies and derived vesicles are involved in biosynthesis and/or transport of polysaccharides (probably hemicelluloses and pectins). Some workers suggested that the ER play an important role in biosynthesis of polysaccharides. The site of hemicellulose synthesis is not elucidated well as in cellulose synthesis, and further investigation on the site of hemicellulose synthesis is needed.

Only a few workers (Pickett-Heaps, 1968a; Wardrop, 1976; Fujita and co-worker, 1979) investigated the cell organella involved in lignin biosynthesis. However, these investigation are still incomplete.

In this chapter, the cell organelle involved in biosynthe-

sis of each cell wall constituents are elucidated by TEM-autoradiography and cytochemical staining(Takabe and co-workers, 1984).

4.1 Materials and methods

4.1.1 Preparation of plant materials

Seven- or eight-year old of cryptomeria (Cryptomeria Japonica D.Don), grown at Kyoto Experimental Nursery of Kyoto University Forest, was used. After the internode was taken from the stem, 130 μCi of tritiated glucose(specific activity, 38 Ci/mmol: concentration, 1.0 mCi/ml, Amersham International plc.) was administered for 4 hours according to the method mentioned in 2.1. 2.1. After administration, the specimen blocks were made, and embedded in epoxy resin according to the method mentioned in 3.1.1.

The specimen blocks made in 3.1.1 were used to investigate the cell organella participating in lignin biosynthesis.

The specimen blocks, in which the cell organella were well preserved, was chosen, and used for the PATAg test.

4.1.2 TEM-autoradiography

Ultra-thin sections were cut on a LKB-ultramicrotome with a diamond knife from the specimen blocks, which were administered with tritiated glucose or phenylalanine, and mounted on 150 mesh collodione-coated Cu-grid. They were stained in 2% uranyl acetate, covered with 5.0 nm thick carbon film, and coated with Sakura NR-H2 emulsion by a loop method or touching method. The grids were stored in a refrigerator for 1 to 7 months, developed with D-19 (19 °C, 3.5 min.) and fixed with F-5 (19 °C, 10 min.). The sections were post-stained for 2 minutes in Reynolds' lead

citrate, and examined in a JEM-7 electron microscope at 80 KV.

4.1.3 PATAg staining

Ultra-thin sections were cut on a LKB-ultramicrotome with a diamond knife, and mounted on 100 mesh Au-grids. PATAg-staining was carried out essentially by the method of Thiéry and co-workers(1967). In this case, the sections were oxidized with 1% periodic acid for 2.5-5 hours.

4.2 Results

4.2.1 TEM-autoradiography of the specimen administered with tritiated glucose

Figure 37 shows the autoradiograph of the tracheids in the S1 formation stage. Silver grains were distributed on the compound middle lamella, and S1. They also located on the boundary between the cell wall and the cytoplasm. A part of them was probably located on the lumen surface of the cell wall, and the other was located on the plasma-membrane. Silver grains were also observed on the Golgi-bodies.

Figures 38 and 39 show the autoradiographs in the early part of the S2 formation. Silver grains were also distributed on the compound middle lamella, S1, S2, boundary between the cell wall and the cytoplasm, and the Golgi-bodies.

Figures 40, 41, 42 and 43 show the autoradiographs in the middle and final parts of S2 formation. The silver grains on the cell wall were distributed on the boundary between the cell wall and the cytoplasm. They also distributed on the ERs and the Golgi-bodies. Especially, strong radioactivity was sometimes observed locally on the ERs.

In the S3 formation stage, the silver grains were distributed all over the secondary wall. The cell organella participating in the cell wall formation could not be observed because

of the poor cytoplasm(Figure 44).

In the tracheids just after the S3 formation stage, the vesicles were fused to the plasma-membrane. The silver grains were distributed on the secondary wall and the vesicles(Figure 45).

Figures 46, 47 and 48 show the autoradiographs of the tracheids, which were forming the borderd pit. In all stages of pit formation, numerous silver grains were distributed on the tips of the developing pit border. The periphery of the pit was relatively rich in the cytoplasm, in which the Golgi-bodies secreted many vesicles. Silver grains were distributed on the Golgi-bodies and vesicles.

4.2.2 TEM-autoradiography of the specimen administered with tritiated phenylalanine

Figures 49 and 50 show TEM-autoradiographs of the differentiating xylem of cryptomeria administered with tritiated phenylalanine for 1 hour. From the S1 formation stage to the early part of S2 formation stage, the silver grains were observed on the cell corners and the compound middle lamella. They were also observed on the Golgi-bodies, Golgi-vesicles, and r-ERs. After S3 formation stage, little silver grains were located on the secondary walls, although a little of those were located on the Golgi-vesicles.

Figures 51, 52, 53 and 54 show the TEM-autoradiographs of

the differentiating xylem administered with tritiated phenylalanine for 2 hours. From the final part of primary wall formation stage to the early part of S1 formation stage, a large amount of Golgi-bodies and Golgi-vesicles were observed. The silver grains were located on those and cell corners (Fig. 51). From the later part of S1 formation to the middle part of S2 formation stage, the silver grains were located obviously on the cell corners, and subsequently on the compound middle lamella and S1. At these stages, many vesicles secreted from the Golgi-bodies were observed. The silver grains were also located on these vesicles and r-ERs(Fig. 52). After these stages, a little silver grains were distributed on S1 and the outer part of S2. In the several tracheids just after the S3 formation stage, a large amount of irregularly swollen smooth-ERs appeared in the cytoplasm, and a part of them fused to the plasma membrane. The Golgi-bodies and their vesicles also were observed in the cytoplasm. At this stage, the silver grains were conspicuously located on the irregularly swollen smooth-ERs, Golgi-bodies, Golgi-vesicles, and secondary walls, although little was observed on the compound middle lamella (Figs. 53 and 54).

Figures 55, 56 and 57 show TEM-autoradiographs of the differentiating xylem administered with tritiated phenylalanine for 4 hours. The distribution of the silver grains on the cell walls and the cell organella in the specimen was almost the same as that in the specimen administered for 2 hours. In the cells

numbered 15-25, obvious silver grains were located on the secondary walls, whereas the cell organella could not be observed due to insufficient fixation of cytoplasm.

4.2.3 The differentiating xylem stained with PATAg

Figure 58 shows the tracheids in the primary wall formation stage. The primary wall was heavily stained with silver proteinate. Outer leaflet of plasma membrane was also stained. The Golgi-bodies secreted relatively small vesicles, which contained the materials stained weakly with silver proteinate. The granular materials, which were positively stained, existed in the narrow space between the plasma membrane and the primary wall.

Figure 59 shows the tracheid just before the S1 formation. Numerous Golgi-bodies appeared in the cytoplasm, and secreted many vesicles. The materials positively stained with silver proteinate were contained in the Golgi-vesicles.

Figures 60 and 61 show the tracheids in the S1 formation stage. The materials, which were heavily stained with silver proteinate, were distributed in the cytoplasm. These materials were ordinarily existed in the tracheids between S1 and S2 formation stages. The cell walls and the Golgi-vesicles were stained positively. Small circular vesicles, which were sometimes distributed near the ER or between the ER-cisternae, were also stained weakly with silver proteinate. Figures 62 and 63 show the tra-

cheids in the S2 formation stage. The contents in the Golgi-vesicles and the materials existed between the cell wall and the plasma membrane were positively stained. It was noteworthy that the tubular inclusions, which also were stained positively with silver proteinate, were observed between the cell wall and the plasma membrane in this stage.

Figures 64 and 65 show the tracheids in the S3 formation stage. The fibrillar materials were seen to be generated from the plasma membrane. Many irregularly swollen s-ERs appeared in the cytoplasm, and the Golgi-bodies secreted vesicles, in which the positively stained materials were contained.

Figures 66 and 67 show the tracheid, which is just after the S3 formation. The cytoplasm was filled with many irregularly swollen s-ERs, and vesicles, which were probably derived from the Golgi-body. The latter was stained positively with silver proteinate, though the former was unstained. Inner surface of the cell wall and warts were heavily stained with silver proteinate.

In the control section, the cell walls, plasma membrane, starch in the plastid, and the Golgi vesicles were not stained with silver proteinate.

4.3 Discussion

The result that almost all of the silver grains were distributed on the boundary between the cell wall and the cytoplasm in the tracheid actively deposited cellulose, and the result shown in Figure 64 suggest that cellulose is synthesized at the plasma membrane or the periplasmic space. It is interesting that the tubular inclusions are observed between the plasma membrane and the inner surface of the cell wall. The role of the tubular inclusion will be elucidated in the near future.

The results in Figures 58, 59, 61, 62 and 65 suggest that the Golgi-body is involved in biosynthesis and/or transport of polysaccharides. It is interesting that the Golgi-vesicles exhibit the three types of staining reaction. Figures 58, 61 and 65 obviously show the difference of staining intensity and pattern among the Golgi-vesicles existed in the different formation stages. These difference may be reflected from the different contents in the Golgi-vesicles. That is, the main contents in the primary wall formation stage probably consist of the pectins and the primary wall-hemicelluloses. The contents in the S1 and S2 formation stages are the secondary wall-hemicelluloses, namely xylan and mannans. In addition, these hemicelluloses seem to be relatively highly-polymerized, because the staining materials show the fibrillar structure. The contents in the Golgi-vesicle after S3 formation stage may also be hemicelluloses. The result

that the inner surface of the developing cell wall and warts were heavily stained from the cell of S3 formation stage to the cell just after the S3 formation suggests that the hemicellulose deposition actively occurs in these stages. The result that the Golgi-cisternae are unstained suggests that the Golgi-cisternae contain water or ethanol soluble materials, namely oligosaccharides and/or hemicellulose precursors. They probably diffuse in the solution during the embedding procedure.

The small circular vesicles were always distributed near the ER and between the ER-cisternae. As the size and the shape of these vesicles are evidently different from those of the Golgi-vesicles, the small circular vesicle is possibly derived from the ER. Both the result that the small circular vesicles were stained positively, and the one shown in Figure 41 suggest that the ER is also involved in biosynthesis and transport of polysaccharides.

The heavily stained materials existed in the cytoplasm during the secondary wall formation is probably mass of glycoprotein or glycolipid.

Figures 49, 50, 51, 52, 53, 54, 55 and 56 suggest that cell organella participating in lignin biosynthesis are the Golgi-body, r-ER, and irregularly swollen s-ER. It is generally accepted that r-ER synthesizes proteins, so that a part of phenylalanine is possibly used as a source in protein synthesis. The role of r-ER in lignin biosynthesis will be elucidated in the

near furture. On the other hand, the Golgi-bodies secreted many vesicles just before and at the active lignification stages of the compound middle lamella and the secondary walls. Administered phenylalanine is probably transported directly to the Golgi-bodies or transported from certain organella to the Golgi-bodies, and converted to a lignin precursor, which is just before polymerization. Then, the lignin precursor may be secreted into cell walls by exocytosis of the Golgi-vesicles. In addition, irregularly swollen s-ERs appear in the cytoplasm at the cells of S3 formation. The phenylalanine is involved in s-ERs and processed. The derivative from phenylalanine may be secreted into the cell walls by fusing irregularly swollen s-ERs to the plasma membrane. The relationship between the Golgi-body and irregularly swollen s-ER was not able to elucidated in this study. The lignin precursor secreted by the Golgi-vesicles and/or irregularly swollen s-ERs is dehydrogenated by peroxidase, which is present in the cell walls, and polymerized. Phenylalanine is probably incorporated into the lignin of compound middle lamella within one hour. Whereas, it takes at least two hours to be incorporated into the lignin of secondary walls.

4.4 SUMMARY

The cell organelle involved in biosynthesis of cellulose, hemicelluloses and lignin were investigated by TEM-autoradiography and cytochemical staining.

When tritiated glucose was administered, the silver grains were abundantly distributed on the plasma membrane and/or the inner surface of the developing cell wall in the tracheids actively depositing cellulose. The fibrillar materials were generated from the plasma membrane. These results suggest that cellulose is synthesized at the plasma membrane or periplasmic zone.

The result that the contents of the Golgi-vesicles were stained positively by PATAg test suggests that the Golgi-vesicle is involved in biosynthesis and/or transport of polysaccharides. The vesicles probably derived from ER also were stained positively by PATAg test. In addition, the strong radioactivity was sometimes observed on the ERs, when the tritiated glucose was administered. These results suggest that the ER is also involved in biosynthesis and/or transport of polysaccharides.

When tritiated phenylalanine was administered, the silver grains were distributed on the Golgi-bodies, Golgi-vesicles, r-ERs and irregularly swollen s-ERs. These results suggest that the Golgi-body and irregularly swollen s-ER are involved in biosynthesis and/or transport of lignin precursor. It is generally accepted that phenylalanine is a protein precursor as well as a

lignin precursor, and that the protein is produced in the r-ER. Hence, a part of the radioactivity on the r-ER is due to the protein. The role of the r-ER in biosynthesis of lignin precursor will be elucidated by me in the near future.

CONCLUSION

The deposition process and the depositing manner of cell wall components, the distribution of the components across the cell wall, and the cell organelle involved in biosynthesis of of cell wall components were investigated by several chemical analyses and microscopic observation.

The deposition process and the depositing manner of polysaccharides were investigated by GLC of sugar residues, chemical analysis using the radioactive precursor, and LM-autoradiography coupled with chemical analysis. The distribution of polysaccharides across the cell wall was discussed on the results of the deposition process and the depositing manner of polysaccharides. The deposition process of cellulose was found to be different from those of hemicelluloses. Cellulose deposited between the S1 and S3 stage, and abundant deposition especially occurred in the middle part of S2 formation stage. Cellulose was supplied to the developing cell wall by apposition. Xylan deposition was active between the later part of S1 stage and the beginning part of S2 stage, and between the final part of S2 stage and S3 stage. Mannans deposited abundantly between the later part of S1 stage and the beginning part of S2 stage, and between the final part of S2 stage and S3 stage. It was noticed that mannans continued to deposit in a few tracheids after the completion of S3 formation. Main chains of xylan and mannans were also supplied to the wall

by apposition. On the other hand, arabinose and galactose, which are the components of side branches of xylan and mannans respectively, were supplied to the pre-existing cell wall by intussusception. S1, outer part of S2 and S3 were rich in hemicelluloses, whereas the middle part of S2 was rich in cellulose.

The lignification process of the tracheid wall was investigated by UV-microscopy, LM-autoradiography using the tritiated lignin precursor, and TEM adapted to observation of the lignin skeleton of differentiating tracheids. Properties of the compound middle lamella lignin and those of the secondary wall lignin were discussed based on the results of LM-autoradiography. Lignification was initiated at the outer surface of the primary wall of the cell corner in the tracheid just before S1 formation or the tracheid at the beginning S1 formation. Lignin was filled up step by step in the intercellular space with the tracheid maturation. Lignification of the intercellular layer and the outermost part of S1 was initiated at the cell corner in the S1 formation stage, and gradually proceeded to the unlignified intercellular layer and outermost part of S1, respectively. The lignification of the primary wall was initiated in the tracheid beginning S2 formation. When the tracheid came to contact with the ray parenchyma, the outer surface of the primary wall, intercellular space, and the outermost part of S1 were lignified earlier in ray parenchyma side than in the opposite side. Lignification of the secondary wall was started from the outermost

part of S1 and gradually proceeded toward the lumen. In the tracheids after the S3 formation stage, lignin accumulation actively occurred all over the secondary wall. The compound middle lamella lignin was supposed to be rich in "bulk polymer", whereas the secondary wall lignin rich in "end-wise polymer".

The cell organelle involved in biosynthesis of cellulose, hemicelluloses and lignin were investigated by TEM-autoradiography and cytochemical staining. When tritiated glucose was administered, the silver grains were abundantly distributed on the plasma membrane and/or the inner surface of the developing cell wall in the tracheids actively depositing cellulose. The fibrillar materials were generated from the plasma membrane. These results suggest that cellulose is synthesized at the plasma membrane or periplasmic zone. The result that the contents of the Golgi-vesicles were stained positively by PATAg test suggest the involvement of the Golgi-vesicle in biosynthesis and/or transport of polysaccharides. The vesicles, probably derived from ER, were also stained positively by PATAg test. The strong radioactivity was sometimes observed on the ERs, when the tritiated glucose was administered. These results suggest that the ER is also involved in biosynthesis and/or transport of polysaccharides. When tritiated phenylalanine was administered, the silver grains were distributed on the Golgi-bodies, Golgi-vesicles, r-ERs and irregularly swollen s-ERs. These results suggest that the Golgi-body and irregularly swollen s-ER are involved in biosynthesis

and/or transport of lignin precursor. It is generally known that phenylalanine is a protein precursor as well as a lignin precursor, and that the protein is produced in the r-ER. Therefore, a part of the radioactivity on the r-ER is probably derived from protein. The role of the r-ER in biosynthesis of lignin precursor will be elucidated in the near future.

ACKNOWLEDGEMENT

The present study has been carried out both in Laboratory of Wood Structure (Department of Wood Science and Technology, Faculty of Agriculture, Kyoto University) and in Laboratory of Radiobiochemistry (Research Institute for Food Science, Kyoto University).

The author wishes to express his sincere thanks to Professor Hiroshi Harada, Department of Wood Science and Technology, Faculty of Agriculture, Kyoto University, for his kind guidance and encouragement during the course of this study.

The author also wishes to express his thanks to Professor Takayoshi Higuchi, Wood Research Institute, Kyoto University, and Professor Zenzaburo Kasai, Research Institute for Food Science, Kyoto University, for their valuable suggestions and critical readings of the manuscript.

The author greatly appreciates to Dr. Masahiro Ogawa(Research Institute for Food Science, Kyoto University) and Dr. Kunisuke Tanaka (Faculty of Agriculture, Kyoto Prefectual University) for their kind help in dealing with the radioactive chemicals and their valuable suggestions on TLC analysis. The author also greatly appreciates to Dr. Tetsuya Suzuki and Dr. Hiroshi Murakami (Research Institute for Food Science, Kyoto University) for providing the GLC analyses, and to Dr. Eiichi Maekawa (Wood Research Institute, Kyoto University) for his

valuable suggestions on GLC analysis.

The author thanks Dr. Keizo Okamura (Faculty of Agriculture, Kyoto University) for his critical reading of the manuscript.

Finally, the author wishes to express his thanks to Associate Professor Hiroshi Saiki, Mr. Tadashi Nobuchi, Dr. Minoru Fujita and other members of Laboratory of Wood Structure, Department of Wood Science and Technology, Kyoto University, for their valuable discussions and assistance during the course of this study.

REFERENCES

Côté, Jr., W. A., N. P. Kutscha, B. W. Simon and T. E. Timell (1968), Tappi 51, 33

Fergus, B. J., A. R. Procter, J. A. N. Scott and D. A. I. Goring (1969), Wood Sci. Tecnol. 3, 117

Fowke, L. C. and J. D. Pickett-Heaps (1972), Protoplasma 74, 19

Fujii, T., H. Harada and H. Saiki (1981), Mokuzai Gakkaishi 27, 149

Fujita, M. and H. Harada (1978), Mokuzai Gakkaishi 24, 435

Fujita, M. and H. Harada (1979), Mokuzai Gakkaishi 25, 89

Fujita, M., H. Saiki and H. Harada (1978), Mokuzai Gakkaishi 24, 158

Fujita, M., K. Takabe and H. Harada (1981) Mokuzai Gakkaishi 27, 337

Gawlick, S. R. and W. F. Millington (1969), Amer. J. Bot. 56, 1084

Giddings, Jr., T. H., D. L. Brower and L. A. Staeherin (1980), J. Cell Biol., 84, 327

Hardell, H. and U. Westermark (1981), The Ekman-Days, Vol. 1, 32

Hepler, P. K., D. E. Fosket and E. H. Newcomb (1970), Amer. J. Bot., 57, 85

Imagawa, H., K. Fukazawa, and S. Ishida (1976), Res. Bull. College Exp. Forests. Hokkaido Univ. 33, 127

Iwakawa, J., H. Kobatake, I. Suzuki and H. Kushida (1980), J. Chromatogr. 193, 333

Kiermayer, O. and U. B. Sleytr (1979), Protoplasma 101, 133

Kishi, K., H. Harada and H. Saiki (1982), Bull. Kyoto Univ. Forests 54, 209

Kushida, H., M. Fujita and H. Harada (1979), J. Electron Microsc., 28, 53

Kutscha, N. P. and J. M. Schwarzmann (1975), Holzforschung 29, 79

Larson, P. R. (1969a), Holzforschung 23, 17

Larson, P. R. (1969b), Tappi 52, 2170

Ledbetter, M. C. and K. R. Porter (1963), J. Cell Biol. 19, 239

Mayor, H. D., J. C. Hampton and B. Rosario (1961), J. Cell Biol. 9, 909

Meier, H. (1961) J. Polymer Sci. 51, 11

Meier, H. and K. C. B. Wilkie (1959), Holzforschung 13, 177

Meuller, S. C., R. M. Brown, Jr. and T. K. Scott (1976), Science 194, 949

Meuller, S. C. and R. M. Brown, Jr. (1980), J. Cell Biol. 84, 315

Newcomb, E. H. and H. T. Bonnett, Jr. (1965), J. Cell Biol. 27, 575

Northcote, D. H. and J. D. Pickett-Heaps (1966), Biochem. J. 98, 159

Parameswaren, N. and W. Liese (1982), Holz als Roh- und Werkstoff 40, 145

Ray, P. M. (1967), J. Cell Biol. 35, 659

Preston, R. D. and R. N. Goodman (1968), J. Roy. Microscop. Soc. 88, 513

Preston, R. D. and B. Kuyper (1951), J. Exp. Bot. 2, 247

Preston, R. D., E. Nicolai and B. Kuyper (1953), J. Exp. Bot. 4, 40

Preston, R. D. and G. W. Ripley (1954), Nature (London) 174, 76

Pickett-Heaps, J. D. (1966), Planta 71, 1

Pickett-Heaps, J. D. (1967), Ultrastructure Res. 18, 287

Pickett-Heaps, J. D. (1968a), Protoplasma 65, 181

Pickett-Heaps, J. D. (1968b), J. Cell Sci. 3, 55

Preston, R. D. (1964), in "The formation of wood in forest trees" ed. by M. H. Zimmermann, Academic Press, p169

Robards, A. W. and P. G. Humpherson (1967), Planta 77, 233

Ryser, U. (1979), Protoplasma 98, 223

Saeman, J. E., W. E. Moore and A. Millett (1963), in "Method in Carbohydrate Chemistry, Vol. 3", Academic Press, New York, 1963, p54

Saleh, T. M., L. Leney and K. V. Sarkanen (1967), Holzforschung 21, 116

Saka, S. and R. J. Thomas (1982), Wood Sci. Technol. 16, 1

Saka, S. and R. J. Thomas (1982), Wood Sci. Technol. 16, 167

Saka, S., P. Whiting, K. Fukazawa and D. A. I. Goring (1982), Wood Sci. Technol. 16, 269

Sarkanen, K. V. (1971), in "Lignins" ed. by K. V. Sarkanen and C. H. Ludwig, Wiley-Interscience, p95

Scott, J. A. N., A. R. Procter, B. J. Fergus and D. A. I. Goring (1969), Wood Sci. Technol. 3, 73

Setterfield, G. and S. T. Bayley (1959), Can. J. Bot. 37, 861

Sinner, M., N. Parameswaren and H. H. Dietrichs (1979), in "Hydrolysis of Cellulose: Mechanisms of Enzymatic and Acid Catalysis" ed. by R. D. Brown, Jr and and L. Jurasek, American Chemical Society, Washington D. C., p303

Sinner, M., N. Parameswaren, H. H. Dietrichs and W. Liese (1973) Holzforschung 27, 36

Sinner, M., N. Parameswaren, N. Yamazaki, W. Liese and H. H. Dietrichs (1976), Appl. Polym. Symp. 28, 993

Takabe, K., M. Fujita, H. Harada and H. Saiki (1981), Mokuzai Gakkaishi 27, 249

Takabe, K., M. Fujita, H. Harada and H. Saiki (1981), Mokuzai Gakkaishi 27, 813

Takabe, K., M. Fujita, H. Harada and H. Saiki (1983), Mokuzai Gakkaishi 29, 183

Takabe, K., M. Fujita, H. Harada and H. Saiki (1984), Mokuzai Gakkaishi 30, 103

Takabe, K., M. Fujita, H. Harada and H. Saiki (198?), Mokuzai Gakkaishi 3?, ???

Thiéry, J. (1967), J. Microscopie 6, 987

Wada, M. and L. A. Staehelin (1981), Planta 151, 462

Wardrop, A. B. (1957), Tappi 40, 225

Wardrop, A. B. (1971), in "Lignins" ed. by K. V. Sarkanen and C. H. Ludwig, Wiley-Interscience, p19

Wardrop, A. B. (1976), Appl. Polym. Symp. 28, 1041

Williams, W. T., R. D. Preston and G. W. Ripley (1955), J. Exp. Bot. 6, 451

Willison, J. H. M. and R. M. Brown, Jr. (1978), J. Cell Biol. 77, 103

Wooding, F. B. P. (1968), J. Cell Sci. 3, 71

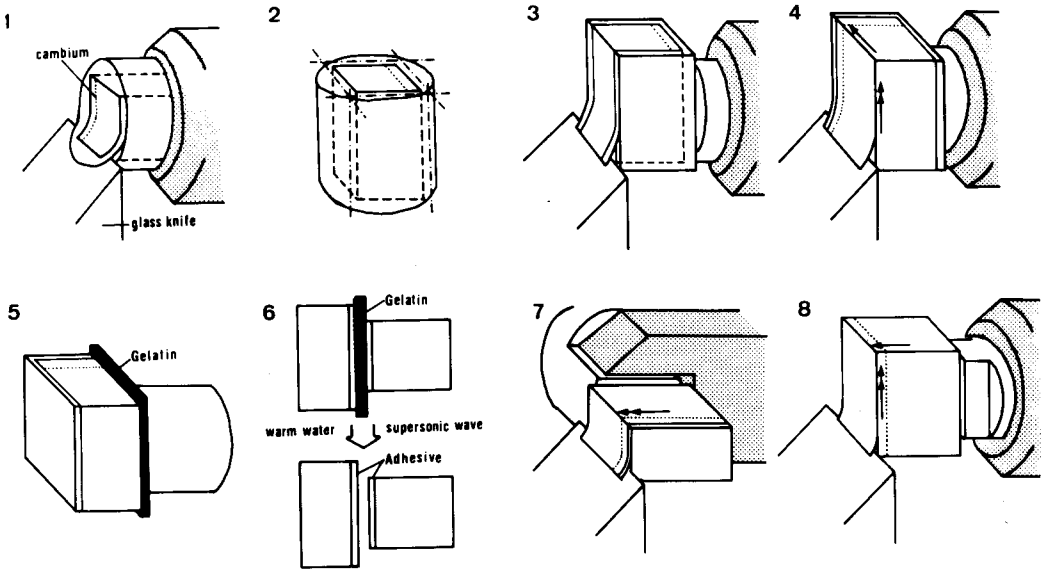

Figure 1 Various steps of slicing accurate transverse, radial and tangential faces. The single arrow shows the direction of radial files of tracheids, and the double arrow shows that of the longitudinal axis of the tracheids.

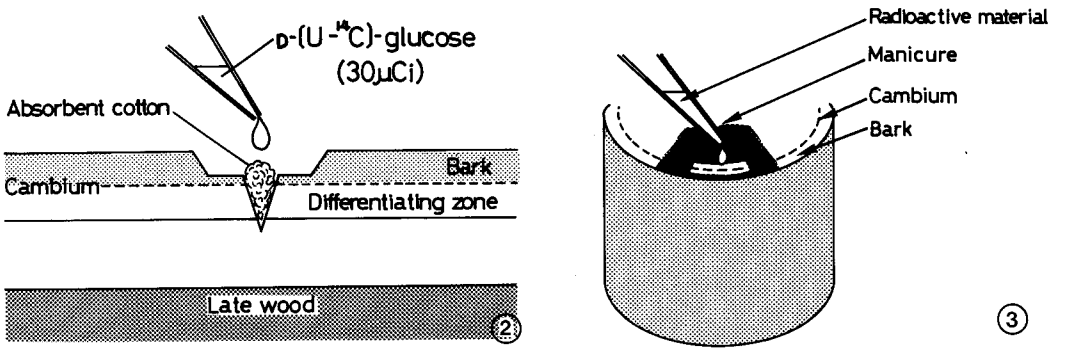

Figures 2 and 3 Administration of precursor.

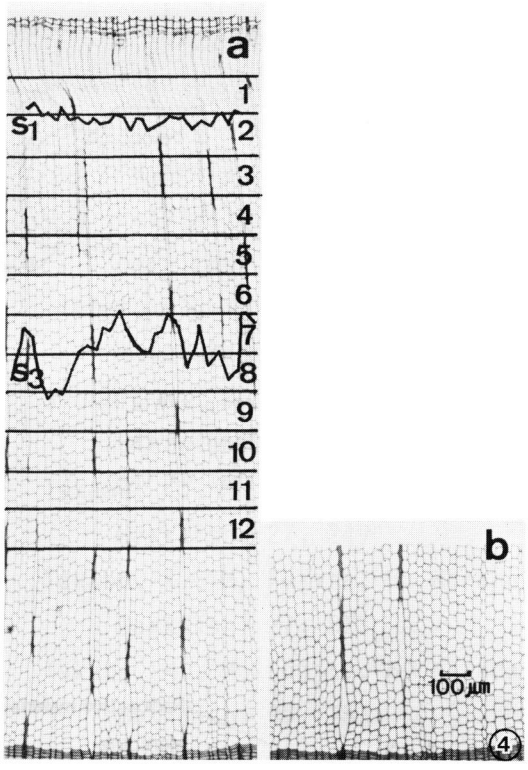

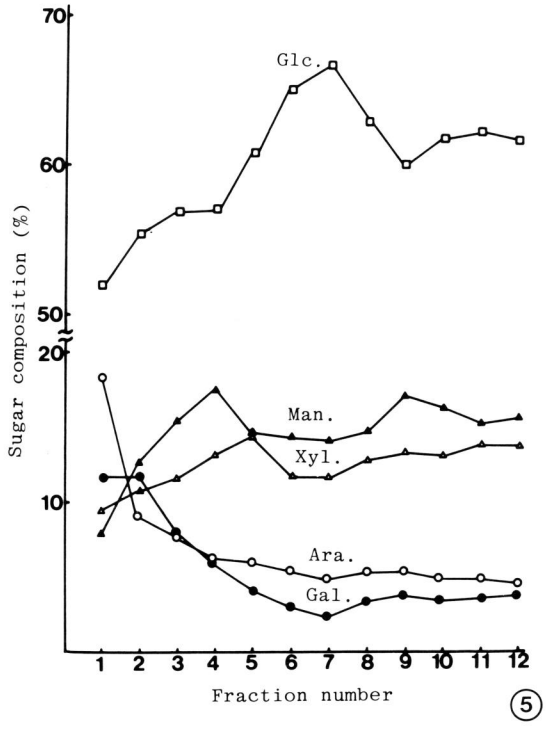

Figure 4 The left photograph shows the transverse section of a specimen block before fractionation, and right photograph the transverse section of a residual specimen block. Arabic numerals indicate the fraction numbers.

Figure 5 Changes in the sugar composition with tracheid maturation. The various components are designated as follows: glucose, □; mannose, ▲; xylose, △; arabinose, ○; and galactose, ●.

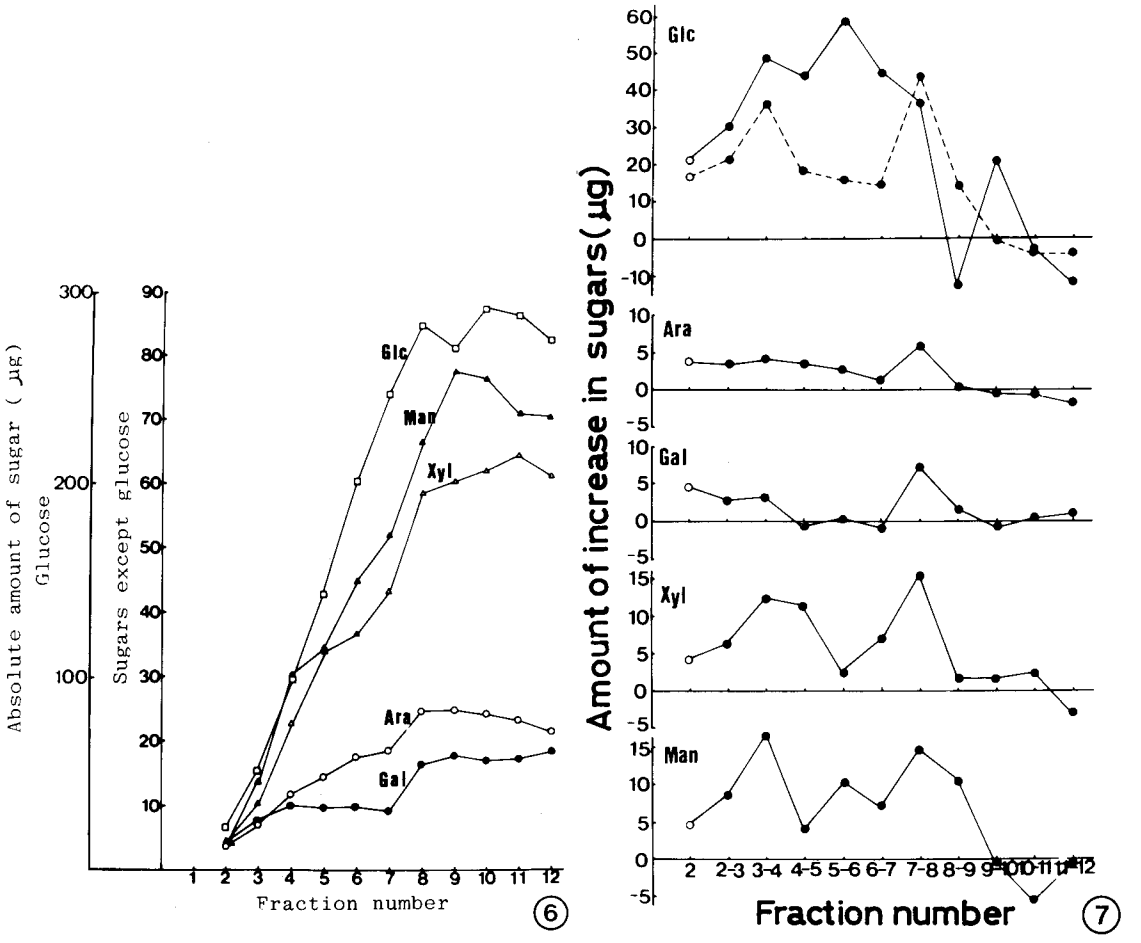

Figure 6 Changes in the amount of sugars with tracheid maturation. Symbols are the same as in Figure 5.

Figure 7 The amount of increase in sugars (the difference of the amounts of sugar between the neighboring fraction). Dashed line shows the sum of arabinose, galactose, xylose and mannose.

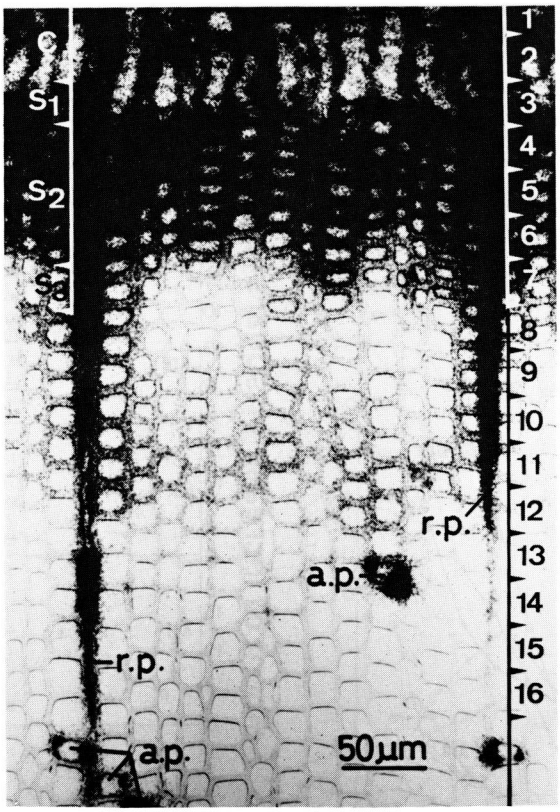

Figure 8 Light microscopic autoradiograph of transverse section of cryptomeria. ^{14}C-glucose was actively incorporated into the differentiating tracheids, ray- and axial-parenchyma cells. Arabic numerals correspond to the fraction numbers shown in Figure 12. C: cambium, S1: S1 deposit stage, S2: S2 deposit stage, S3: S3 deposit stage, a.p.: axial parenchyma cell, r.p.: ray parenchyma cell.

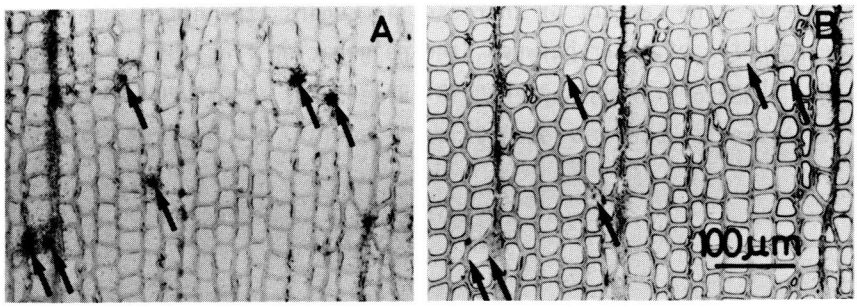

Figure 9 Light microscopic autoradiographs of transverse sections before(A) and after(B) treatment with α-amylase. The radioactivity of the axial parenchyma cell (arrows) was removed completely by the treatment.

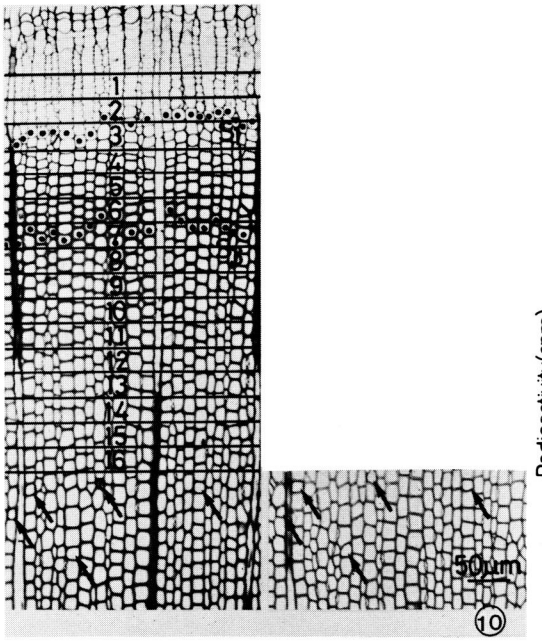

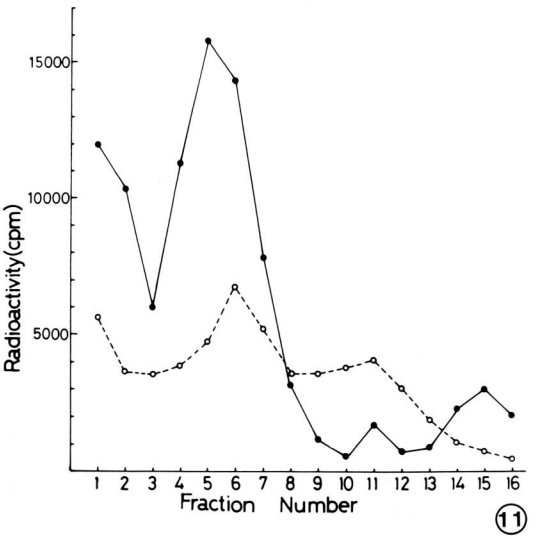

Figure 10 The left photograph shows the transverse section of the specimen block before fractionation, and the right photograph the transverse section of a residual specimen block. The existence of axial parenchyma cells (arrows) makes it easy to compare the transverse sections. Arabic numerals are the fraction numbers.

Figure 11 The radioactivity of hydrolyzates and Klason lignin in each fraction. Symbols are as follows: —●—, hydrolyzate; - -○- -, Klason lignin.

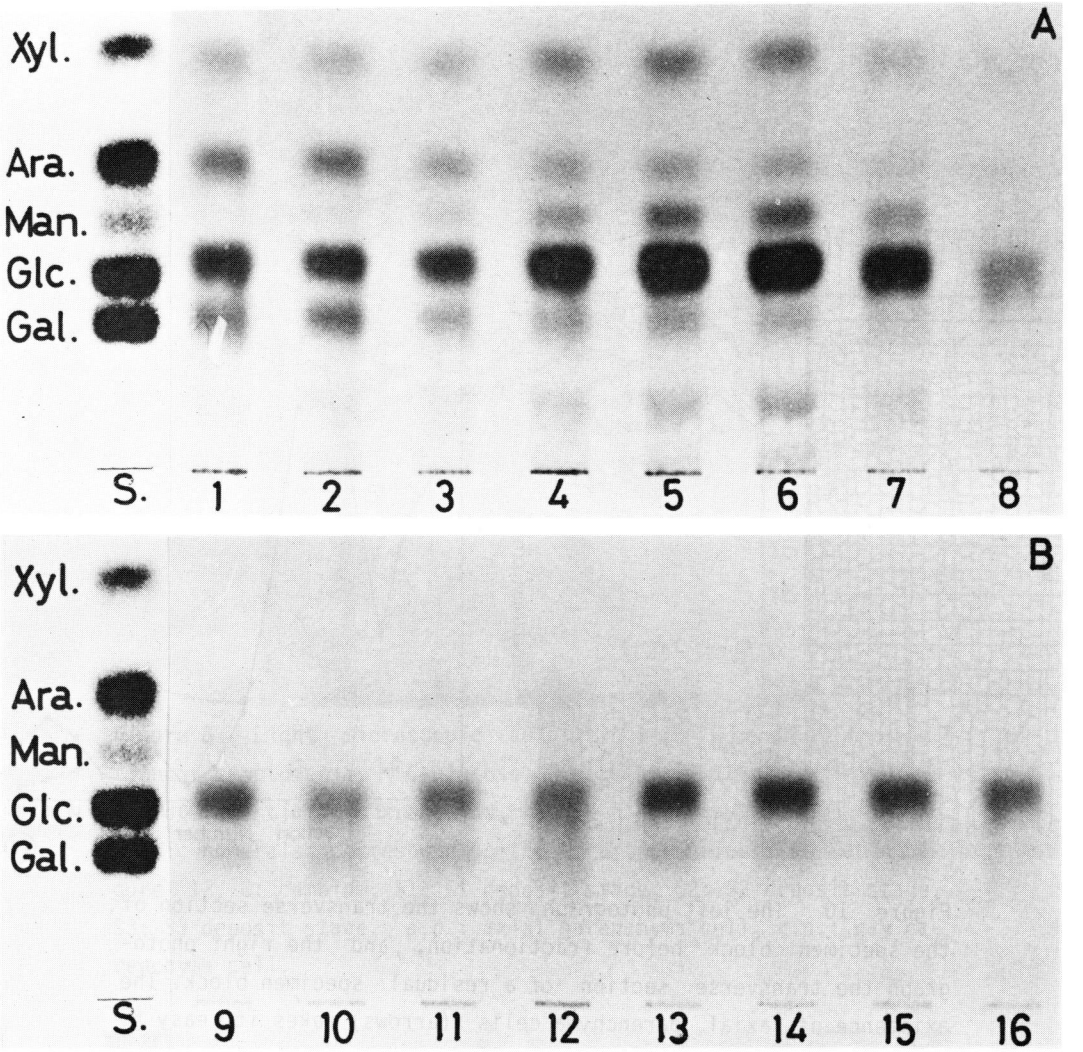

Figure 12 TLC-autoradiographs. Autoradiographs A and B were obtained after 2- and 13-weeks exposures, respectively. S., standard; Xyl., xylose; Ara., arabinose; Man., mannose; Glc., glucose; Gal., galactose. Arabic numerals are the same as in Figure 10.

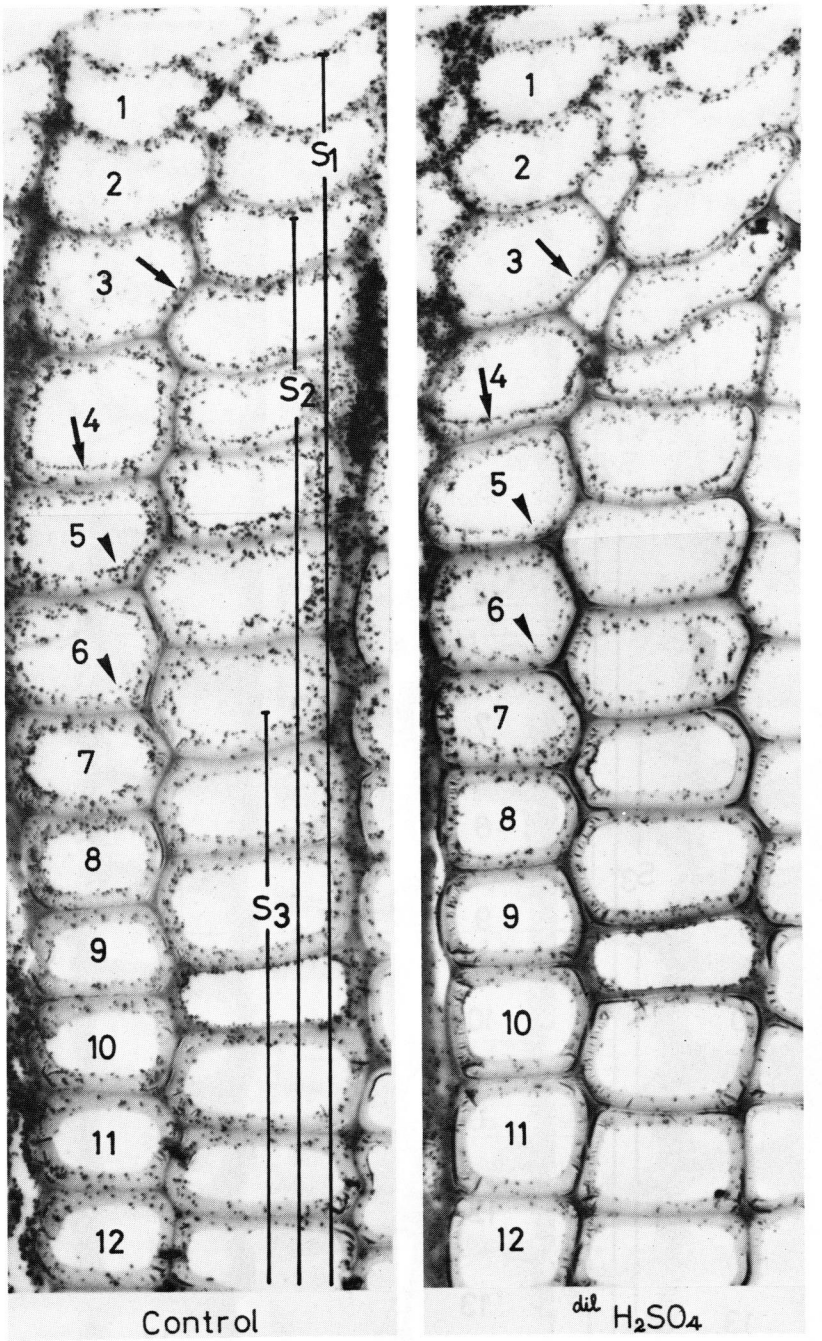

Figure 13 LM-autoradiographs of the control section (left) and the section treated with hot diluted sulfuric acid(right). Cell number is started from the cell just before S1 formation. The radioactivity at the interior of the cell wall were removed by the treatment with hot diluted sulfuric acid (arrow heads), whereas the radioactivity at the inner surface of the cell wall remains (arrows).

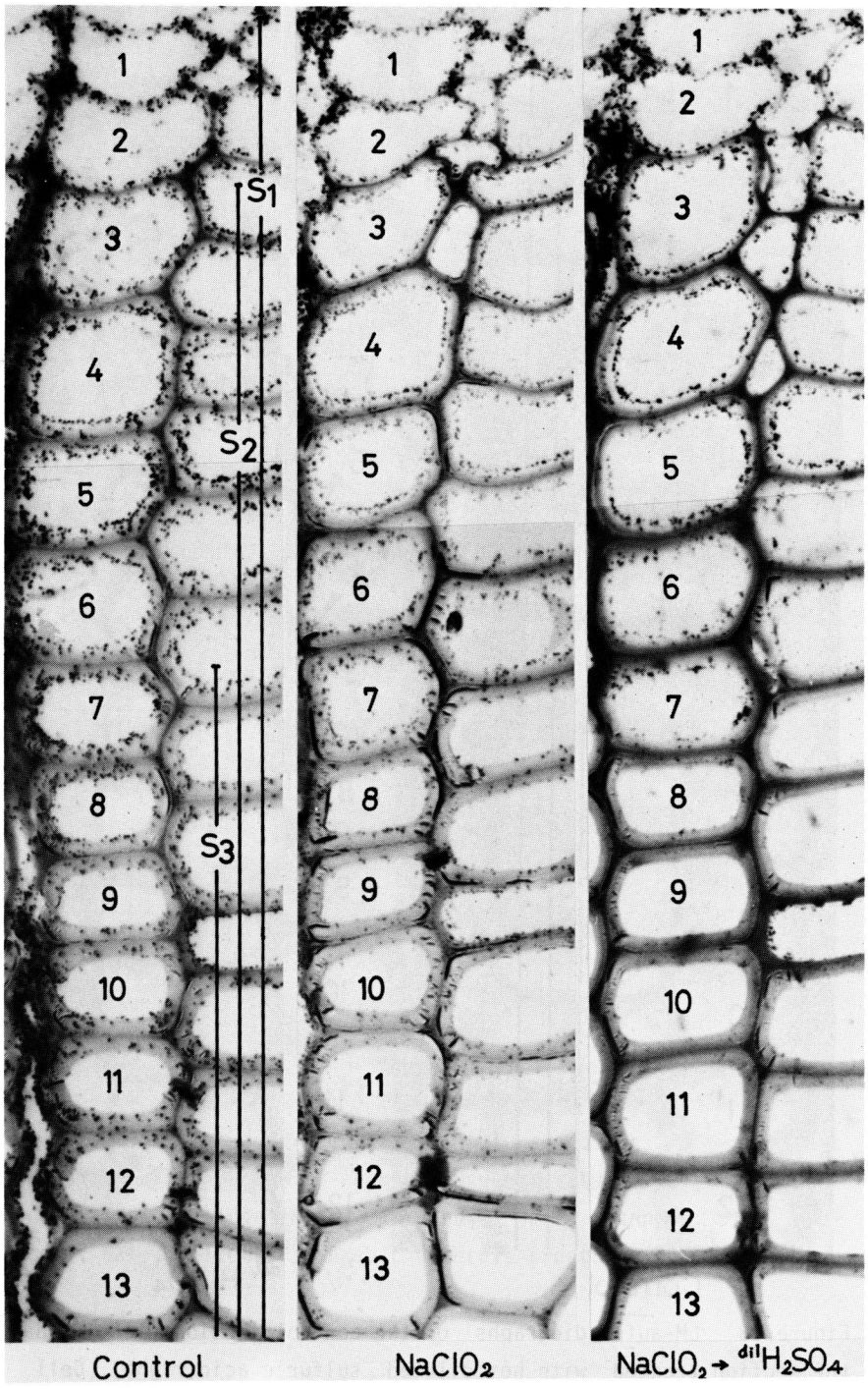

Figure 14 LM-autoradiographs of the control section (left), the section treated with acidified $NaClO_2$ (center) and the section treated with hot diluted sulfuric acid after $NaClO_2$ extraction (right).

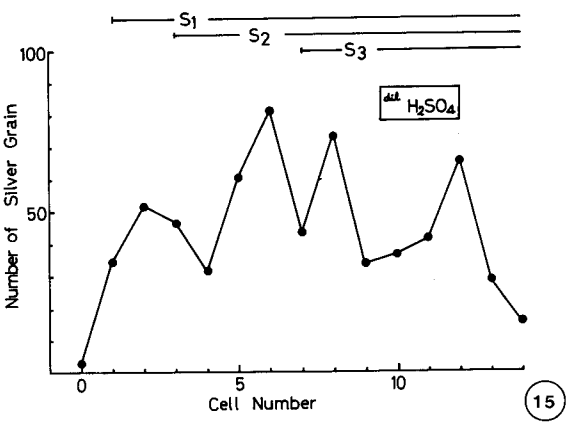

Figure 15 The radioactivity removed by the treatment with hot diluted sulfuric acid. The horizontal axis indicates the cell number and the vertical axis the number of silver grains.

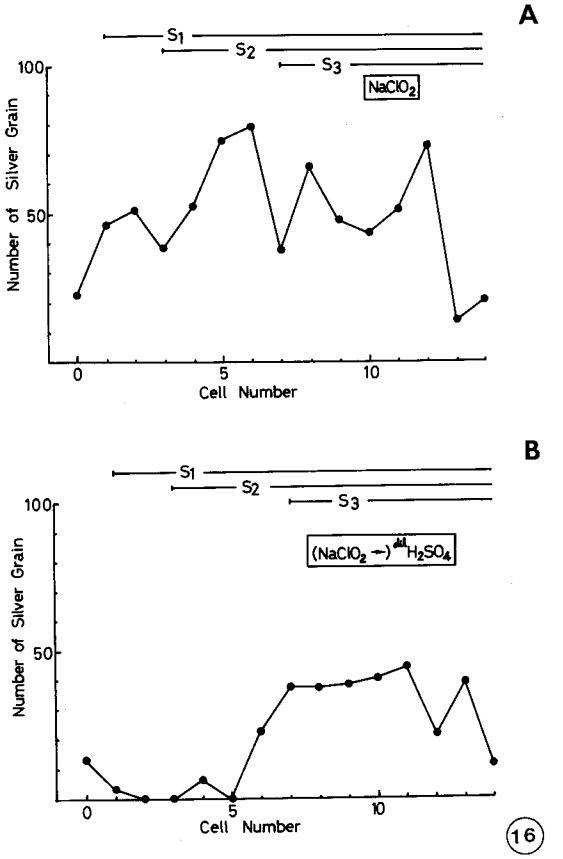

Figure 16 A, The radioactivity removed by the treatment with acidified $NaClO_2$. B, The radioactivity removed by the treatment with hot diluted sulfuric acid after $NaClO_2$ extraction.

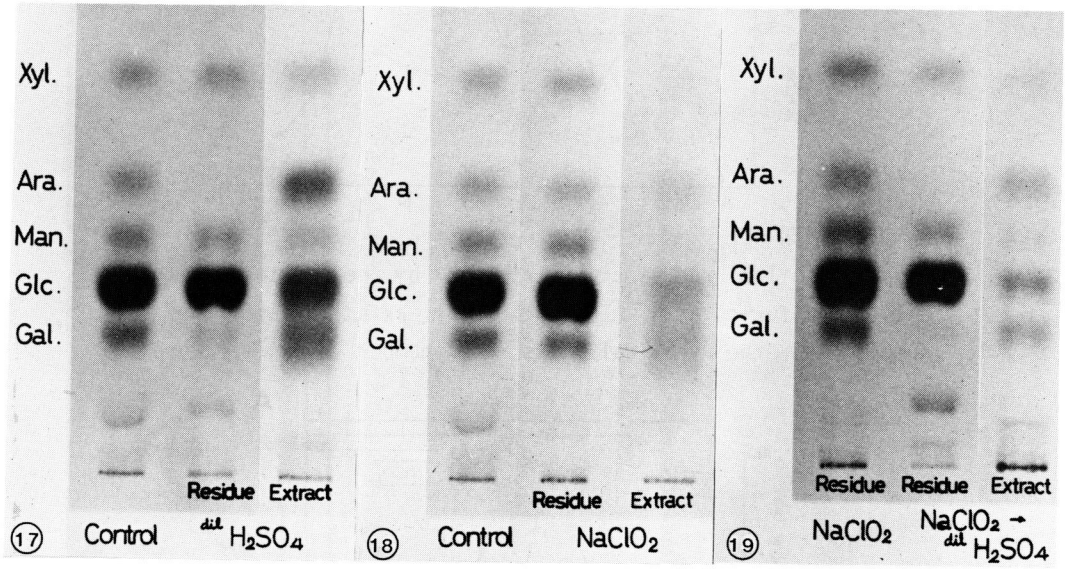

Figure 17 TLC-autoradiograph. Control (left), and the residue (center) and the extracts (right) by the treatment with hot diluted sulfuric acid.

Figure 18 TLC-autoradiograph. Control (left), and the residue (center) and the extracts (right) by the treatment with acidified $NaClO_2$.

Figure 19 TLC-autoradiograph. The residue (left) by the treatment with acidified $NaClO_2$, the residue (center) by the treatment with acidified $NaClO_2$ followed by the treatment with hot diluted sulfuric acid, and the extracts (right) by the treatment with hot diluted sulfuric acid after $NaClO_2$ extraction.

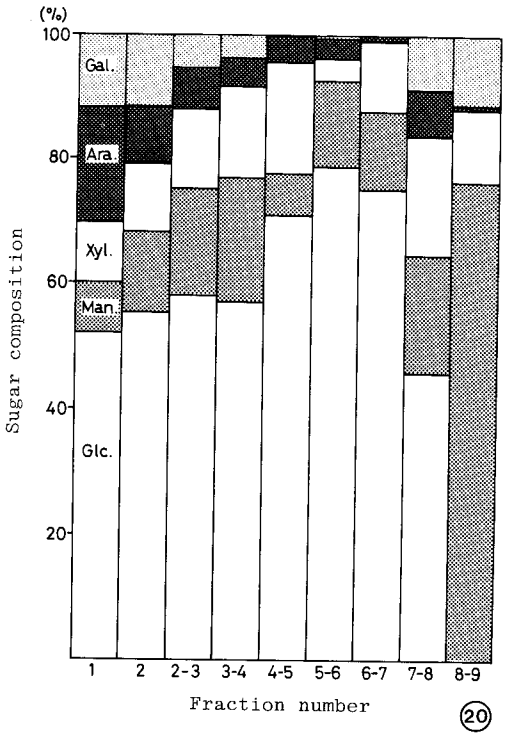

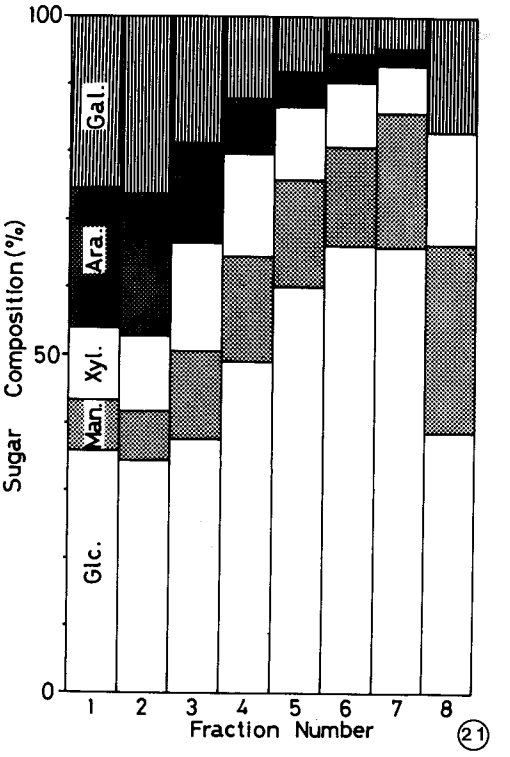

Figure 20 The composition of the amount of increase in neutral sugars. The numbers on the horizontal axis indicate the fraction number and the numbers on the vertical axis the sugar composition.

Figure 21 The composition of radioactive neutral sugars after recalculation.

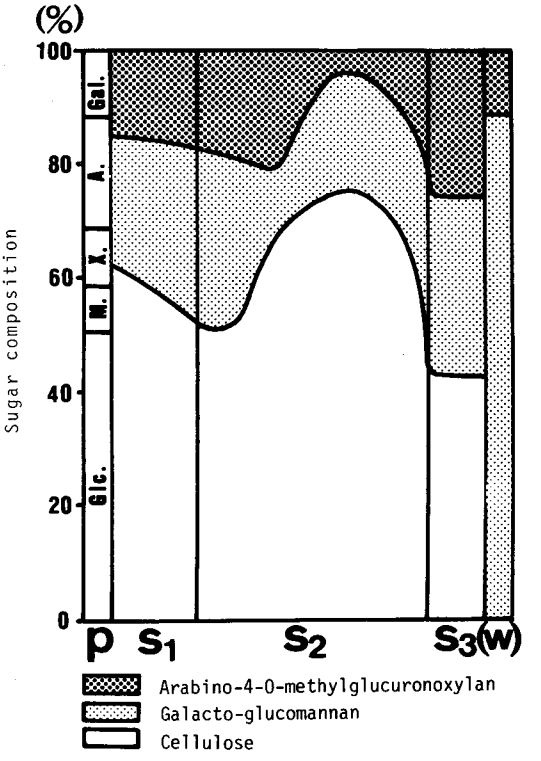

Figure 22 The distribution of polysaccharides across the cell wall of cryptomeria.

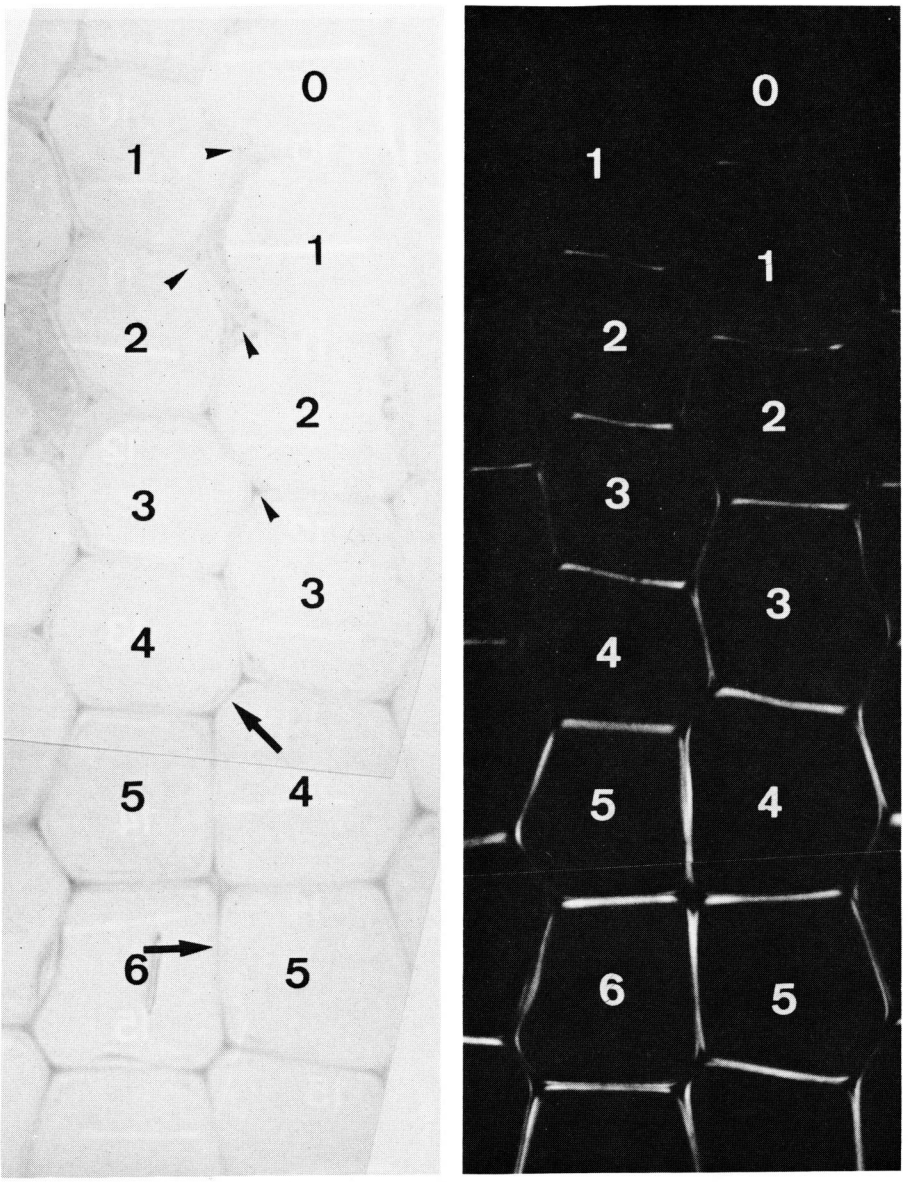

Figure 23 Differentiating xylem of cryptomeria photographed in ultraviolet light of wavelength 280 nm (left). Polarizing photomicrograph of the same tracheids (right). Arabic numerals indicate the cell number started from the cell just before S1 formation. In the tracheid begining S1 formation, weak UV-absorption can be seen at the cell corners (arrow heads). After that, UV-absorption appears at the middle lamella (arrows).

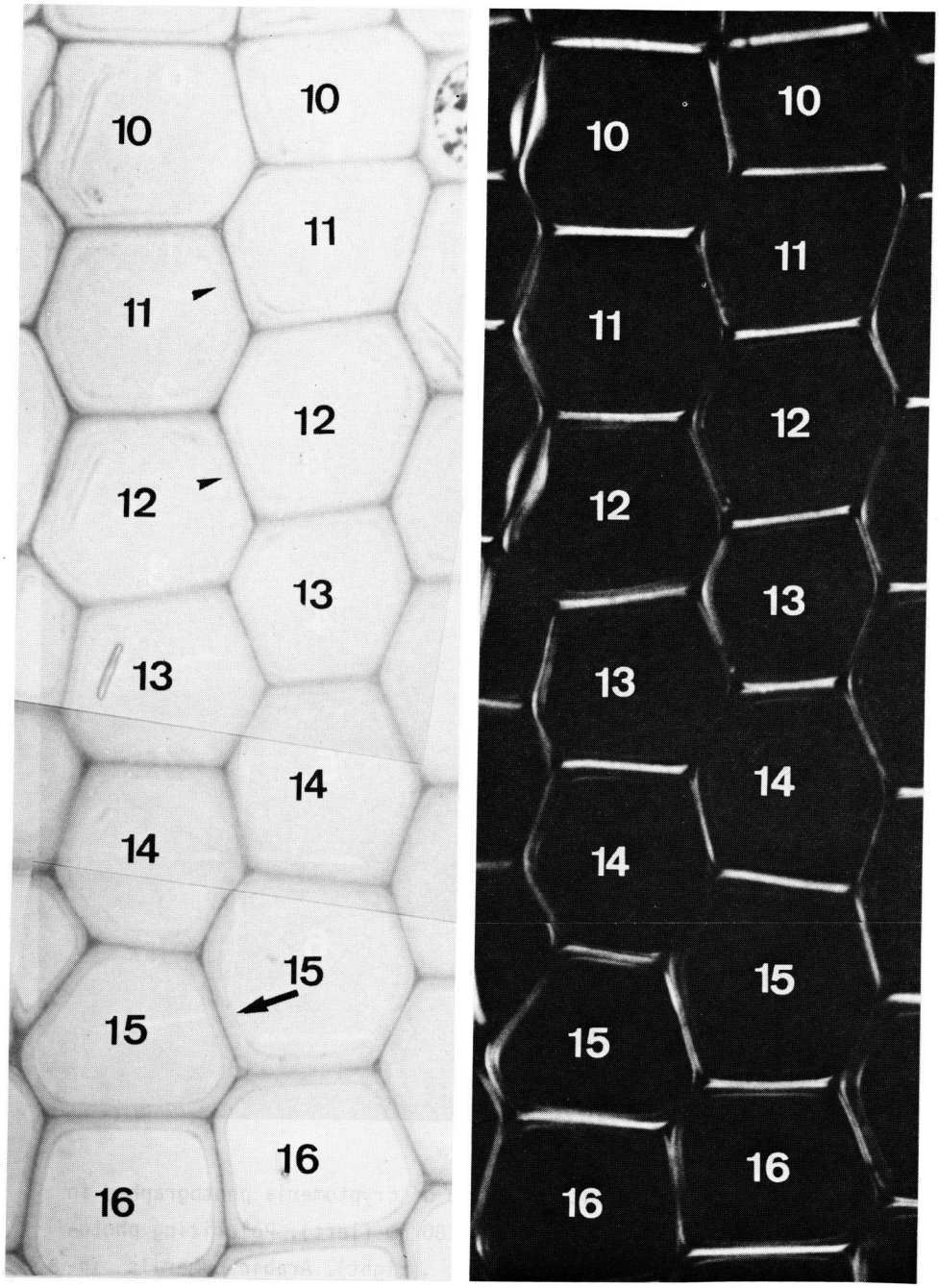

Figure 24 UV-photograph (left) and polarizing photograph (right) of the differentiating xylem of cryptomeria. UV-absorption of the secondary wall can be seen at the outer portion in the final part of S2 formation (arrow heads). In the tracheid just after S3 formation, UV-absorption is seen all over the secondary wall (arrow).

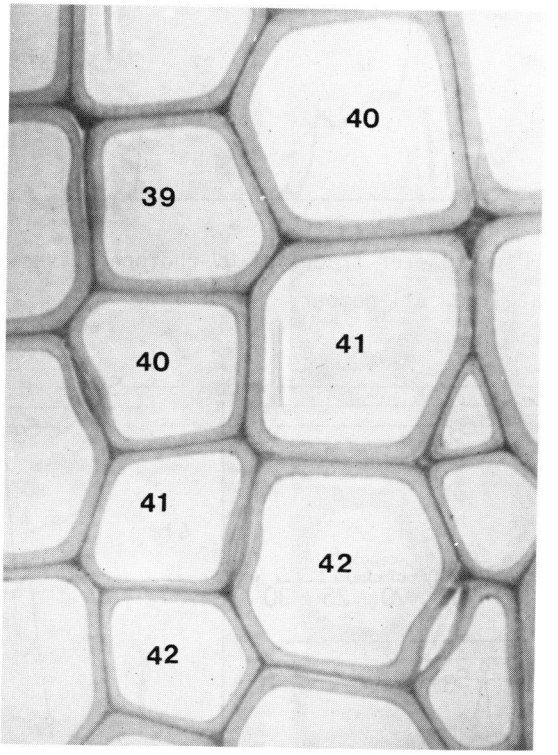

Figure 25 UV-photograph of mature tracheids. The secondary walls show the approximately a uniform UV-absorption.

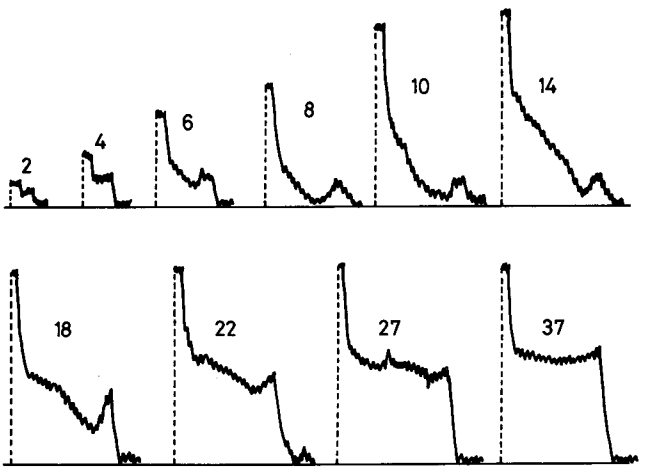

Figure 26 Densitometer traces of UV-photonegatives. Arabic numerals indicate the cell number.

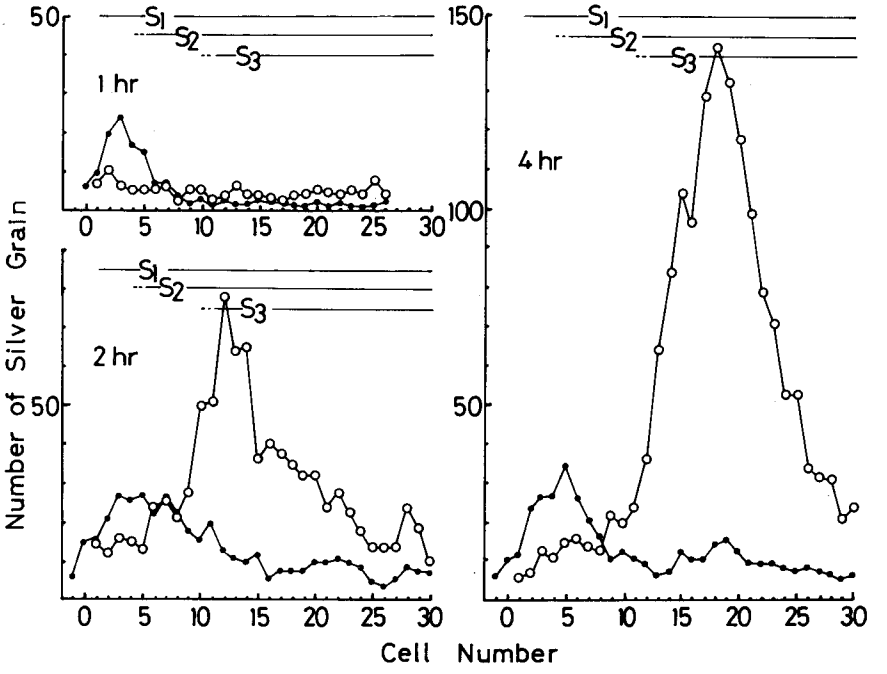

Figure 27 Incorporation of the radioactive phenylalanine into the compound middle lamella lignin and the secondary wall lignin determined by counting silver grains. The horizontal axis shows the cell number and the vertical axis the number of silver grains. Cell number is started from the tracheid just before S1 formation. Symbols are as follows: ○, secondary wall; ●, compound middle lamella.

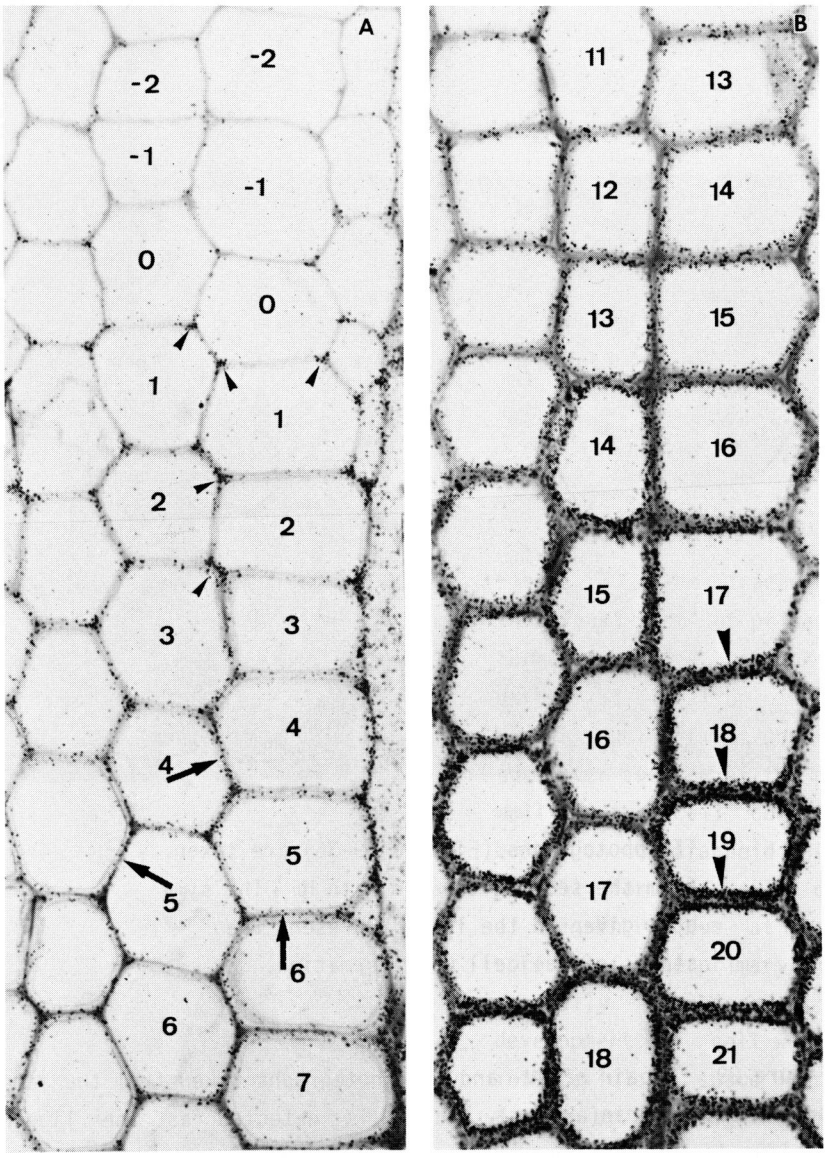

Figure 28 LM-autoradiographs of differentiating xylem of cryptomeria administered with tritiated phenylalanine for 4 hours. A: Silver grains are concentrated at the cell corners from the tracheids just before S1 formation to those of S1 formation (arrow heads). Subsequently, silver grains appear on the compound middle lamella(arrows). B: Numerous silver grains are distributed on the secondary wall in the tracheids just after the S3 formation (arrow heads).

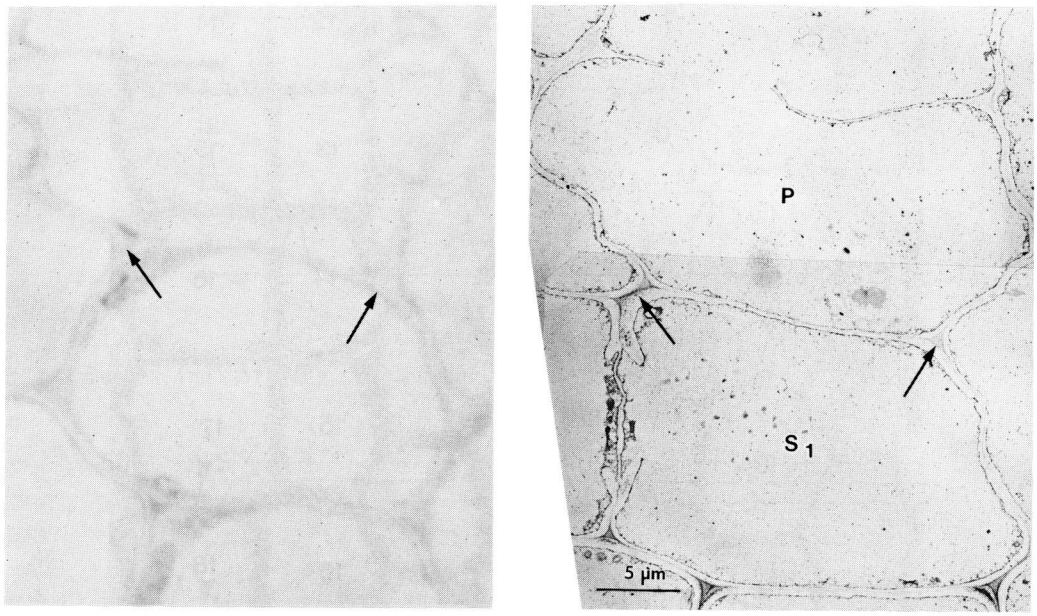

TEM-photographs (Figures 29-36) are taken from the section treated with HF. The symbols given in the lumen represent the stages of the cell wall formation.

Figure 29 A pair of UV- and TEM-photographs taken from the same tracheids. Lignin(arrows), which is detected as the lignin residue in TEM-photograph, can not be detected in UV-photograph. The resolving power of TEM is properly higher than that of UV-microscope.

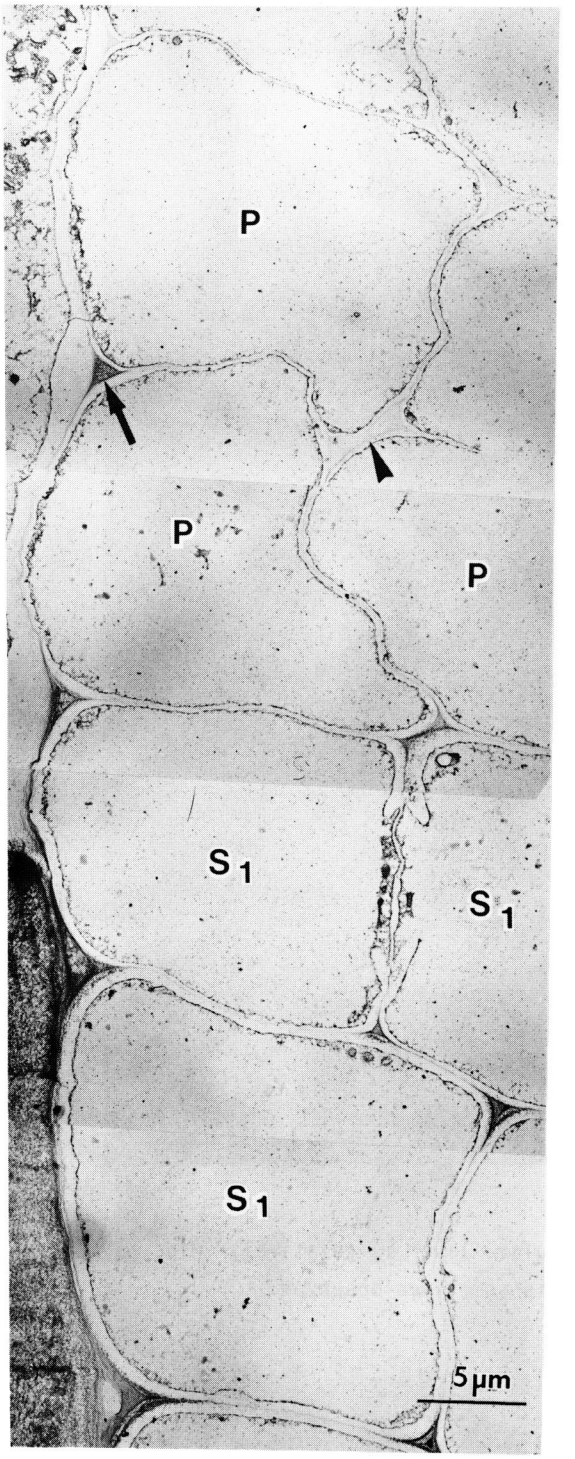

Figure 30 The tracheids from the final part of primary wall formation stage to the early part of S1 formation stage. Lignin residue is first observed at the outer surface of the primary wall of the cell corner(arrow head) in the tracheid just before S1 formation. The density of lignin residue at the outer surface of the primary wall is gradually increased with the development of cell wall. The intercellular space is also filled up with lignin residue. When the tracheid comes into contact with the ray parenchyma, the lignin residues at the outer surface of the primary wall and the intercellular space adjacent to the ray parenchyma(arrow) are detected earlier than those of the opposite side.

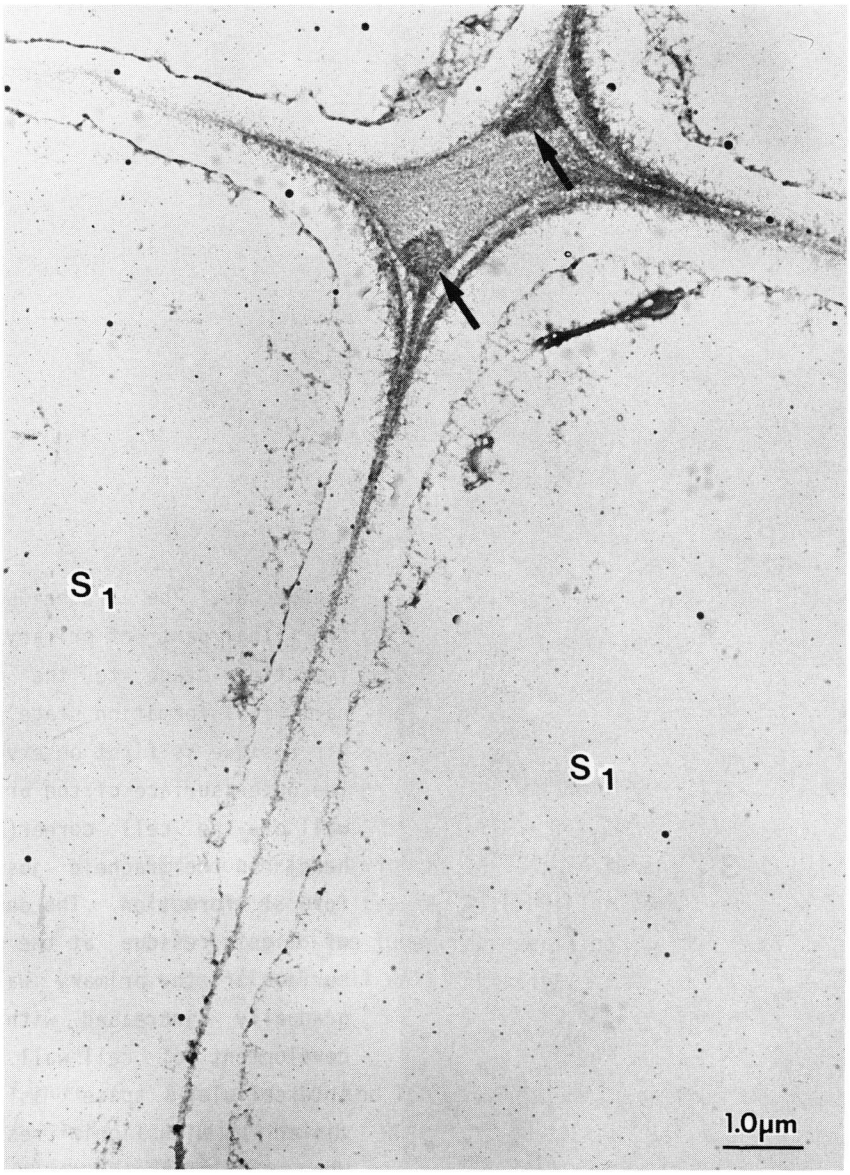

Figure 31 When the intercellular layer is relatively wide, a mass of lignin residue(arrows) is sometimes observed.

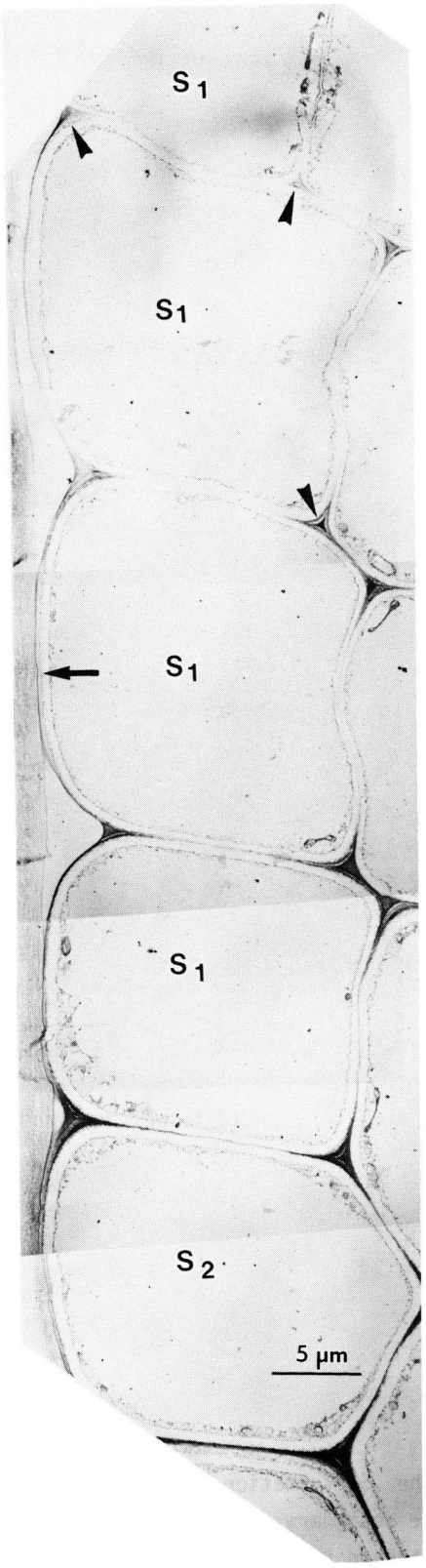

Figure 32 The tracheids from the S1 formation to the early part of S2 formation stage. The lignin residue at the intercellular layer is spreaded from the cell corners. The lignin residue is observed at the outermost part of S1 of the cell corner (arrow heads) in the early part of S1 formation stage and spreaded to the unlignified outermost part of S1. The lignin residue at the outermost part of S1 is also observed earlier in the ray parenchyma side(arrow) than in the opposite side.

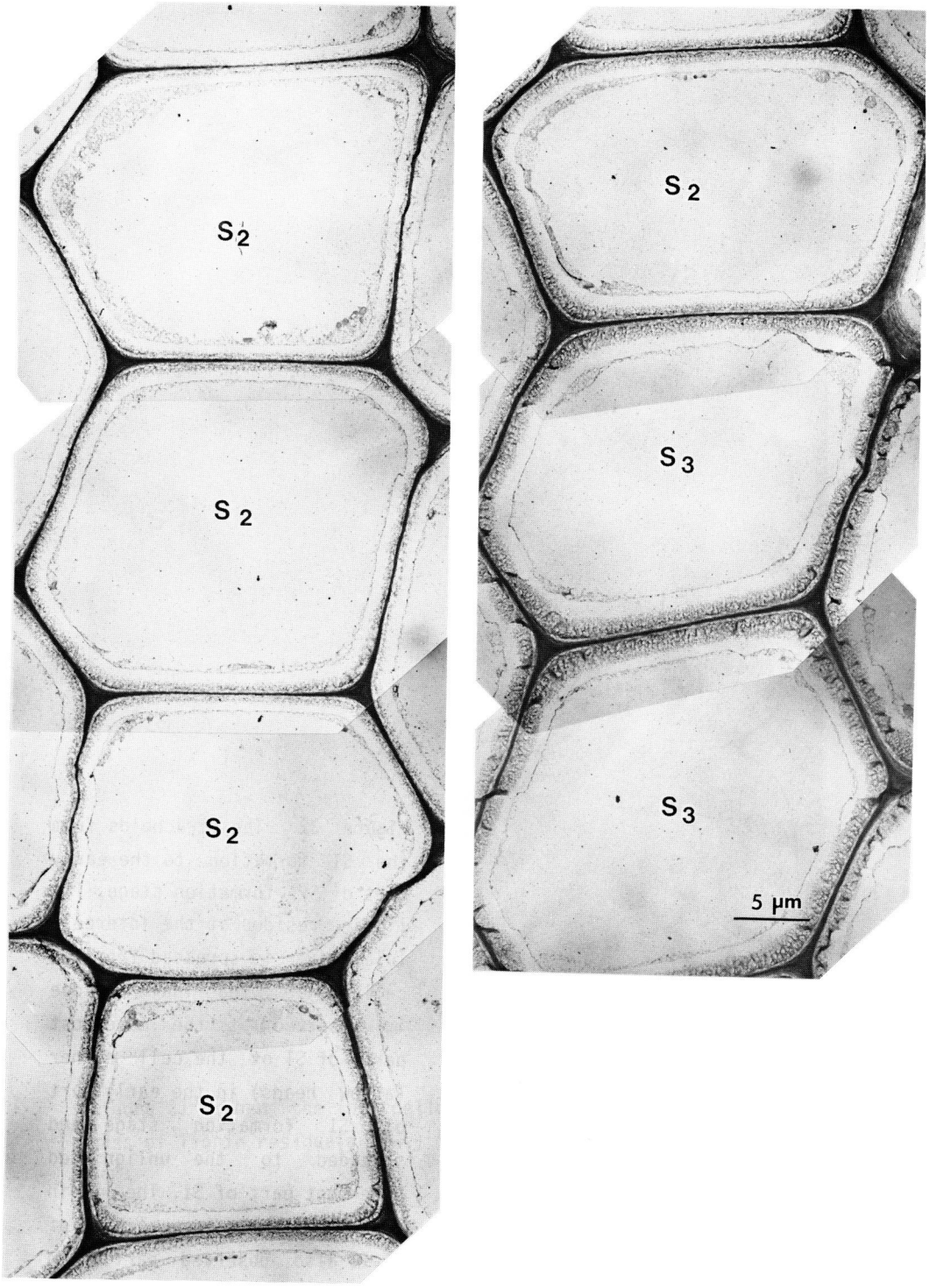

Figure 33 The tracheids from the S2 formation stage to the S3 stage. The lignin residue of the secondary wall gradually proceeds toward the lumen, lagging behind the cell wall thickening.

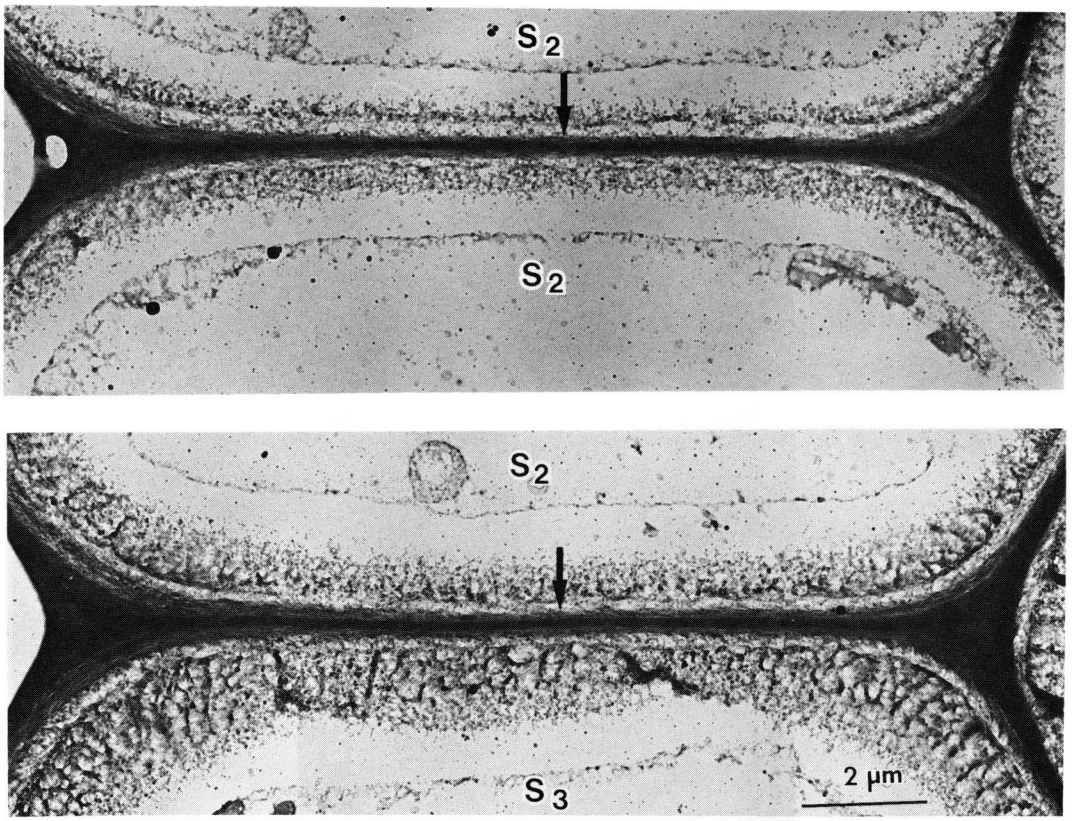

Figure 34 The tracheids in the S2 formation stage. The outer portion S1(arrows) has much more dense lignin residue than the inner portion of S1.

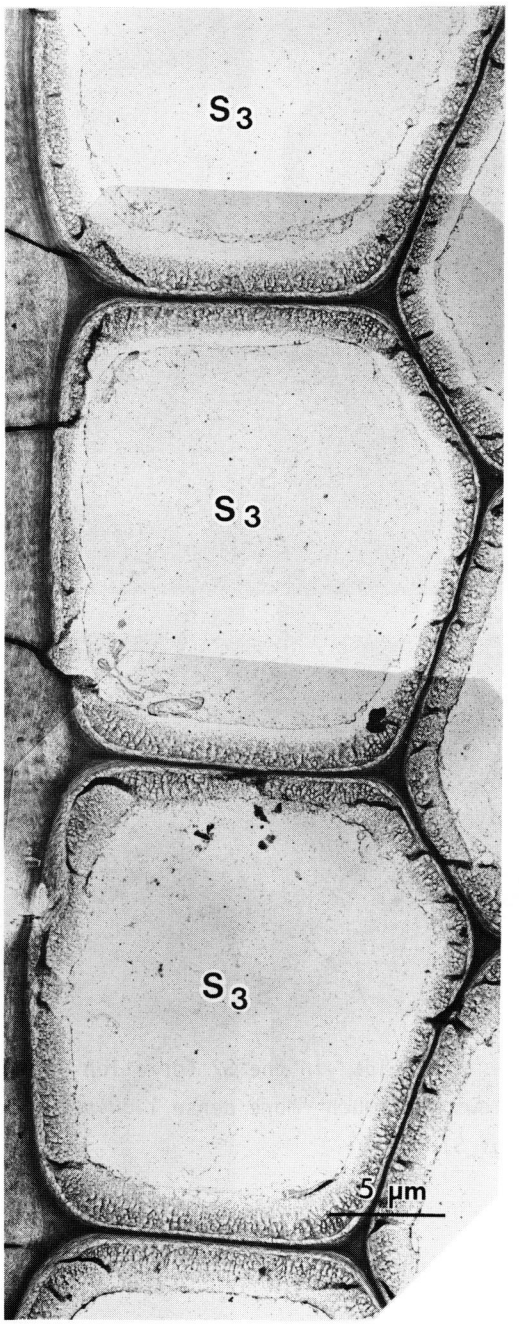

Figure 35 The tracheids in the S3 formation stage. The lignin residue of the secondary wall proceeds toward the lumen and reached to the lumen surface of the cell wall. At this time, the density of lignin residue at the outer portion of the secondary wall is still higher than that at the inner portion.

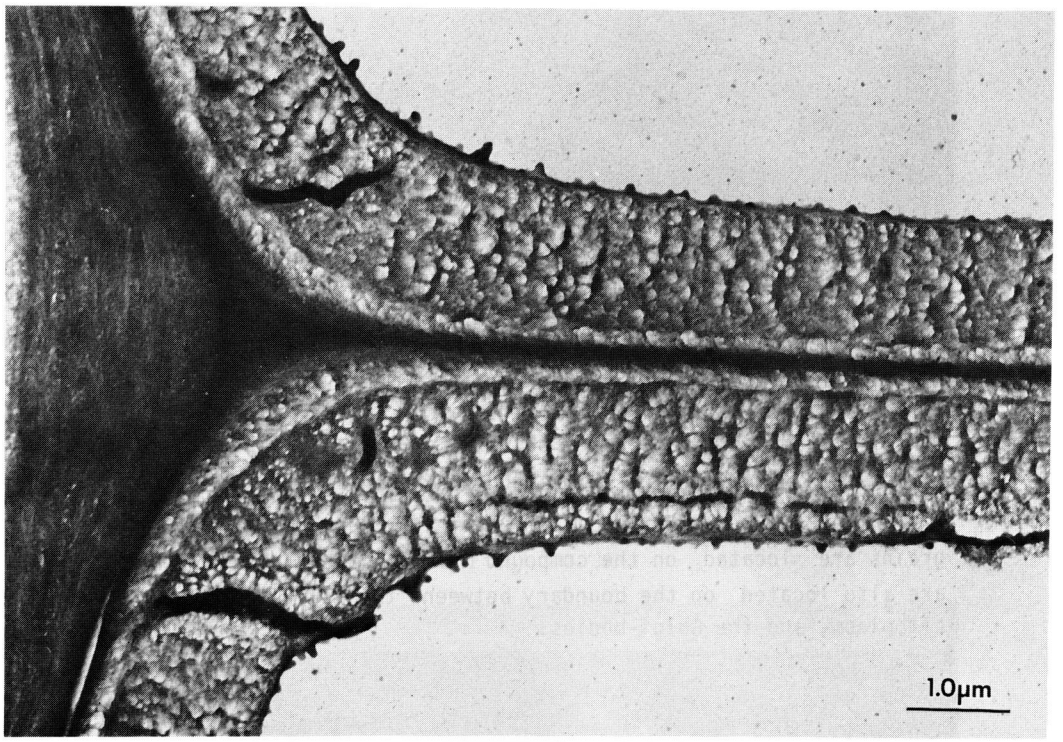

Figure 36 Mature tracheids. Secondary wall has approximately a uniform density of lignin residue, though the warty layer has slightly higher density. Compound middle lamella and ray parenchyma cell wall show a high density of lignin residue.

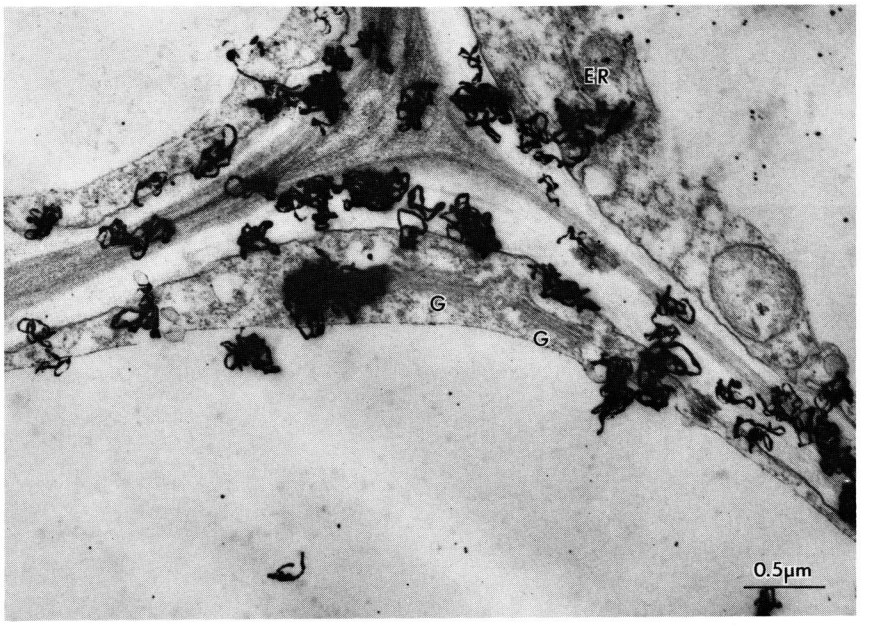

Figures 37-48 are obtained from the specimen administered with tritiated glucose for 4 hours.

Figure 37 The tracheids in the S1 formation stage. Silver grains are located on the compound middle lamella and S1. They are also located on the boundary between the cell wall and the cytoplasm, and the Golgi-bodies.

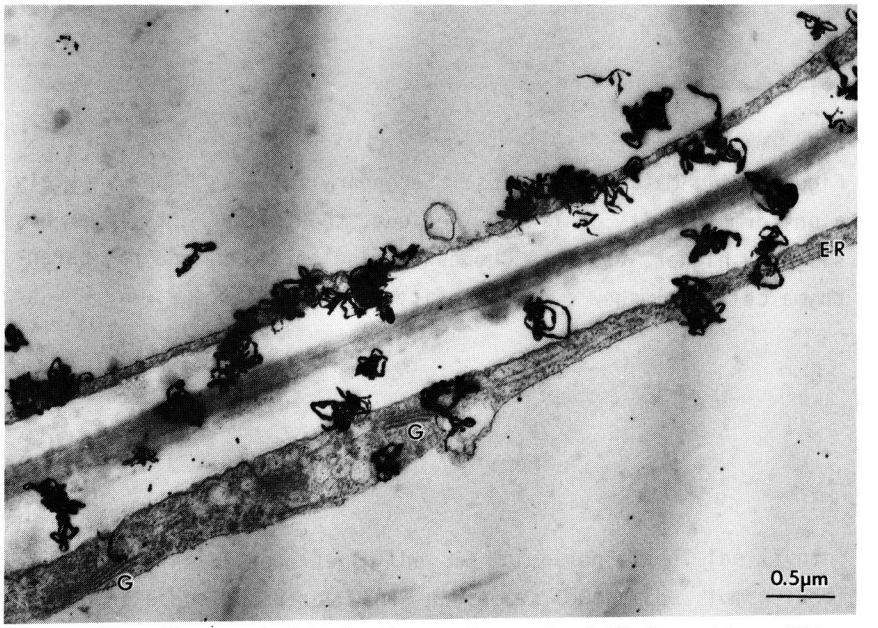

Figure 38 The tracheids in the early part of S2 formation. Silver grains are located on the compound middle lamella, S1, S2 and the boundary between the cell wall and the cytoplasm. They are also located on the Golgi-body.

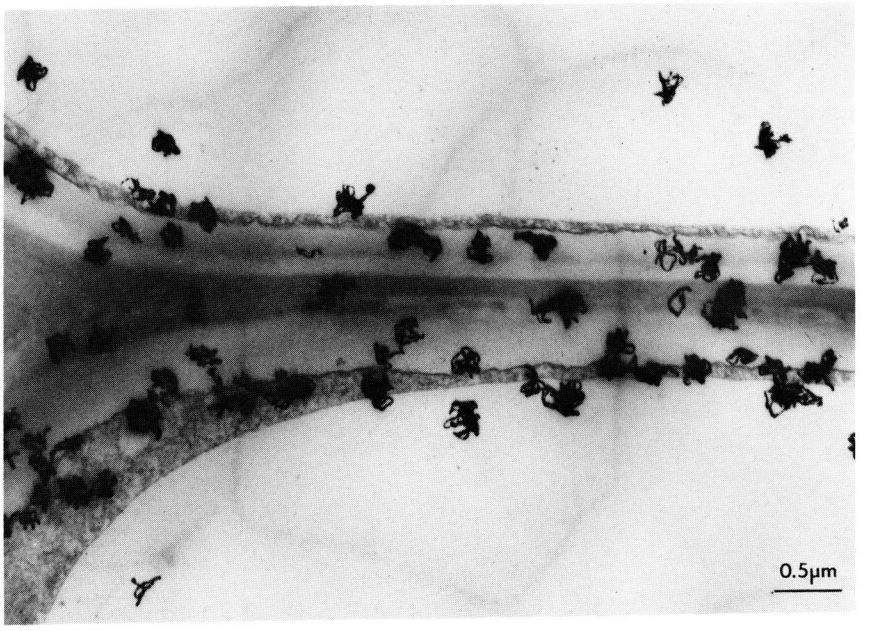

Figure 39 The tracheids in the early part of S2 formation stage. Silver grains are distributed on the compound middle lamella and the secondary wall.

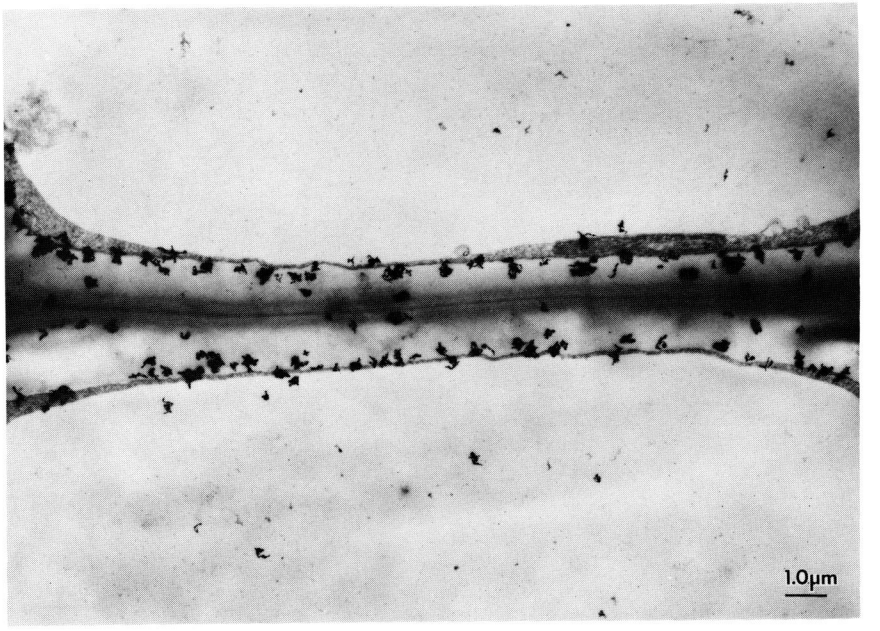

Figure 40 The tracheids in the S2 formation stage. Many silver grains are distributed on the inner surface of the cell wall.

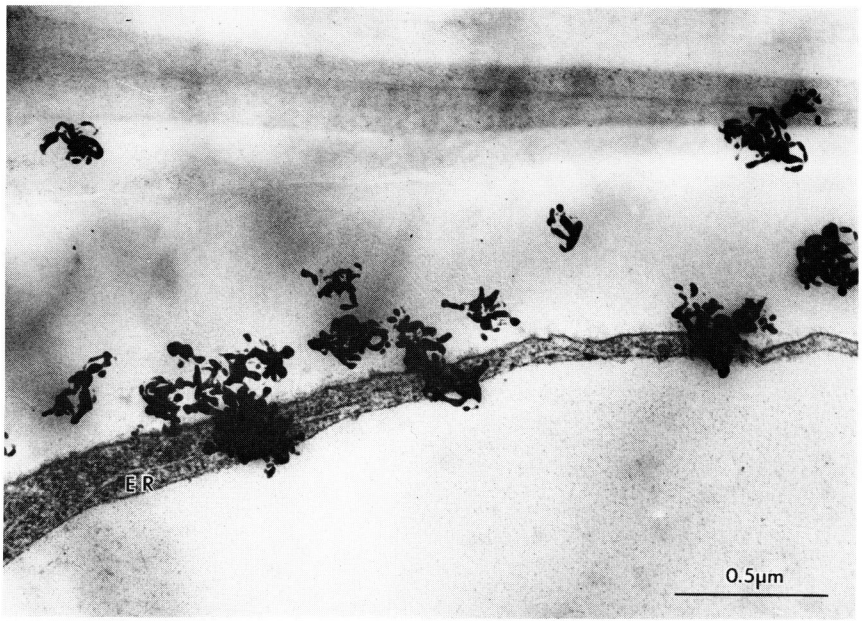

Figure 41 The tracheid in the S2 formation stage. Strong radioactivity is sometimes observed locally on the ER.

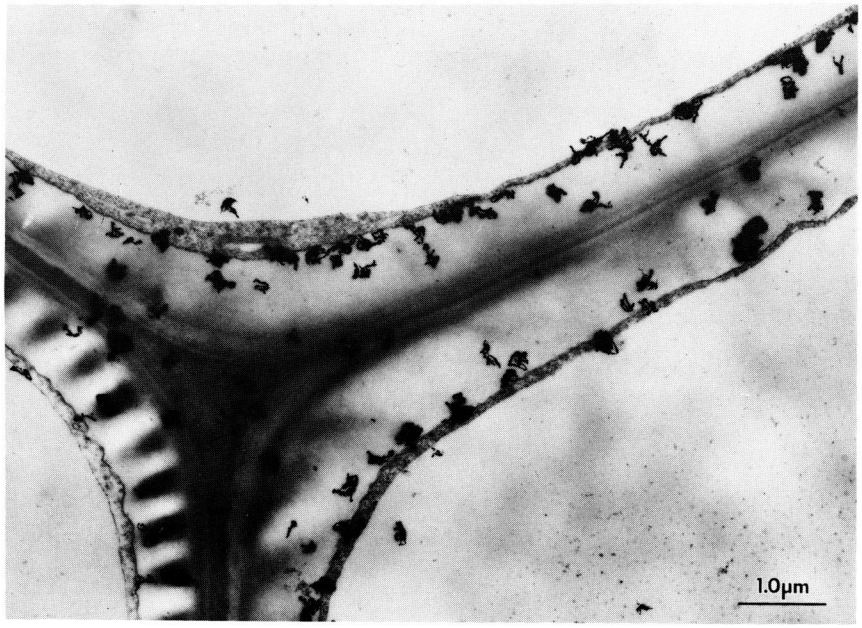

Figure 42 The tracheids in the S2 formation stage. Many silver grains are distributed on the boundary between the cytoplasm and the developing cell wall.

Figure 43 The tracheids in the final part of the S2 formation stage. Almost all of the silver grains are distributed on the boundary between the cytoplasm and the developing cell wall.

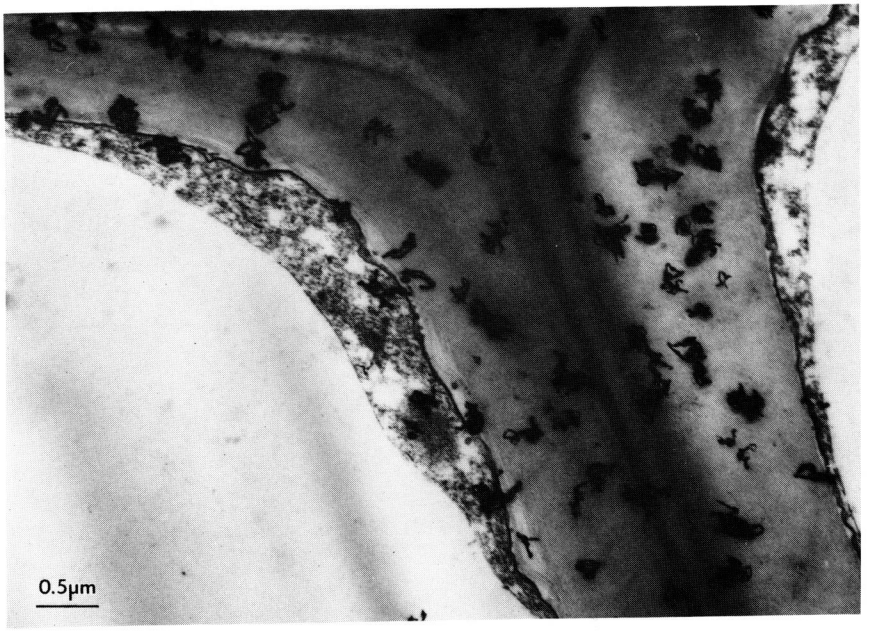

Figure 44 The tracheids in the S3 formation stage. Silver grains are distributed all over the secondary wall.

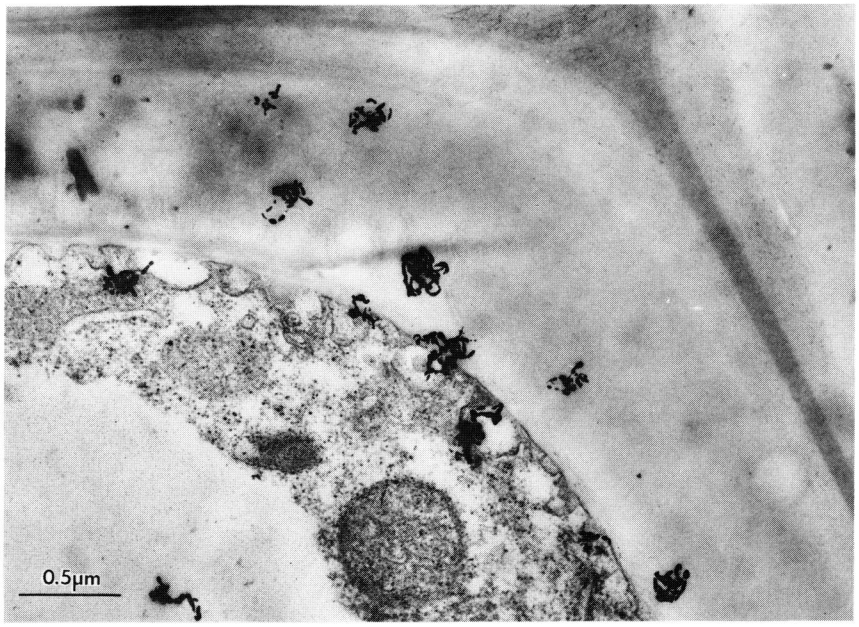

Figure 45 The tracheid after the S3 formation stage. The vesicles are fused to the plasma membrane. Silver grains are distributed on the vesicles and the secondary wall.

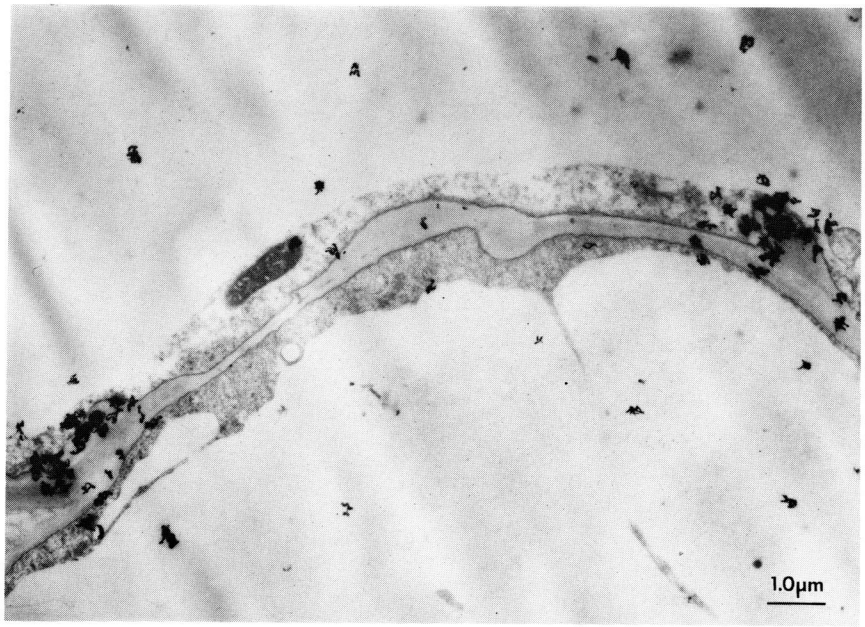

Figure 46 The tracheids in the S1 formation stage. Silver grains are concentrated on the tips of the developing bordered pit.

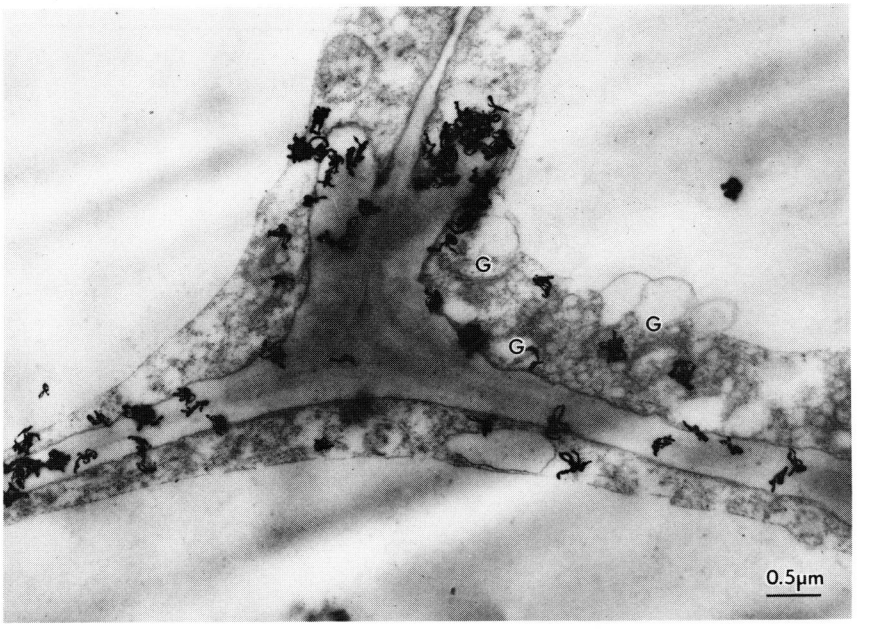

Figure 47 The tracheids in the S1 formation stage. Many sliver grains are distributed on the tips of the developing bordered pit. The Golgi bodies secreted many vesicles. Silver grains are also distributed on the Golgi bodies and the Golgi vesicles.

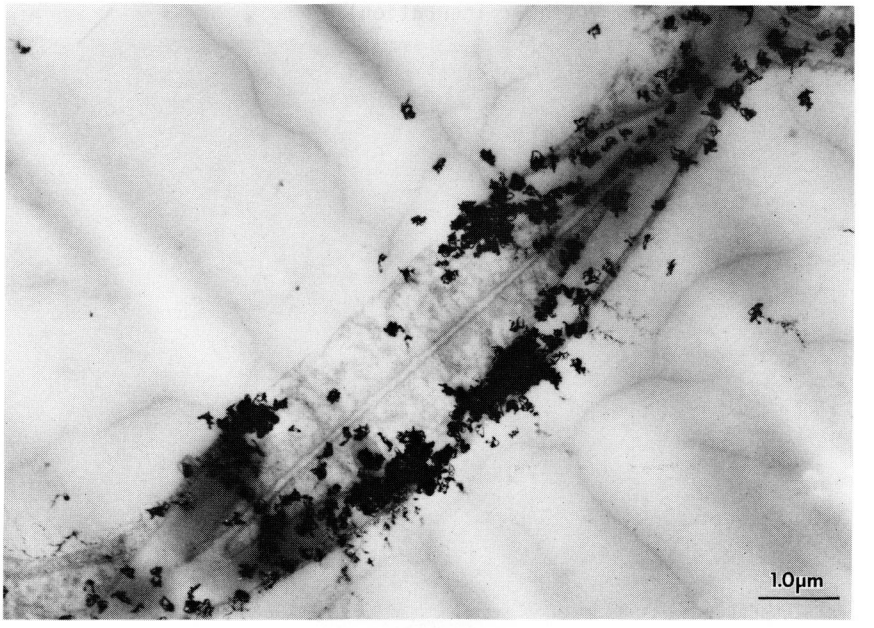

Figure 48 The tracheids in the S2 formation stage. Silver grains are abundantly distributed on the tips of the bordered pits.

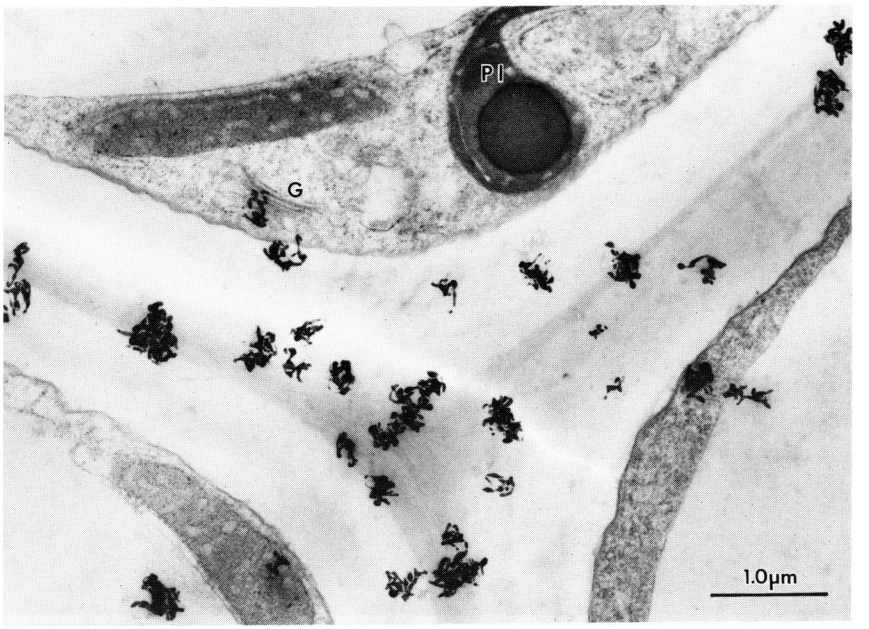

Figures 49-57 are obtained from the specimens administered with tritiated phenylalanine for 1-4 hours.

Figure 49 The tracheids at the early part of S2 formation stage. Silver grains are located on the compound middle lamella and the Golgi-body. (1 hour incubation)

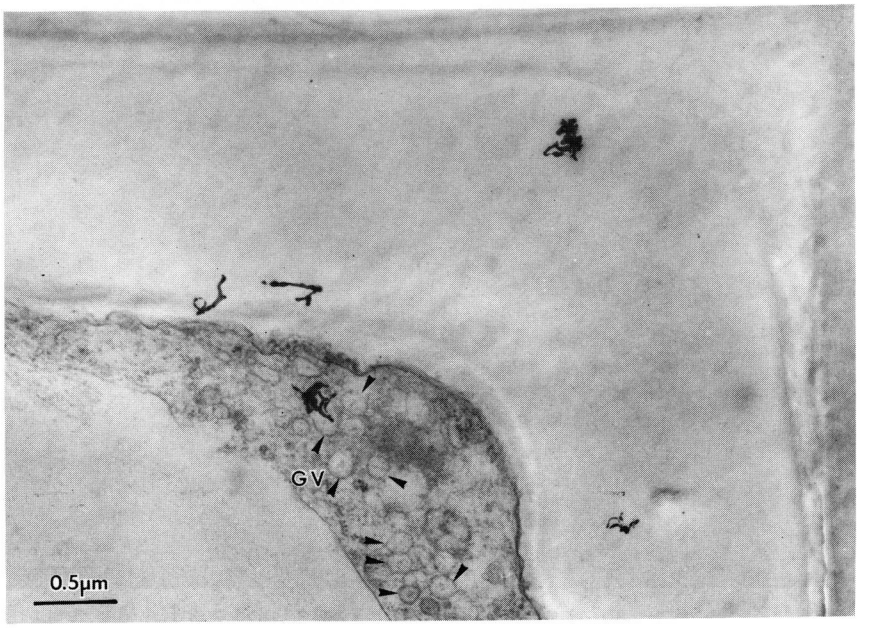

Figure 50 The tracheid just after S3 formation stage. A small amount of silver grains are located on the Golgi-vesicles(arrow heads), and secondary wall. (1 hour incubation)

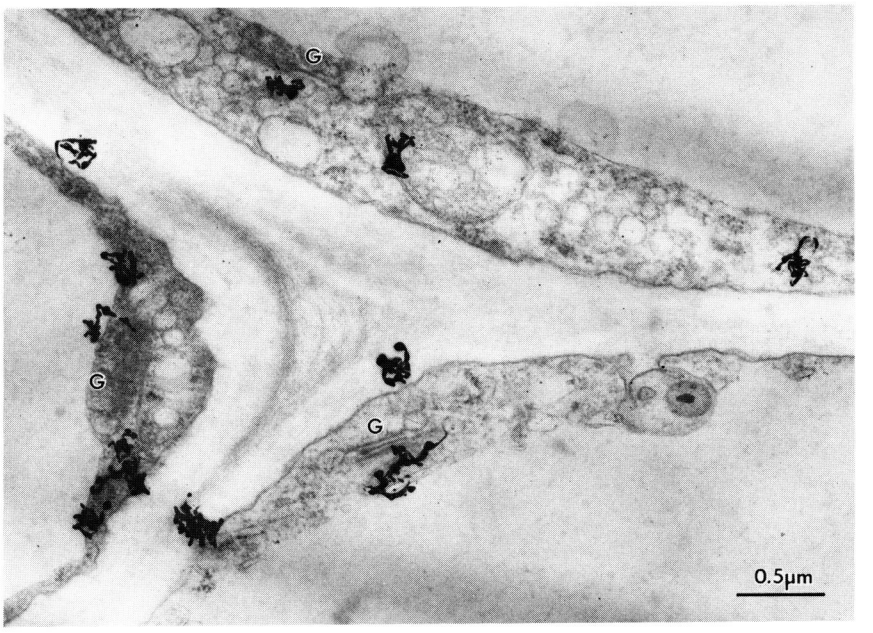

Figure 51 The tracheids at the final part of primary wall formation stage. The Golgi-bodies produce many vesicles. Silver grains are located on the Golgi-bodies, Golgi-vesicles, and compound middle lamella. (2 hour incubation)

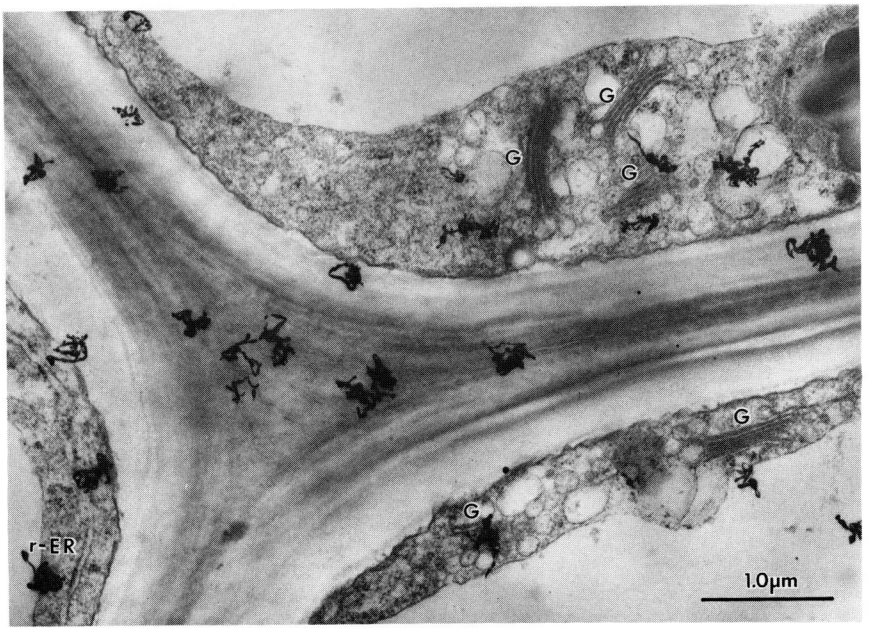

Figure 52 The tracheids at the early part of S2 formation stage. Radioactivity is observed on the Golgi-bodies, Golgi-vesicles, r-ER, and compound middle lamella. (2 hour incubation)

Figure 53 The tracheid just after S3 formation stage. The Golgi-bodies secrete vesicles, which fuse to the plasma membrane. Radioactivity is observed on the secondary wall, and Golgi-bodies, whereas it is scarcely observed on the compound middle lamella. (2 hour incubation)

Figure 54 The tracheid after S3 formation stage. Irregularly swollen smooth-ERs are filled in the cytoplasm. Numerous silver grains are located on the smooth-ERs and secondary wall. (2 hour incubation)

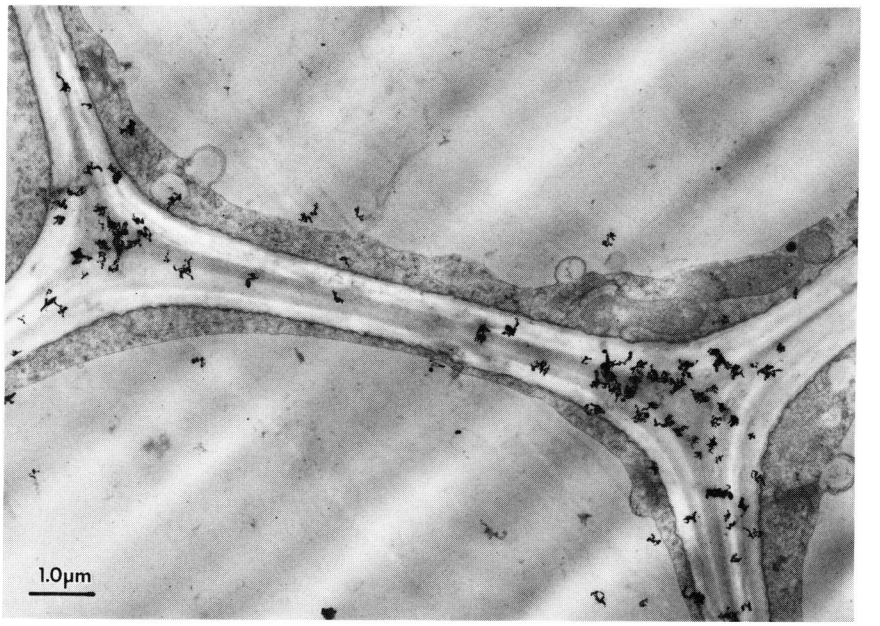

Figure 55 The tracheids at the early part of S2 formation stage. Radioactivity is concentrated on the cell corners. (4 hour incubation)

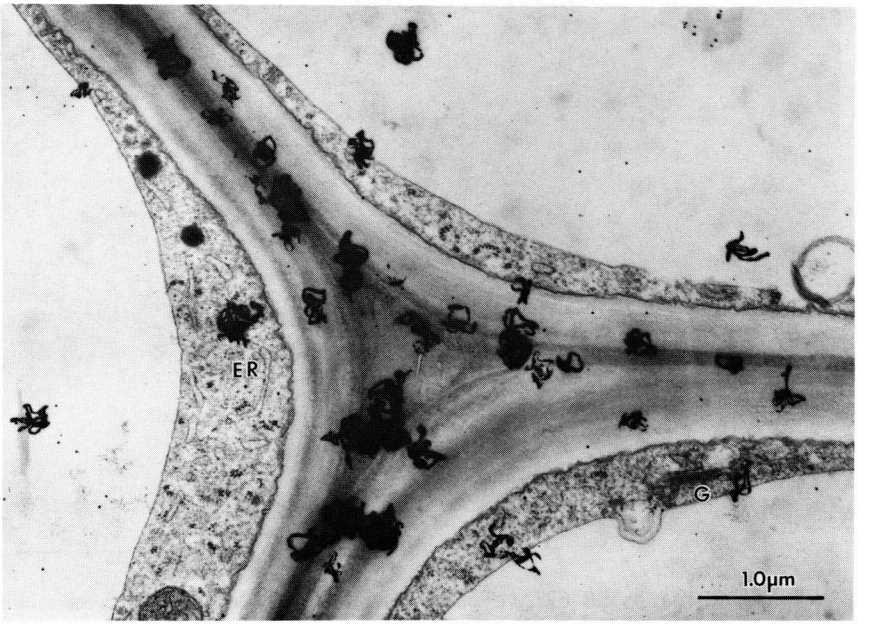

Figure 56 The tracheids in the early part of S2 formation. Silver grains are abundantly distributed on the compound middle lamella. They are also distributed on the Golgi body and ER. (4 hour incubation)

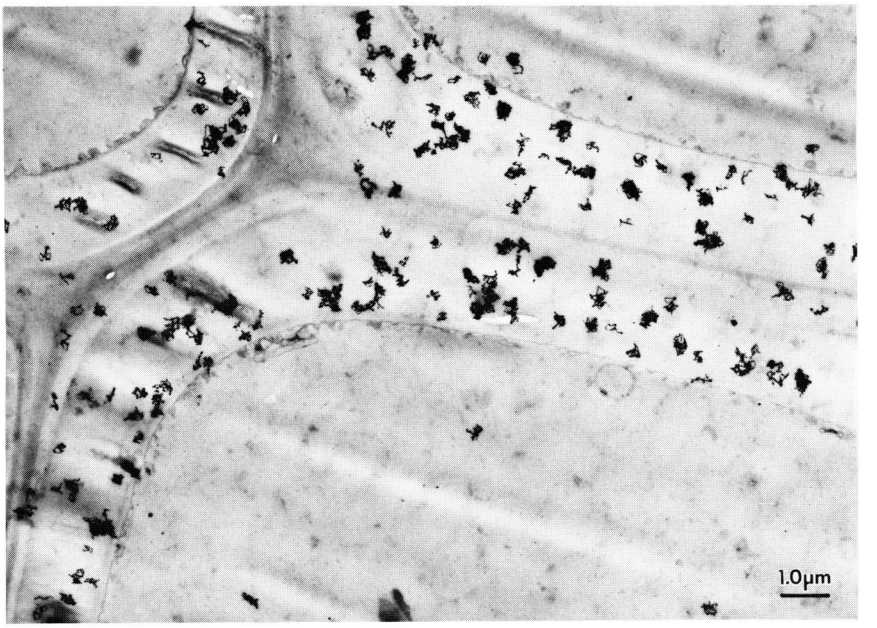

Figure 57 The tracheids after S3 formation stage. Numerous silver grains are observed on the secondary walls. (4 hour incubation)

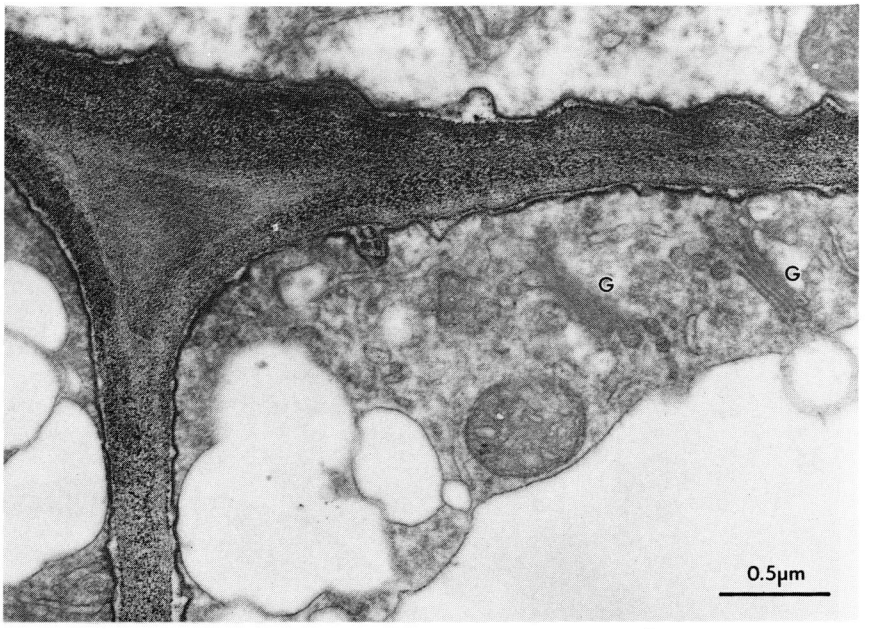

Figures 58-67 are obtained from the sections stained with PATAg reagent.

Figure 58 The tracheids in the primary wall formation stage. Primary wall is heavily stained with PATAg. Outer leaflet of the plasma memgrane is stained positively. The Golgi-vesicles are also stained weakly.

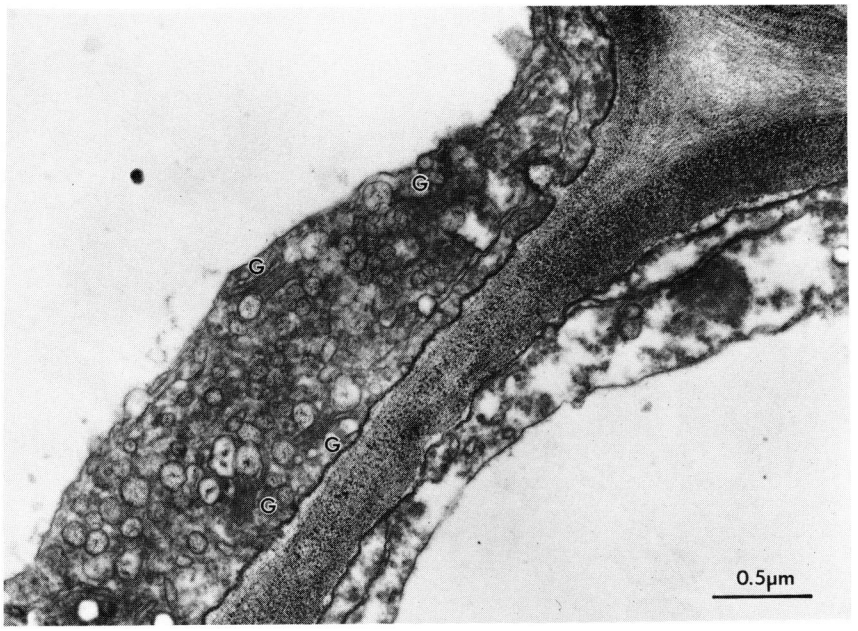

Figure 59 The tracheids just before S1 formation. Numerous Golgi bodies appear in the cytoplasm. The contents of the Golgi-vesicles are stained positively with PATAg.

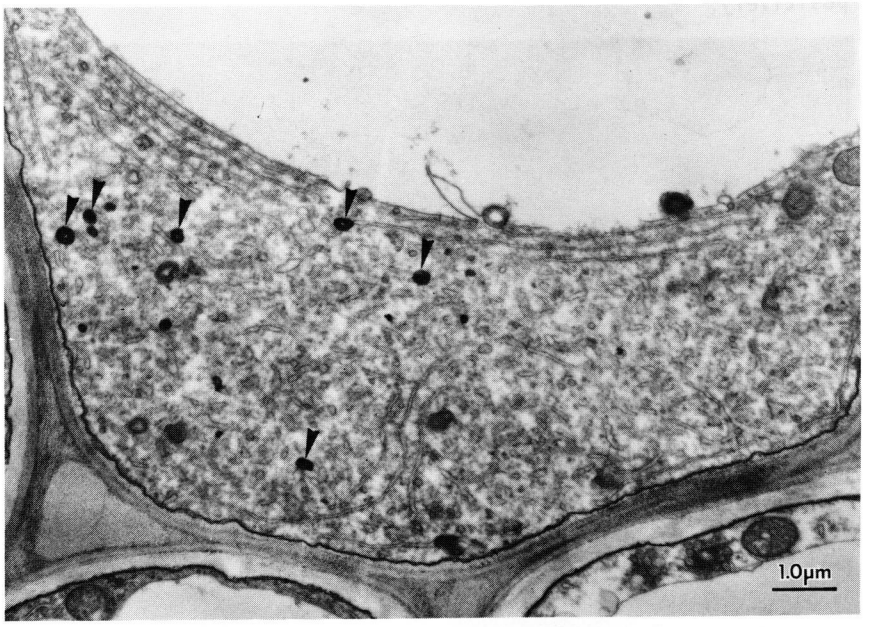

Figure 60 The tracheids just begining S1 formation. The materials stained heavily with PATAg (arrow heads) are distributed in the cytoplasm.

Figure 61 The tracheids just begining S1 formation. The Golgi-vesicles are positively stained with PATAg, whereas the Golgi-cisternae stained negatively. Small circular vesicles(arrow heads), which are distributed near the ER, are also stained positively.

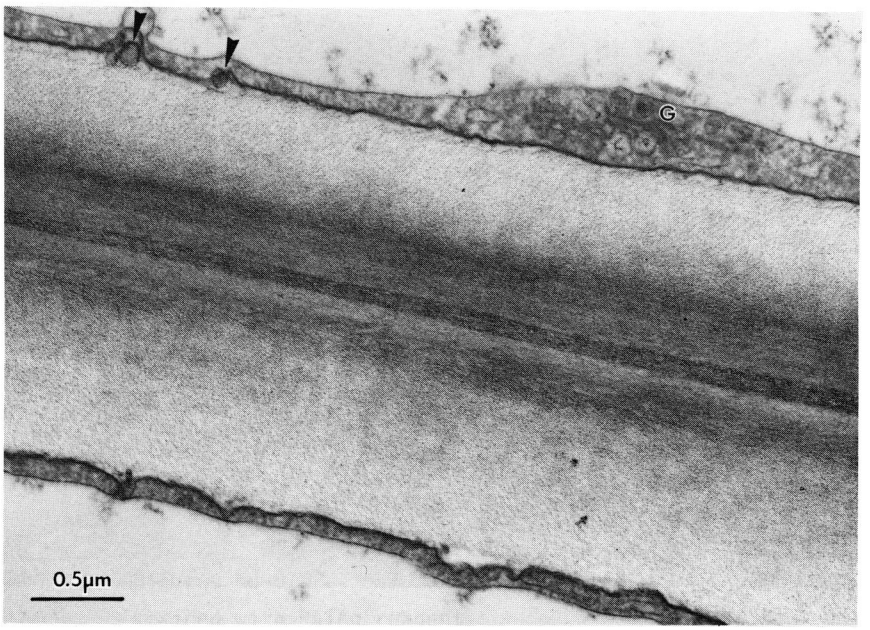

Figure 62 The tracheids in the S2 formation stage. The contents of the Golgi-vesicles and the materials between the developing cell wall and the plasma membrane(arrow heads) are positively stained with PATAg.

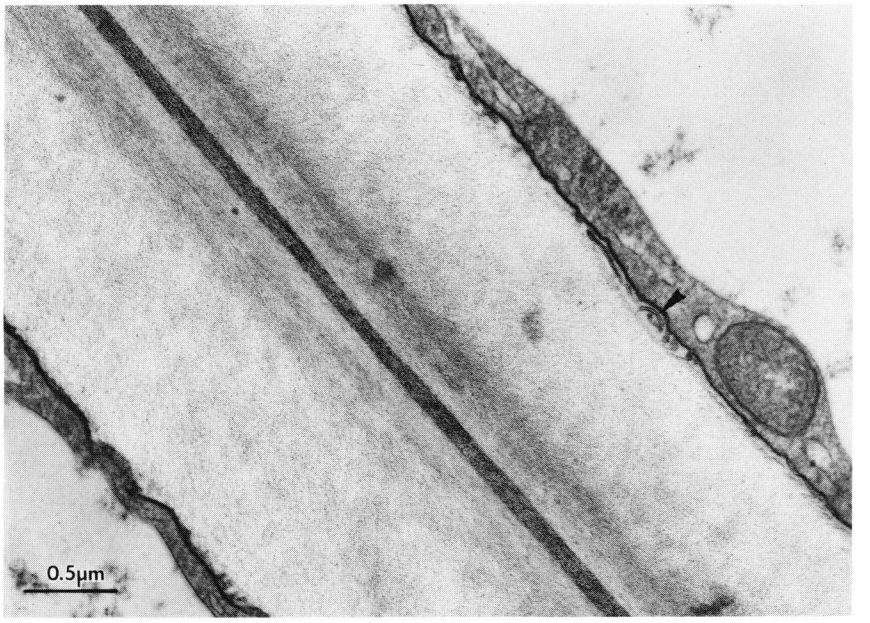

Figure 63 The tracheids in the S2 formation stage. Tubular inclusions(arrow head), which are stained positively with PATAg, are observed between the developing cell wall and the plasma membrane.

Figure 64 The tracheid in the S3 formation stage. Fibrillar materials (arrows) are generated from the plasma membrane. Numerous irregularly swollen s-ERs, which are unstained, appear in the cytoplasm.

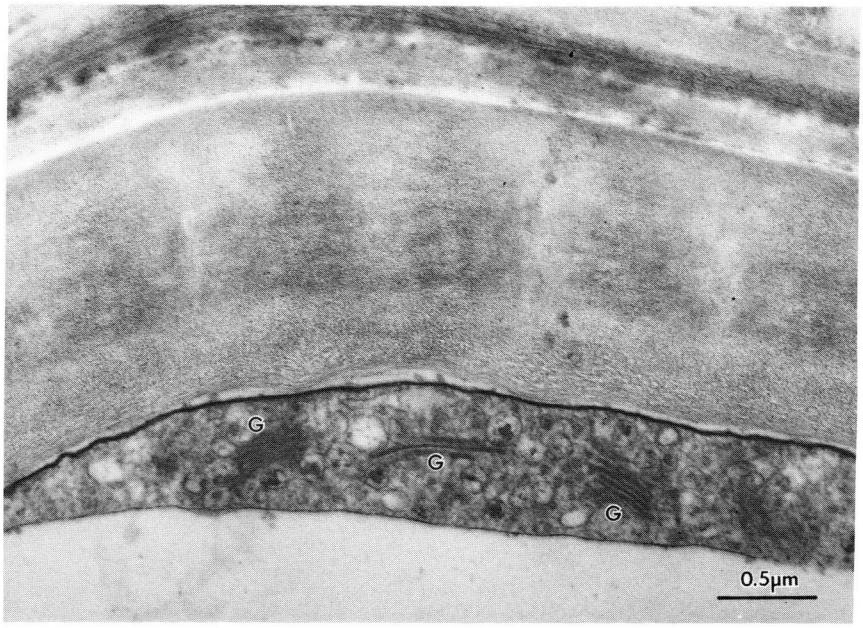

Figure 65 The tracheid in the S3 formation stage. The contents of the Golgi-vesicles are stained positively.

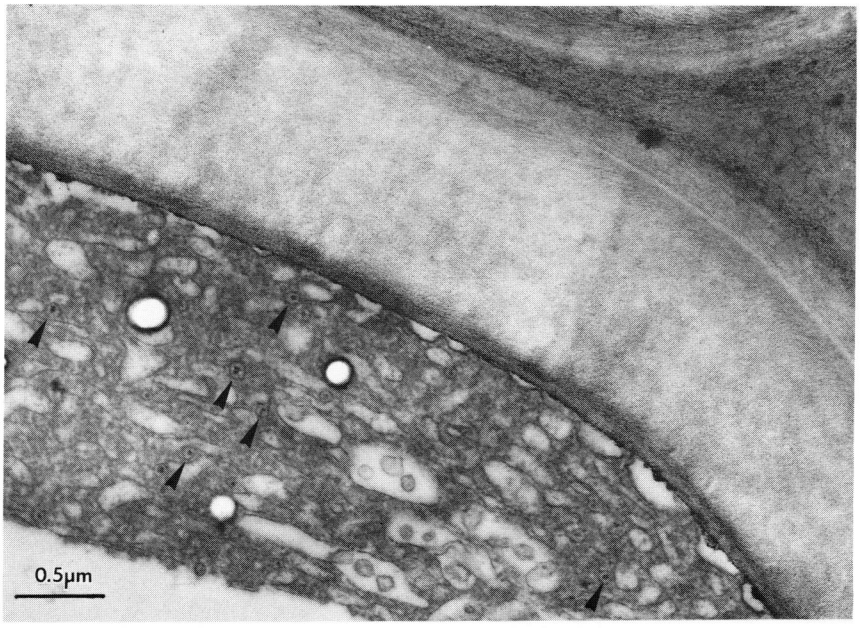

Figure 66 The tracheid just after the S3 formation stage. Numerous irregularly swollen s-ERs and the vesicles (arrow heads) probably derived from the Golgi-body appear in the cytoplasm. The former is stained negatively with PATAg, whereas the latter stained positively. Warts are heavily stained.

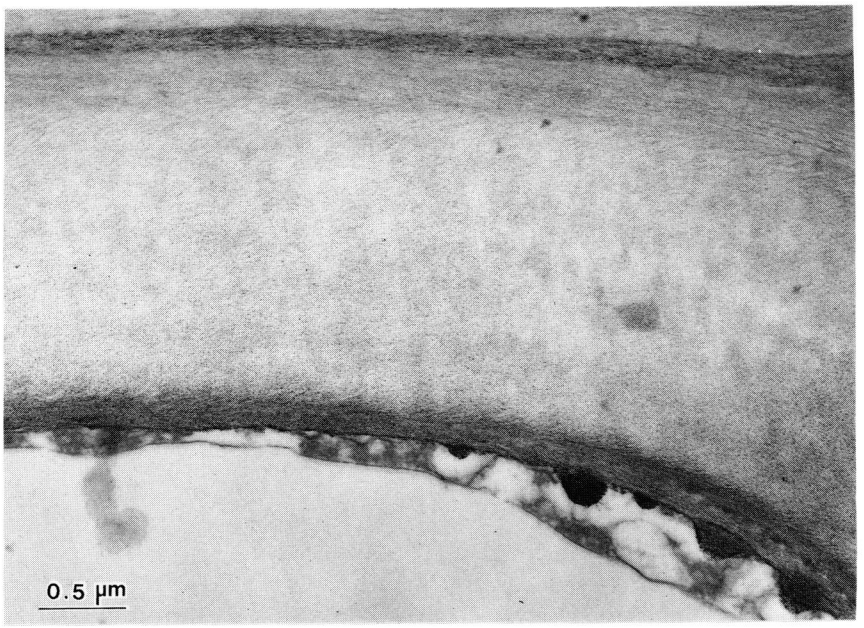

Figure 67 The tracheid just after the S3 formation stage. Warts are heavily stained with PATAg. S3 is also stained more dense than S1 and S2.